10. ELECTROWEAK MODEL AND CONSTRAINTS ON NEW PHYSICS

Revised December 2011 by J. Erler (U. Mexico and Institute for Advanced Study) and P. Langacker (Princeton University and Institute for Advanced Study).

10.1. Introduction

The standard model of the electroweak interactions (SM) [1] is based on the gauge group SU(2) × U(1), with gauge bosons W^i_μ, $i = 1, 2, 3$, and B_μ for the SU(2) and U(1) factors, respectively, and the corresponding gauge coupling constants g and g'. The left-handed fermion fields of the i^{th} fermion family transform as doublets $\Psi_i = \begin{pmatrix} \nu_i \\ \ell_i^- \end{pmatrix}$ and $\begin{pmatrix} u_i \\ d'_i \end{pmatrix}$ under SU(2), where $d'_i \equiv \sum_j V_{ij}\, d_j$, and V is the Cabibbo-Kobayashi-Maskawa mixing matrix. (Constraints on V and tests of universality are discussed in Ref. 2 and in the Section on "The CKM Quark-Mixing Matrix". The extension of the formalism to allow an analogous leptonic mixing matrix is discussed in the Section on "Neutrino Mass, Mixing, and Oscillations".) The right-handed fields are SU(2) singlets. In the minimal model there are three fermion families.

A complex scalar Higgs doublet, $\phi \equiv \begin{pmatrix} \phi^+ \\ \phi^0 \end{pmatrix}$, is added to the model for mass generation through spontaneous symmetry breaking with potential* given by,

$$V(\phi) = \mu^2 \phi^\dagger \phi + \frac{\lambda^2}{2} (\phi^\dagger \phi)^2. \tag{10.1}$$

For μ^2 negative, ϕ develops a vacuum expectation value, $v/\sqrt{2}$, where $v \approx 246.22$ GeV, breaking part of the electroweak (EW) gauge symmetry, after which only one neutral Higgs scalar, H, remains in the physical particle spectrum. In non-minimal models there are additional charged and neutral scalar Higgs particles [3].

After the symmetry breaking the Lagrangian for the fermion fields, ψ_i, is

$$\mathscr{L}_F = \sum_i \overline{\psi}_i \left(i \not{\partial} - m_i - \frac{g m_i H}{2 M_W} \right) \psi_i$$

* There is no generally accepted convention to write the quartic term. Our numerical coefficient simplifies Eq. (10.3*a*) below and the squared coupling preserves the relation between the number of external legs and the power counting of couplings at a given loop order. This structure also naturally emerges from physics beyond the SM, such as supersymmetry.

$$
\begin{aligned}
&- \frac{g}{2\sqrt{2}} \sum_i \overline{\Psi}_i \, \gamma^\mu \, (1-\gamma^5)(T^+ \, W_\mu^+ + T^- \, W_\mu^-) \, \Psi_i \\
&- e \sum_i q_i \, \overline{\psi}_i \, \gamma^\mu \, \psi_i \, A_\mu \\
&- \frac{g}{2\cos\theta_W} \sum_i \overline{\psi}_i \, \gamma^\mu (g_V^i - g_A^i \gamma^5) \, \psi_i \, Z_\mu \ . \qquad (10.2)
\end{aligned}
$$

$\theta_W \equiv \tan^{-1}(g'/g)$ is the weak angle; $e = g \sin\theta_W$ is the positron electric charge; and $A \equiv B\cos\theta_W + W^3 \sin\theta_W$ is the photon field (γ). $W^\pm \equiv (W^1 \mp iW^2)/\sqrt{2}$ and $Z \equiv -B\sin\theta_W + W^3 \cos\theta_W$ are the charged and neutral weak boson fields, respectively. The Yukawa coupling of H to ψ_i in the first term in $\mathscr{L}_F$, which is flavor diagonal in the minimal model, is $g m_i / 2M_W$. The boson masses in the EW sector are given (at tree level, *i.e.*, to lowest order in perturbation theory) by,

$$M_H = \lambda \, v, \qquad (10.3a)$$

$$M_W = \frac{1}{2} \, g \, v = \frac{e \, v}{2 \sin\theta_W}, \qquad (10.3b)$$

$$M_Z = \frac{1}{2} \sqrt{g^2 + g'^2} \, v = \frac{e \, v}{2 \sin\theta_W \cos\theta_W} = \frac{M_W}{\cos\theta_W}, \qquad (10.3c)$$

$$M_\gamma = 0. \qquad (10.3d)$$

The second term in $\mathscr{L}_F$ represents the charged-current weak interaction [4–7], where T^+ and T^- are the weak isospin raising and lowering operators. For example, the coupling of a W to an electron and a neutrino is

$$-\frac{e}{2\sqrt{2}\sin\theta_W} \left[W_\mu^- \, \overline{e} \, \gamma^\mu (1-\gamma^5) \nu + W_\mu^+ \, \overline{\nu} \, \gamma^\mu \, (1-\gamma^5) e \right]. \qquad (10.4)$$

For momenta small compared to M_W, this term gives rise to the effective four-fermion interaction with the Fermi constant given by $G_F/\sqrt{2} = 1/2v^2 = g^2/8M_W^2$. CP violation is incorporated into the EW model by a single observable phase in V_{ij}.

The third term in $\mathscr{L}_F$ describes electromagnetic interactions (QED) [8–10], and the last is the weak neutral-current interaction [5–7]. The vector and axial-vector couplings are

$$g_V^i \equiv t_{3L}(i) - 2 q_i \sin^2\theta_W, \qquad (10.5a)$$

$$g_A^i \equiv t_{3L}(i), \qquad (10.5b)$$

where $t_{3L}(i)$ is the weak isospin of fermion i ($+1/2$ for u_i and ν_i; $-1/2$ for d_i and e_i) and q_i is the charge of ψ_i in units of e.

The first term in Eq. (10.2) also gives rise to fermion masses, and in the presence of right-handed neutrinos to Dirac neutrino masses. The possibility of Majorana masses is discussed in the Section on "Neutrino Mass, Mixing, and Oscillations".

10.2. Renormalization and radiative corrections

In addition to the Higgs boson mass, M_H, the fermion masses and mixings, and the strong coupling constant, α_s, the SM has three parameters. A particularly useful set contains the Z mass[**], the Fermi constant, and the fine structure constant, which will be discussed in turn:

The Z boson mass, $M_Z = 91.1876 \pm 0.0021$ GeV, has been determined from the Z lineshape scan at LEP 1 [11].

The Fermi constant, $G_F = 1.1663787(6) \times 10^{-5}$ GeV^{-2}, is derived from the muon lifetime formula[***],

$$\frac{\hbar}{\tau_\mu} = \frac{G_F^2 m_\mu^5}{192\pi^3} F(\rho) \left[1 + H_1(\rho)\frac{\widehat{\alpha}(m_\mu)}{\pi} + H_2(\rho)\frac{\widehat{\alpha}^2(m_\mu)}{\pi^2}\right], \tag{10.6}$$

where $\rho = m_e^2/m_\mu^2$, and where

$$F(\rho) = 1 - 8\rho + 8\rho^3 - \rho^4 - 12\rho^2 \ln\rho = 0.99981295, \tag{10.7a}$$

$$H_1(\rho) = \frac{25}{8} - \frac{\pi^2}{2} - \left(9 + 4\pi^2 + 12\ln\rho\right)\rho + 16\pi^2\rho^{3/2} + \mathcal{O}(\rho^2) = -1.80793, \tag{10.7b}$$

$$H_2(\rho) = \frac{156815}{5184} - \frac{518}{81}\pi^2 - \frac{895}{36}\zeta(3) + \frac{67}{720}\pi^4 + \frac{53}{6}\pi^2\ln 2 - (0.042 \pm 0.002)_{\rm had} - \frac{5}{4}\pi^2\sqrt{\rho} + \mathcal{O}(\rho) = 6.64, \tag{10.7c}$$

$$\widehat{\alpha}(m_\mu)^{-1} = \alpha^{-1} + \frac{1}{3\pi}\ln\rho + \mathcal{O}(\alpha) = 135.901 \tag{10.7d}$$

The massless corrections to H_1 and H_2 have been obtained in Refs. 13 and 14, respectively, where the term in parentheses is from the hadronic vacuum polarization [14]. The mass corrections to H_1 have been known for some time [15], while those to H_2 are more recent [16]. Notice the term linear in m_e whose appearance was unforeseen and can be traced to the use of the muon pole mass in the prefactor [16]. The remaining uncertainty in G_F is experimental and has recently been reduced by an order of magnitude by the MuLan collaboration [12] at the PSI.

** We emphasize that in the fits described in Sec. 10.6 and Sec. 10.7 the values of the SM parameters are affected by all observables that depend on them. This is of no practical consequence for α and G_F, however, since they are very precisely known.

*** In the spirit of the Fermi theory, we incorporated the small propagator correction, $3/5\ m_\mu^2/M_W^2$, into Δr (see below). This is also the convention adopted by the MuLan collaboration [12]. While this breaks with historical consistency, the numerical difference was negligible in the past.

The fine structure constant, $\alpha = 1/137.035999074(44)$, is currently dominated by the $e^{\pm}$ anomalous magnetic moment [10]. In most EW renormalization schemes, it is convenient to define a running α dependent on the energy scale of the process, with $\alpha^{-1} \sim 137$ appropriate at very low energy, *i.e.* close to the Thomson limit. (The running has also been observed [17] directly.) For scales above a few hundred MeV this introduces an uncertainty due to the low energy hadronic contribution to vacuum polarization. In the modified minimal subtraction ($\overline{\rm MS}$) scheme [18] (used for this *Review*), and with $\alpha_s(M_Z) = 0.120$, we have $\widehat{\alpha}(m_\tau)^{-1} = 133.471 \pm 0.014$ and $\widehat{\alpha}(M_Z)^{-1} = 127.944 \pm 0.014$. (In this Section we denote quantities defined in the modified minimal subtraction ($\overline{\rm MS}$) scheme by a caret; the exception is the strong coupling constant, α_s, which will always correspond to the $\overline{\rm MS}$ definition and where the caret will be dropped.) The latter corresponds to a quark sector contribution (without the top) to the conventional (on-shell) QED coupling, $\alpha(M_Z) = \dfrac{\alpha}{1 - \Delta\alpha(M_Z)}$, of $\Delta\alpha^{(5)}_{\rm had}(M_Z) \approx 0.02772 \pm 0.00010$. These values are updated from Ref. 19 with $\Delta\alpha^{(5)}_{\rm had}(M_Z)$ moved downwards and its uncertainty halved (partly due to a more precise charm quark mass). Its correlation with the $\mu^{\pm}$ anomalous magnetic moment (see Sec. 10.5), as well as the non-linear α_s dependence of $\widehat{\alpha}(M_Z)$ and the resulting correlation with the input variable α_s, are fully taken into account in the fits. This is done by using as actual input (fit constraint) instead of $\Delta\alpha^{(5)}_{\rm had}(M_Z)$ the analogous low energy contribution by the three light quarks, $\Delta\alpha^{(3)}_{\rm had}(1.8\ \text{GeV}) = (55.50 \pm 0.78) \times 10^{-4}$ [20], and by calculating the perturbative and heavy quark contributions to $\widehat{\alpha}(M_Z)$ in each call of the fits according to Ref. 19. Part of the uncertainty ($\pm 0.49 \times 10^{-4}$) is from e^+e^- annihilation data below 1.8 GeV and τ decay data (including uncertainties from isospin breaking effects), but uncalculated higher order perturbative ($\pm 0.41 \times 10^{-4}$) and non-perturbative ($\pm 0.44 \times 10^{-4}$) QCD corrections and the $\overline{\rm MS}$ quark mass values (see below) also contribute. Various recent evaluations of $\Delta\alpha^{(5)}_{\rm had}$ are summarized in Table 10.1, where the leading order relation[†] between the $\overline{\rm MS}$ and on-shell definitions is given by,

$$\Delta\widehat{\alpha}(M_Z) - \Delta\alpha(M_Z) = \frac{\alpha}{\pi}\left(\frac{100}{27} - \frac{1}{6} - \frac{7}{4}\ln\frac{M_Z^2}{M_W^2}\right) \approx 0.0072, \tag{10.8}$$

and where the first term is from fermions and the other two are from $W^{\pm}$ loops which are usually excluded from the on-shell definition. Most of the older results relied on $e^+e^- \to$ hadrons cross-section measurements up to energies of 40 GeV, which were somewhat higher than the QCD prediction, suggested stronger running, and were less precise. The most recent results typically assume the validity of perturbative QCD (PQCD) at scales of 1.8 GeV and above, and are in reasonable agreement with each other. There

[†] Eq. (10.8) is for illustration only. Higher order contributions are directly evaluated in the $\overline{\rm MS}$ scheme using the FORTRAN package GAPP [21], including three-loop QED contributions of both leptons and quarks. The leptonic three-loop contribution in the on-shell scheme has been obtained in Ref. 22.

Table 10.1: Recent evaluations of the on-shell $\Delta\alpha^{(5)}_{\rm had}(M_Z)$. For better comparison we adjusted central values and errors to correspond to a common and fixed value of $\alpha_s(M_Z) = 0.120$. References quoting results without the top quark decoupled are converted to the five flavor definition. Ref. [33] uses $\Lambda_{\rm QCD} = 380 \pm 60$ MeV; for the conversion we assumed $\alpha_s(M_Z) = 0.118 \pm 0.003$.

Reference	Result	Comment
Martin, Zeppenfeld [23]	0.02744 ± 0.00036	PQCD for $\sqrt{s} > 3$ GeV
Eidelman, Jegerlehner [24]	0.02803 ± 0.00065	PQCD for $\sqrt{s} > 40$ GeV
Geshkenbein, Morgunov [25]	0.02780 ± 0.00006	$\mathcal{O}(\alpha_s)$ resonance model
Burkhardt, Pietrzyk [26]	0.0280 ± 0.0007	PQCD for $\sqrt{s} > 40$ GeV
Swartz [27]	0.02754 ± 0.00046	use of fitting function
Alemany *et al.* [28]	0.02816 ± 0.00062	incl. τ decay data
Krasnikov, Rodenberg [29]	0.02737 ± 0.00039	PQCD for $\sqrt{s} > 2.3$ GeV
Davier & Höcker [30]	0.02784 ± 0.00022	PQCD for $\sqrt{s} > 1.8$ GeV
Kühn & Steinhauser [31]	0.02778 ± 0.00016	complete $\mathcal{O}(\alpha_s^2)$
Erler [19]	0.02779 ± 0.00020	conv. from $\overline{\rm MS}$ scheme
Davier & Höcker [32]	0.02770 ± 0.00015	use of QCD sum rules
Groote *et al.* [33]	0.02787 ± 0.00032	use of QCD sum rules
Martin *et al.* [34]	0.02741 ± 0.00019	incl. new BES data
Burkhardt, Pietrzyk [35]	0.02763 ± 0.00036	PQCD for $\sqrt{s} > 12$ GeV
de Troconiz, Yndurain [36]	0.02754 ± 0.00010	PQCD for $s > 2$ GeV^2
Jegerlehner [37]	0.02765 ± 0.00013	conv. from MOM scheme
Hagiwara *et al.* [38]	0.02757 ± 0.00023	PQCD for $\sqrt{s} > 11.09$ GeV
Burkhardt, Pietrzyk [39]	0.02760 ± 0.00035	incl. KLOE data
Hagiwara *et al.* [40]	0.02770 ± 0.00022	incl. selected KLOE data
Jegerlehner [41]	0.02755 ± 0.00013	Adler function approach
Davier *et al.* [20]	0.02750 ± 0.00010	e^+e^- data
Davier *et al.* [20]	0.02762 ± 0.00011	incl. τ decay data
Hagiwara *et al.* [42]	0.02764 ± 0.00014	e^+e^- data

is, however, some discrepancy between analyses based on $e^+e^- \to$ hadrons cross-section data and those based on τ decay spectral functions [20]. The latter utilize data from OPAL [43], CLEO [44], ALEPH [45], and Belle [46] and imply lower central values

for the extracted M_H of about 6%. This discrepancy is smaller than in the past and at least some of it appears to be experimental. The dominant $e^+e^- \to \pi^+\pi^-$ cross-section was measured with the CMD-2 [47] and SND [48] detectors at the VEPP-2M e^+e^- collider at Novosibirsk and the results are (after an initial discrepancy due to a flaw in the Monte Carlo event generator used by SND) in good agreement with each other. As an alternative to cross-section scans, one can use the high statistics radiative return events at e^+e^- accelerators operating at resonances such as the Φ or the $\Upsilon(4S)$. The method [49] is systematics limited but dominates over the Novosibirsk data throughout. The BaBar collaboration [50] studied multi-hadron events radiatively returned from the $\Upsilon(4S)$, reconstructing the radiated photon and normalizing to $\mu^\pm\gamma$ final states. Their result is higher compared to VEPP-2M and in fact agrees quite well with the τ analysis including the energy dependence (shape). In contrast, the shape and smaller overall cross-section from the $\pi^+\pi^-$ radiative return results from the Φ obtained by the KLOE collaboration [51] differs significantly from what is observed by BaBar. The discrepancy originates from the kinematic region $\sqrt{s} \gtrsim 0.6$ GeV, and is most pronounced for $\sqrt{s} \gtrsim 0.85$ GeV. All measurements including older data [52] and multi-hadron final states (there are also discrepancies in the $e^+e^- \to 2\pi^+2\pi^-$ channel [20]) are accounted for and corrections have been applied for missing channels [20]. Further improvement of this dominant theoretical uncertainty in the interpretation of precision data will require better measurements of the cross-section for $e^+e^- \to$ hadrons below the charmonium resonances including multi-pion and other final states. To improve the precisions in $\widehat{m}_c(\widehat{m}_c)$ and $\widehat{m}_b(\widehat{m}_b)$ it would help to remeasure the threshold regions of the heavy quarks as well as the electronic decay widths of the narrow $c\bar{c}$ and $b\bar{b}$ resonances.

Further free parameters entering into Eq. (10.2) are the quark and lepton masses, where m_i is the mass of the i^{th} fermion ψ_i. For the quarks these are the current masses. For the light quarks, as described in the note on "Quark Masses" in the Quark Listings, $\widehat{m}_u = 2.5^{+0.6}_{-0.8}$ MeV, $\widehat{m}_d = 5.0^{+0.7}_{-0.9}$ MeV, and $\widehat{m}_s = 100^{+30}_{-20}$ MeV. These are running $\overline{\rm MS}$ masses evaluated at the scale $\mu = 2$ GeV. For the heavier quarks we use QCD sum rule [53] constraints [54] and recalculate their masses in each call of our fits to account for their direct α_s dependence. We find[¶], $\widehat{m}_c(\mu = \widehat{m}_c) = 1.267^{+0.032}_{-0.040}$ GeV and $\widehat{m}_b(\mu = \widehat{m}_b) = 4.197 \pm 0.025$ GeV, with a correlation of 24%.

The top quark "pole" mass (the quotation marks are a reminder that quarks do not form asymptotic states), $m_t = 173.4 \pm 0.9$ GeV, is an average of published and preliminary CDF and DØ results from run I and II [56] with first results by the CMS [57] and ATLAS [58] collaborations averaged in ignoring correlations. To gauge the possible

[¶] Other authors [55] advocate to evaluate and quote $\widehat{m}_c(\mu = 3$ GeV) instead. We use $\widehat{m}_c(\mu = \widehat{m}_c)$ because in the global analysis it is convenient to nullify any explicitly m_c dependent logarithms. Note also that our uncertainty for m_c (and to a lesser degree for m_b) is larger than the one in Ref. 55, for example. The reason is that we determine the continuum contribution for charm pair production using only resonance data and theoretical consistency across various sum rule moments, and then use any difference to the experimental continuum data as an additional uncertainty. We also include an uncertainty for the condensate terms which grows rapidly for higher moments in the sum rule analysis.

impact of the neglect of correlations involving the LHC experiments, we also averaged the results conservatively assuming that the entire 0.75 GeV systematic of the Tevatron average is fully correlated with a 0.75 GeV component in both CMS and ATLAS. Incidentally, this yields correlations of similar size as those between the two Tevatron experiments and the two Runs and reduces the central value by 0.15 GeV. Within round-off we expect a more refined average to coincide with ours. Our average[$] differs slightly from the value, $m_t = 173.5 \pm 0.6 \pm 0.8$ GeV, which appears in the top quark Listings in this *Review* and which is based exclusively on published results. We are working, however, with $\overline{\rm MS}$ masses in all expressions to minimize theoretical uncertainties. Such a short distance mass definition (unlike the pole mass) is free from non-perturbative and renormalon [59] uncertainties. We therefore convert to the top quark $\overline{\rm MS}$ mass,

$$\widehat{m}_t(\mu = \widehat{m}_t) = m_t[1 - \frac{4}{3}\frac{\alpha_s}{\pi} + \mathcal{O}(\alpha_s^2)], \tag{10.9}$$

using the three-loop formula [60]. This introduces an additional uncertainty which we estimate to 0.5 GeV (the size of the three-loop term) and add in quadrature to the experimental pole mass error. This is convenient because we use the pole mass as an external constraint while fitting to the $\overline{\rm MS}$ mass. We are assuming that the kinematic mass extracted from the collider events corresponds within this uncertainty to the pole mass. Using the BLM optimized [61] version of the two-loop perturbative QCD formula [62] (as we did in previous editions of this *Review*) gives virtually identical results. In summary, we will use $m_t = 173.4 \pm 0.9$ (exp.) ± 0.5 (QCD) GeV $= 173.4 \pm 1.0$ GeV (together with $M_H = 117$ GeV) for the numerical values quoted in Sec. 10.2–Sec. 10.5.

$\sin^2\theta_W$ and M_W can be calculated from M_Z, $\widehat{\alpha}(M_Z)$, and G_F, when values for m_t and M_H are given; conversely (as is done at present), M_H can be constrained by $\sin^2\theta_W$ and M_W. The value of $\sin^2\theta_W$ is extracted from neutral-current processes (see Sec. 10.3) and Z pole observables (see Sec. 10.4) and depends on the renormalization prescription. There are a number of popular schemes [63–70] leading to values which differ by small factors depending on m_t and M_H. The notation for these schemes is shown in Table 10.2.

(*i*) The on-shell scheme [63] promotes the tree-level formula $\sin^2\theta_W = 1 - M_W^2/M_Z^2$ to a definition of the renormalized $\sin^2\theta_W$ to all orders in perturbation theory, *i.e.*, $\sin^2\theta_W \to s_W^2 \equiv 1 - M_W^2/M_Z^2$:

$$M_W = \frac{A_0}{s_W(1-\Delta r)^{1/2}}\ , \qquad M_Z = \frac{M_W}{c_W}\ , \tag{10.10}$$

where $c_W \equiv \cos\theta_W$, $A_0 = (\pi\alpha/\sqrt{2}G_F)^{1/2} = 37.28039(1)$ GeV, and Δr includes the radiative corrections relating α, $\alpha(M_Z)$, G_F, M_W, and M_Z. One finds $\Delta r \sim \Delta r_0 - \rho_t/\tan^2\theta_W$, where $\Delta r_0 = 1 - \alpha/\widehat{\alpha}(M_Z) = 0.06635(10)$ is due to the

[$] At the time of writing this review, the efforts to establish a top quark averaging group involving both the Tevatron and the LHC were still in progress. Therefore we perform a simplified average ourselves.

Table 10.2: Notations used to indicate the various schemes discussed in the text. Each definition of $\sin^2\theta_W$ leads to values that differ by small factors depending on m_t and M_H. Approximate values are also given for illustration.

Scheme	Notation	Value
On-shell	s^2_W	0.2231
NOV	$s^2_{M_Z}$	0.2310
$\overline{\rm MS}$	$\widehat{s}^2_Z$	0.2312
$\overline{\rm MS}$ ND	$\widehat{s}^2_{\rm ND}$	0.2314
Effective angle	$\overline{s}^2_f$	0.2315

running of α, and $\rho_t = 3G_F m_t^2/8\sqrt{2}\pi^2 = 0.00943\,(m_t/173.4\ \text{GeV})^2$ represents the dominant (quadratic) m_t dependence. There are additional contributions to Δr from bosonic loops, including those which depend logarithmically on M_H. One has $\Delta r = 0.0358 \mp 0.0004 \pm 0.00010$, where the first uncertainty is from m_t and the second is from $\alpha(M_Z)$. Thus the value of s^2_W extracted from M_Z includes an uncertainty (∓ 0.00012) from the currently allowed range of m_t. This scheme is simple conceptually. However, the relatively large ($\sim 3\%$) correction from ρ_t causes large spurious contributions in higher orders.

(*ii*) A more precisely determined quantity $s^2_{M_Z}$ [64] can be obtained from M_Z by removing the (m_t, M_H) dependent term from Δr [65], *i.e.*,

$$s^2_{M_Z}(1 - s^2_{M_Z}) \equiv \frac{\pi\alpha(M_Z)}{\sqrt{2}\,G_F\,M_Z^2}\ . \tag{10.11}$$

Using $\alpha(M_Z)^{-1} = 128.93 \pm 0.02$ yields $s^2_{M_Z} = 0.23102 \mp 0.00005$. The small uncertainty in $s^2_{M_Z}$ compared to other schemes is because the m_t dependence has been removed by definition. However, the m_t uncertainty reemerges when other quantities (*e.g.*, M_W or other Z pole observables) are predicted in terms of M_Z.

Both s^2_W and $s^2_{M_Z}$ depend not only on the gauge couplings but also on the spontaneous-symmetry breaking, and both definitions are awkward in the presence of any extension of the SM which perturbs the value of M_Z (or M_W). Other definitions are motivated by the tree-level coupling constant definition $\theta_W = \tan^{-1}(g'/g)$:

(*iii*) In particular, the modified minimal subtraction ($\overline{\rm MS}$) scheme introduces the quantity $\sin^2\widehat{\theta}_W(\mu) \equiv \widehat{g}'^2(\mu)/\big[\widehat{g}^{\,2}(\mu) + \widehat{g}'^2(\mu)\big]$, where the couplings $\widehat{g}$ and $\widehat{g}'$ are defined by modified minimal subtraction and the scale μ is conveniently chosen to be M_Z for many EW processes. The value of $\widehat{s}^{\,2}_Z = \sin^2\widehat{\theta}_W(M_Z)$ extracted from M_Z is less sensitive than s^2_W to m_t (by a factor of $\tan^2\theta_W$), and is less sensitive to most types of new physics than s^2_W or $s^2_{M_Z}$. It is also very useful for comparing with the predictions

of grand unification. There are actually several variant definitions of $\sin^2\widehat{\theta}_W(M_Z)$, differing according to whether or how finite $\alpha\ln(m_t/M_Z)$ terms are decoupled (subtracted from the couplings). One cannot entirely decouple the $\alpha\ln(m_t/M_Z)$ terms from all EW quantities because $m_t \gg m_b$ breaks SU(2) symmetry. The scheme that will be adopted here decouples the $\alpha\ln(m_t/M_Z)$ terms from the γ–Z mixing [18,66], essentially eliminating any $\ln(m_t/M_Z)$ dependence in the formulae for asymmetries at the Z pole when written in terms of $\widehat{s}^2_Z$. (A similar definition is used for $\widehat{\alpha}$.) The various definitions are related by

$$\widehat{s}^2_Z = c\,(m_t, M_H) s^2_W = \overline{c}\,(m_t, M_H)\, s^2_{M_Z}\ , \tag{10.12}$$

where $c = 1.0362 \pm 0.0004$ and $\overline{c} = 1.0009 \mp 0.0002$. The quadratic m_t dependence is given by $c \sim 1 + \rho_t/\tan^2\theta_W$ and $\overline{c} \sim 1 - \rho_t/(1-\tan^2\theta_W)$, respectively. The expressions for M_W and M_Z in the $\overline{\rm MS}$ scheme are

$$M_W = \frac{A_0}{\widehat{s}_Z(1-\Delta\widehat{r}_W)^{1/2}}\ , \qquad\qquad M_Z = \frac{M_W}{\widehat{\rho}^{\,1/2}\,\widehat{c}_Z}\ , \tag{10.13}$$

and one predicts $\Delta\widehat{r}_W = 0.06951 \pm 0.00001 \pm 0.00010$. $\Delta\widehat{r}_W$ has no quadratic m_t dependence, because shifts in M_W are absorbed into the observed G_F, so that the error in $\Delta\widehat{r}_W$ is dominated by $\Delta r_0 = 1 - \alpha/\widehat{\alpha}(M_Z)$ which induces the second quoted uncertainty. The quadratic m_t dependence has been shifted into $\widehat{\rho} \sim 1 + \rho_t$, where including bosonic loops, $\widehat{\rho} = 1.01051 \pm 0.00011$. Quadratic M_H effects are deferred to two-loop order, while the leading logarithmic M_H effect is a good approximation only for large M_H values which are clearly disfavored by the precision data. As an illustration, the shift in M_W due to a large M_H (for fixed M_Z) is given by

$$\begin{aligned}\Delta_H M_W &= -\frac{11}{96}\frac{\alpha}{\pi}\frac{M_W}{c^2_W - s^2_W}\ln\frac{M^2_H}{M^2_W} + \mathcal{O}(\alpha^2)\\ &\sim -200\ \text{MeV (for } M_H = 10\ M_W).\end{aligned} \tag{10.14}$$

(*iv*) A variant $\overline{\rm MS}$ quantity $\widehat{s}^2_{\rm ND}$ (used in the 1992 edition of this *Review*) does not decouple the $\alpha\ln(m_t/M_Z)$ terms [67]. It is related to $\widehat{s}^2_Z$ by

$$\widehat{s}^2_Z = \widehat{s}^2_{\rm ND}/\Big(1 + \frac{\widehat{\alpha}}{\pi}d\Big), \tag{10.15a}$$

$$d = \frac{1}{3}\left(\frac{1}{\widehat{s}^2} - \frac{8}{3}\right)\left[(1+\frac{\alpha_s}{\pi})\ln\frac{m_t}{M_Z} - \frac{15\alpha_s}{8\pi}\right], \tag{10.15b}$$

Thus, $\widehat{s}^2_Z - \widehat{s}^2_{\rm ND} \approx -0.0002$.

(*v*) Yet another definition, the effective angle [68–70] $\overline{s}^2_f$ for the Z vector coupling to fermion f, is based on Z pole observables and described below.

Experiments are at such level of precision that complete $\mathcal{O}(\alpha)$ radiative corrections must be applied. For neutral-current and Z pole processes, these corrections are conveniently divided into two classes:

1. QED diagrams involving the emission of real photons or the exchange of virtual photons in loops, but not including vacuum polarization diagrams. These graphs often yield finite and gauge-invariant contributions to observable processes. However, they are dependent on energies, experimental cuts, *etc.*, and must be calculated individually for each experiment.
2. EW corrections, including $\gamma\gamma$, γZ, ZZ, and WW vacuum polarization diagrams, as well as vertex corrections, box graphs, *etc.*, involving virtual W and Z bosons. The one-loop corrections are included for all processes, and certain two-loop corrections are also important. In particular, two-loop corrections involving the top quark modify ρ_t in $\widehat{\rho}$, Δr, and elsewhere by

$$\rho_t \to \rho_t[1 + R(M_H, m_t)\rho_t/3]. \tag{10.16}$$

$R(M_H, m_t)$ is best described as an expansion in M_Z^2/m_t^2. The unsuppressed terms were first obtained in Ref. 71, and are known analytically [72]. Contributions suppressed by M_Z^2/m_t^2 were first studied in Ref. 73 with the help of small and large Higgs mass expansions, which can be interpolated. These contributions are about as large as the leading ones in Refs. 71 and 72. The complete two-loop calculation of Δr (without further approximation) has been performed in Refs. 74 and 75 for fermionic and purely bosonic diagrams, respectively. Similarly, the EW two-loop calculation for the relation between $\overline{s}_\ell^2$ and s_W^2 is complete [76] including the recently obtained purely bosonic contribution [77]. For M_H above its lower direct limit, $-17 < R \leq -13$.

Mixed QCD-EW contributions to gauge boson self-energies of order $\alpha\alpha_s m_t^2$ [78] and $\alpha\alpha_s^2 m_t^2$ [79] increase the predicted value of m_t by 6%. This is, however, almost entirely an artifact of using the pole mass definition for m_t. The equivalent corrections when using the $\overline{\rm MS}$ definition $\widehat{m}_t(\widehat{m}_t)$ increase m_t by less than 0.5%. The subleading $\alpha\alpha_s$ corrections [80] are also included. Further three-loop corrections of order $\alpha\alpha_s^2$ [81], $\alpha^3 m_t^6$ [82,83], and $\alpha^2\alpha_s m_t^4$ (for $M_H = 0$) [82], are rather small. The same is true for $\alpha^3 M_H^4$ [84] corrections unless M_H approaches 1 TeV. Also known are the singlet contributions (pure gluonic intermediate states) of order $\alpha\alpha_s^2$ [85] and $\alpha\alpha_s^3$ [86]. Recently, the corresponding non-singlet contributions have been computed as well [87].

The leading EW two-loop terms for the $Z \to b\bar{b}$-vertex of $\mathcal{O}(\alpha^2 m_t^4)$ have been obtained in Refs. 71 and 72, and the mixed QCD-EW contributions in Refs. 88 and 89. The authors of Ref. 90 completed the two-loop EW fermionic corrections to $\overline{s}_b^2$. The $\mathcal{O}(\alpha\alpha_s)$-vertex corrections involving massless quarks [91] add coherently, resulting in a sizable effect and shift $\alpha_s(M_Z)$ when extracted from Z lineshape observables (see Sec. 10.4) by $\approx +0.0007$.

Many of the EW corrections are absorbed into the renormalized Fermi constant defined in Eq. (10.6). Others modify the tree-level expressions for Z pole observables and neutral-current amplitudes. In particular, the relations in Eq. (10.5) now read,

$$\overline{g}_V^f = \sqrt{\rho_f}\,(t_{3L}^{(f)} - 2q_f\kappa_f \sin^2\theta_W), \qquad \overline{g}_A^f = \sqrt{\rho_f}\,t_{3L}^{(f)}, \tag{10.17}$$

where the EW radiative corrections have been absorbed into corrections $\rho_f - 1$ and $\kappa_f - 1$, which depend on the fermion f and on the renormalization scheme. In the on-shell scheme, the quadratic m_t dependence is given by $\rho_f \sim 1 + \rho_t$, $\kappa_f \sim 1 + \rho_t/\tan^2\theta_W$, while in $\overline{\rm MS}$, $\widehat{\rho}_f \sim \widehat{\kappa}_f \sim 1$, for $f \neq b$ ($\widehat{\rho}_b \sim 1 - \frac{4}{3}\rho_t$, $\widehat{\kappa}_b \sim 1 + \frac{2}{3}\rho_t$). In the $\overline{\rm MS}$ scheme the normalization is changed according to $G_F M_Z^2/2\sqrt{2}\pi \to \widehat{\alpha}/4\widehat{s}^2_Z\widehat{c}^2_Z$. (If one continues to normalize amplitudes by $G_F M_Z^2/2\sqrt{2}\pi$, as in the 1996 edition of this *Review*, then $\widehat{\rho}_f$ contains an additional factor of $\widehat{\rho}(1-\Delta\widehat{r}_W)\widehat{\alpha}/\alpha$.) In practice, additional bosonic and fermionic loops, vertex corrections, leading higher order contributions, *etc.*, must be included. For example, in the $\overline{\rm MS}$ scheme one has $\widehat{\rho}_\ell = 0.9981$, $\widehat{\kappa}_\ell = 1.0013$, $\widehat{\rho}_b = 0.9869$, and $\widehat{\kappa}_b = 1.0067$. It is convenient to define an effective angle $\overline{s}^2_f \equiv \sin^2\overline{\theta}_{Wf} \equiv \widehat{\kappa}_f \widehat{s}^2_Z = \kappa_f s^2_W$, in terms of which $\overline{g}^f_V$ and $\overline{g}^f_A$ are given by $\sqrt{\rho_f}$ times their tree-level formulae. Because $\overline{g}^\ell_V$ is very small, not only $A^0_{LR} = A_e$, $A^{(0,\ell)}_{FB}$, and $\mathcal{P}_\tau$, but also $A^{(0,b)}_{FB}$, $A^{(0,c)}_{FB}$, $A^{(0,s)}_{FB}$, and the hadronic asymmetries are mainly sensitive to $\overline{s}^2_\ell$. One finds that $\widehat{\kappa}_f$ ($f \neq b$) is almost independent of (m_t, M_H), so that one can write

$$\overline{s}^2_\ell \sim \widehat{s}^2_Z + 0.00029\ . \tag{10.18}$$

Thus, the asymmetries determine values of $\overline{s}^2_\ell$ and $\widehat{s}^2_Z$ almost independent of m_t, while the κ's for the other schemes are m_t dependent.

Throughout this *Review* we utilize EW radiative corrections from the program GAPP [21], which works entirely in the $\overline{\rm MS}$ scheme, and which is independent of the package ZFITTER [70]. Another resource is the recently developed modular fitting toolkit Gfitter [92].

10.3. Low energy electroweak observables

In the following we discuss EW precision observables obtained at low momentum transfers [6], *i.e.* $Q^2 \ll M_Z^2$. It is convenient to write the four-fermion interactions relevant to ν-hadron, ν-e, as well as parity violating e-hadron and e-e neutral-current processes in a form that is valid in an arbitrary gauge theory (assuming massless left-handed neutrinos). One has,

$$\begin{aligned} -\mathscr{L}^{\nu h} =& \frac{G_F}{\sqrt{2}}\,\overline{\nu}\,\gamma^\mu(1-\gamma^5)\nu \\ & \times \sum_i [\epsilon_L(i)\overline{q}_i\,\gamma_\mu(1-\gamma^5)q_i + \epsilon_R(i)\overline{q}_i\,\gamma_\mu(1+\gamma^5)q_i], \end{aligned} \tag{10.19}$$

$$-\mathscr{L}^{\nu e} = \frac{G_F}{\sqrt{2}}\,\overline{\nu}_\mu\gamma^\mu(1-\gamma^5)\nu_\mu\,\overline{e}\,\gamma_\mu(g_V^{\nu e} - g_A^{\nu e}\gamma^5)e, \tag{10.20}$$

$$-\mathscr{L}^{eh} = -\frac{G_F}{\sqrt{2}}\sum_i \left[C_{1i}\,\overline{e}\,\gamma_\mu\gamma^5 e\,\overline{q}_i\,\gamma^\mu q_i + C_{2i}\,\overline{e}\,\gamma_\mu e\,\overline{q}_i\,\gamma^\mu\gamma^5 q_i\right], \tag{10.21}$$

$$-\mathscr{L}^{ee} = -\frac{G_F}{\sqrt{2}}\, C_{2e}\, \overline{e}\,\gamma_\mu\gamma^5 e\; \overline{e}\,\gamma^\mu e, \tag{10.22}$$

where one must include the charged-current contribution for ν_e-e and $\overline{\nu}_e$-e and the parity-conserving QED contribution for electron scattering.

Table 10.3: Standard Model expressions for the neutral-current parameters for ν-hadron, ν-e, and e^--scattering processes. At tree level, $\rho = \kappa = 1$, $\lambda = 0$. If radiative corrections are included, $\rho_{\nu N} = 1.0082$, $\widehat{\kappa}_{\nu N}(\langle Q^2\rangle = -20\ \mathrm{GeV}^2) = 0.9972$, $\widehat{\kappa}_{\nu N}(\langle Q^2\rangle = -35\ \mathrm{GeV}^2) = 0.9965$, $\lambda_{uL} = -0.0031$, $\lambda_{dL} = -0.0025$ and $\lambda_R = 3.7\times10^{-5}$. For ν-e scattering, $\rho_{\nu e} = 1.0128$ and $\widehat{\kappa}_{\nu e} = 0.9963$ (at $\langle Q^2\rangle = 0.$). For atomic parity violation and the polarized DIS experiment at SLAC, $\rho'_e = 0.9887$, $\rho_e = 1.0007$, $\widehat{\kappa}'_e = 1.0038$, $\widehat{\kappa}_e = 1.0297$, $\lambda' = -1.8\times10^{-5}$, $\lambda_u = -0.0118$ and $\lambda_d = 0.0029$. And for polarized Møller scattering with SLAC (JLab) kinematics, $\lambda_e = -0.0002$ ($\lambda_e = -0.0004$). The dominant m_t dependence is given by $\rho \sim 1 + \rho_t$, while $\widehat{\kappa} \sim 1$ ($\overline{\rm MS}$) or $\kappa \sim 1 + \rho_t/\tan^2\theta_W$ (on-shell).

Quantity	Standard Model Expression
$\epsilon_L(u)$	$\rho_{\nu N}\left(\frac{1}{2} - \frac{2}{3}\,\widehat{\kappa}_{\nu N}\,\widehat{s}^2_Z\right) + \lambda_{uL}$
$\epsilon_L(d)$	$\rho_{\nu N}\left(-\frac{1}{2} + \frac{1}{3}\,\widehat{\kappa}_{\nu N}\,\widehat{s}^2_Z\right) + \lambda_{dL}$
$\epsilon_R(u)$	$\rho_{\nu N}\left(-\frac{2}{3}\,\widehat{\kappa}_{\nu N}\,\widehat{s}^2_Z\right) + \lambda_R$
$\epsilon_R(d)$	$\rho_{\nu N}\left(\frac{1}{3}\,\widehat{\kappa}_{\nu N}\,\widehat{s}^2_Z\right) + 2\,\lambda_R$
$g_V^{\nu e}$	$\rho_{\nu e}\left(-\frac{1}{2} + 2\,\widehat{\kappa}_{\nu e}\,\widehat{s}^2_Z\right)$
$g_A^{\nu e}$	$\rho_{\nu e}\left(-\frac{1}{2}\right)$
C_{1u}	$\rho'_e\left(-\frac{1}{2} + \frac{4}{3}\,\widehat{\kappa}'_e\,\widehat{s}^2_Z\right) + \lambda'$
C_{1d}	$\rho'_e\left(\frac{1}{2} - \frac{2}{3}\,\widehat{\kappa}'_e\,\widehat{s}^2_Z\right) - 2\,\lambda'$
C_{2u}	$\rho_e\left(-\frac{1}{2} + 2\,\widehat{\kappa}_e\,\widehat{s}^2_Z\right) + \lambda_u$
C_{2d}	$\rho_e\left(\frac{1}{2} - 2\,\widehat{\kappa}_e\,\widehat{s}^2_Z\right) + \lambda_d$
C_{2e}	$\rho_e\left(\frac{1}{2} - 2\,\widehat{\kappa}_e\,\widehat{s}^2_Z\right) + \lambda_e$

The SM expressions for $\epsilon_{L,R}(i)$, $g_{V,A}^{\nu e}$, and C_{ij} are given in Table 10.3. Note, that $g_{V,A}^{\nu e}$ and the other quantities are coefficients of effective four-Fermi operators, which differ

from the quantities defined in Eq. (10.5) in the radiative corrections and in the presence of possible physics beyond the SM.

10.3.1. ***Neutrino scattering*** : For a general review on ν-scattering we refer to Ref. 93 (nonstandard neutrino scattering interactions are surveyed in Ref. 94).

The cross-section in the laboratory system for $\nu_\mu e \to \nu_\mu e$ or $\overline{\nu}_\mu e \to \overline{\nu}_\mu e$ elastic scattering [95] is

$$\frac{d\sigma_{\nu,\bar{\nu}}}{dy} = \frac{G_F^2 m_e E_\nu}{2\pi}\left[(g_V^{\nu e} \pm g_A^{\nu e})^2 + (g_V^{\nu e} \mp g_A^{\nu e})^2(1-y)^2 - (g_V^{\nu e 2} - g_A^{\nu e 2})\frac{y\, m_e}{E_\nu}\right], \quad (10.23)$$

where the upper (lower) sign refers to $\nu_\mu(\overline{\nu}_\mu)$, and $y \equiv T_e/E_\nu$ (which runs from 0 to $(1 + m_e/2E_\nu)^{-1}$) is the ratio of the kinetic energy of the recoil electron to the incident ν or $\overline{\nu}$ energy. For $E_\nu \gg m_e$ this yields a total cross-section

$$\sigma = \frac{G_F^2 m_e E_\nu}{2\pi}\left[(g_V^{\nu e} \pm g_A^{\nu e})^2 + \frac{1}{3}(g_V^{\nu e} \mp g_A^{\nu e})^2\right]. \quad (10.24)$$

The most accurate measurements [95–100] of $\sin^2\theta_W$ from ν-lepton scattering (see Sec. 10.6) are from the ratio $R \equiv \sigma_{\nu_\mu e}/\sigma_{\bar{\nu}_\mu e}$ in which many of the systematic uncertainties cancel. Radiative corrections (other than m_t effects) are small compared to the precision of present experiments and have negligible effect on the extracted $\sin^2\theta_W$. The most precise experiment (CHARM II) [98] determined not only $\sin^2\theta_W$ but $g_{V,A}^{\nu e}$ as well, which are shown in Fig. 10.1. The cross-sections for ν_e-e and $\overline{\nu}_e$-e may be obtained from Eq. (10.23) by replacing $g_{V,A}^{\nu e}$ by $g_{V,A}^{\nu e} + 1$, where the 1 is due to the charged-current contribution.

A precise determination of the on-shell s_W^2, which depends only very weakly on m_t and M_H, is obtained from deep inelastic scattering (DIS) of neutrinos from (approximately) isoscalar targets [101]. The ratio $R_\nu \equiv \sigma_{\nu N}^{NC}/\sigma_{\nu N}^{CC}$ of neutral-to-charged-current cross-sections has been measured to 1% accuracy by CDHS [102] and CHARM [103] at CERN. CCFR [104] at Fermilab has obtained an even more precise result, so it is important to obtain theoretical expressions for R_ν and $R_{\bar{\nu}} \equiv \sigma_{\bar{\nu}N}^{NC}/\sigma_{\bar{\nu}N}^{CC}$ to comparable accuracy. Fortunately, many of the uncertainties from the strong interactions and neutrino spectra cancel in the ratio. A large theoretical uncertainty is associated with the c-threshold, which mainly affects σ^{CC}. Using the slow rescaling prescription [105] the central value of $\sin^2\theta_W$ from CCFR varies as $0.0111(m_c\ [\mathrm{GeV}] - 1.31)$, where m_c is the effective mass which is numerically close to the $\overline{\rm MS}$ mass $\widehat{m}_c(\widehat{m}_c)$, but their exact relation is unknown at higher orders. For $m_c = 1.31 \pm 0.24$ GeV (determined from ν-induced dimuon production [106]) this contributes ± 0.003 to the total uncertainty $\Delta \sin^2\theta_W \sim \pm 0.004$. (The experimental uncertainty is also ± 0.003.) This uncertainty largely cancels, however, in the Paschos-Wolfenstein ratio [107],

$$R^- = \frac{\sigma_{\nu N}^{NC} - \sigma_{\bar{\nu}N}^{NC}}{\sigma_{\nu N}^{CC} - \sigma_{\bar{\nu}N}^{CC}}\ . \quad (10.25)$$

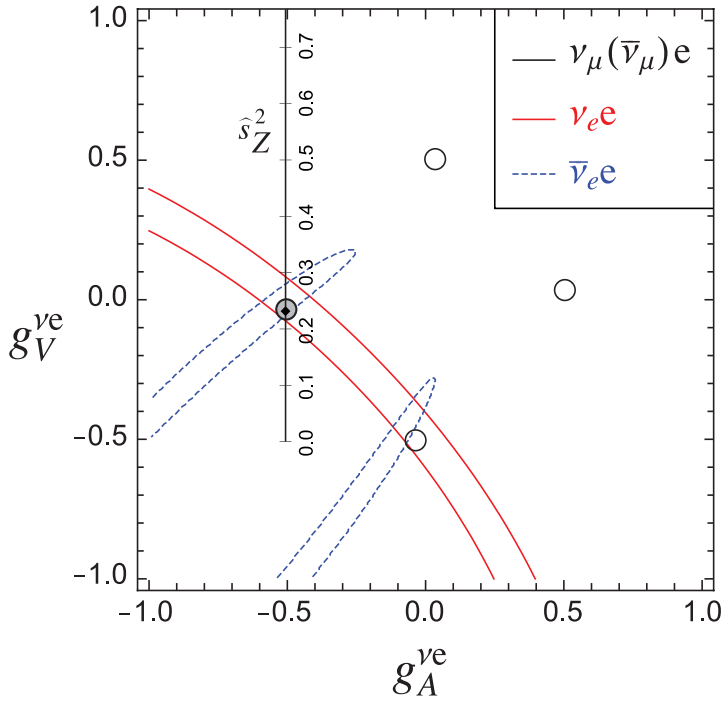

Figure 10.1: Allowed contours in $g_A^{\nu e}$ *vs.* $g_V^{\nu e}$ from neutrino-electron scattering and the SM prediction as a function of the weak mixing angle $\widehat{s}^2_Z$. (The SM best fit value $\widehat{s}^2_Z = 0.23116$ is also indicated.) The $\nu_e e$ [99] and $\bar{\nu}_e e$ [100] constraints are at 1 σ, while each of the four equivalent $\nu_\mu(\bar{\nu}_\mu)e$ [95–98] solutions ($g_{V,A} \to -g_{V,A}$ and $g_{V,A} \to g_{A,V}$) are at 90% C.L. The global best fit region (shaded) almost exactly coincides with the corresponding $\nu_\mu(\bar{\nu}_\mu)e$ region. The solution near $g_A = 0, g_V = -0.5$ is eliminated by $e^+e^- \to \ell^+\ell^-$ data under the weak additional assumption that the neutral current is dominated by the exchange of a single Z boson.

It was measured by Fermilab's NuTeV collaboration [108] for the first time, and required a high-intensity and high-energy anti-neutrino beam.

A simple zeroth-order approximation is

$$R_\nu = g_L^2 + g_R^2 r, \quad R_{\bar{\nu}} = g_L^2 + \frac{g_R^2}{r}, \quad R^- = g_L^2 - g_R^2, \tag{10.26}$$

where

$$g_L^2 \equiv \epsilon_L(u)^2 + \epsilon_L(d)^2 \approx \frac{1}{2} - \sin^2\theta_W + \frac{5}{9}\sin^4\theta_W, \tag{10.27a}$$

$$g_R^2 \equiv \epsilon_R(u)^2 + \epsilon_R(d)^2 \approx \frac{5}{9}\sin^4\theta_W, \tag{10.27b}$$

and $r \equiv \sigma^{CC}_{\bar{\nu}N}/\sigma^{CC}_{\nu N}$ is the ratio of $\overline{\nu}$ to ν charged-current cross-sections, which can be measured directly. (In the simple parton model, ignoring hadron energy cuts,

$r \approx (\frac{1}{3} + \epsilon)/(1 + \frac{1}{3}\epsilon)$, where $\epsilon \sim 0.125$ is the ratio of the fraction of the nucleon's momentum carried by anti-quarks to that carried by quarks.) In practice, Eq. (10.26) must be corrected for quark mixing, quark sea effects, c-quark threshold effects, non-isoscalarity, W–Z propagator differences, the finite muon mass, QED and EW radiative corrections. Details of the neutrino spectra, experimental cuts, x and Q^2 dependence of structure functions, and longitudinal structure functions enter only at the level of these corrections and therefore lead to very small uncertainties. CCFR quotes $s^2_W = 0.2236 \pm 0.0041$ for $(m_t, M_H) = (175, 150)$ GeV with very little sensitivity to (m_t, M_H).

The NuTeV collaboration found $s^2_W = 0.2277 \pm 0.0016$ (for the same reference values), which was 3.0 σ higher than the SM prediction [108]. The deviation was in g^2_L (initially 2.7 σ low) while g^2_R was consistent with the SM. Since then a number of experimental and theoretical developments changed the interpretation of the measured cross section ratios, affecting the extracted $g^2_{L,R}$ (and thus s^2_W) including their uncertainties and correlation. In the following paragraph we give a semi-quantitative and preliminary discussion of these effects, but we stress that the precise impact of them needs to be evaluated carefully by the collaboration with a new and self-consistent set of PDFs, including new radiative corrections, while simultaneously allowing isospin breaking and asymmetric strange seas. This is an effort which is currently on its way and until it is completed we do not include the NuTeV constraints on $g^2_{L,R}$ in our default set of fits.

(i) In the original analysis NuTeV worked with a symmetric strange quark sea but subsequently measured [109] the difference between the strange and antistrange momentum distributions, $S^- \equiv \int_0^1 \mathrm{d}x x[s(x) - \bar{s}(x)] = 0.00196 \pm 0.00143$, from dimuon events utilizing the first complete next-to-leading order QCD description [110] and parton distribution functions (PDFs) according to Ref. 111. The global PDF fits in Ref. 112 give somewhat smaller values, $S^- = 0.0013(9)$ [$S^- = 0.0010(13)$], where the semi-leptonic charmed-hadron branching ratio, $B_\mu = 8.8 \pm 0.5\%$, has [not] been used as an external constraint. The resulting S^- also depends on the PDF model used and on whether theoretical arguments (see Ref. 113 and references therein) are invoked favoring a zero crossing of $x[s(x) - \bar{s}(x)]$ at values much larger than seen by NuTeV and suggesting an effect of much smaller and perhaps negligible size. (ii) The measured branching ratio for K_{e3} decays enters crucially in the determination of the $\nu_e(\bar{\nu}_e)$ contamination of the $\nu_\mu(\bar{\nu}_\mu)$ beam. This branching ratio has moved from $4.82 \pm 0.06\%$ at the time of the original publication [108] to the current value of $5.07 \pm 0.04\%$, *i.e.,* a change by more than $4\,\sigma$. This moves s^2_W about one standard deviation further away from the SM prediction while reducing the $\nu_e(\bar{\nu}_e)$ uncertainty. (iii) PDFs seem to violate isospin symmetry at levels much stronger than generally expected [114]. A minimum χ^2 set of PDFs [115] allowing charge symmetry violation for both valence quarks [$d^p_V(x) \neq u^n_V(x)$] and sea quarks [$\bar{d}^p(x) \neq \bar{u}^n(x)$] shows a reduction in the NuTeV discrepancy by about $1\,\sigma$. But isospin symmetry violating PDFs are currently not well constrained phenomenologically and within uncertainties the NuTeV anomaly could be accounted for in full or conversely made larger [115]. Still, the leading contribution from quark mass differences turns out to be largely model-independent [116] (at least in sign) and

a shift, $\delta s^2_W = -0.0015 \pm 0.0003$ [113], has been estimated. (iv) QED splitting effects also violate isospin symmetry with an effect on s^2_W whose sign (reducing the discrepancy) is model-independent. The corresponding shift of $\delta s^2_W = -0.0011$ has been calculated in Ref. 117 but has a large uncertainty. (v) Nuclear shadowing effects [118] are likely to affect the interpretation of the NuTeV result at some level, but the NuTeV collaboration argues that their data are dominated by values of Q^2 at which nuclear shadowing is expected to be relatively small. However, another nuclear effect, the isovector EMC effect [119], is much larger (because it affects all neutrons in the nucleus, not just the excess ones) and model-independently works to reduce the discrepancy. It is estimated to lead to a shift of $\delta s^2_W = -0.0019 \pm 0.0006$ [113]. It would be important to verify and quantify this kind of effect experimentally, *e.g.*, in polarized electron scattering. (vi) The extracted s^2_W may also shift at the level of the quoted uncertainty when analyzed using the most recent QED and EW radiative corrections [120,121], as well as QCD corrections to the structure functions [122]. However, these are scheme-dependent and in order to judge whether they are significant they need to be adapted to the experimental conditions and kinematics of NuTeV, and have to be obtained in terms of observable variables and for the differential cross-sections. In addition, there is the danger of double counting some of the QED splitting effects. (vii) New physics could also affect $g^2_{L,R}$ [123] but it is difficult to convincingly explain the entire effect that way.

10.3.2. *Parity violation* :

The SLAC polarized electron-deuteron DIS experiment [124] measured the right-left asymmetry,

$$A = \frac{\sigma_R - \sigma_L}{\sigma_R + \sigma_L} \ , \tag{10.28}$$

where $\sigma_{R,L}$ is the cross-section for the deep-inelastic scattering of a right- or left-handed electron: $e_{R,L}N \to e\mathrm{X}$. In the quark parton model,

$$\frac{A}{Q^2} = a_1 + a_2 \frac{1-(1-y)^2}{1+(1-y)^2} \ , \tag{10.29}$$

where $Q^2 > 0$ is the momentum transfer and y is the fractional energy transfer from the electron to the hadrons. For the deuteron or other isoscalar targets, one has, neglecting the s-quark and anti-quarks,

$$a_1 = \frac{3G_F}{5\sqrt{2}\pi\alpha}\left(C_{1u} - \frac{1}{2}C_{1d}\right) \approx \frac{3G_F}{5\sqrt{2}\pi\alpha}\left(-\frac{3}{4} + \frac{5}{3}\sin^2\theta_W\right), \tag{10.30a}$$

$$a_2 = \frac{3G_F}{5\sqrt{2}\pi\alpha}\left(C_{2u} - \frac{1}{2}C_{2d}\right) \approx \frac{9G_F}{5\sqrt{2}\pi\alpha}\left(\sin^2\theta_W - \frac{1}{4}\right). \tag{10.30b}$$

In another polarized-electron scattering experiment on deuterons, but in the quasi-elastic kinematic regime, the SAMPLE experiment [125] at MIT-Bates extracted the combination $C_{2u} - C_{2d}$ at Q^2 values of 0.1 GeV^2 and 0.038 GeV^2. What was actually determined

were nucleon form factors from which the quoted results were obtained by the removal of a multi-quark radiative correction [126]. Other linear combinations of the C_{iq} have been determined in polarized-lepton scattering at CERN in μ-C DIS, at Mainz in e-Be (quasi-elastic), and at Bates in e-C (elastic). See the review articles in Refs. 127 and 128 for more details. Recent polarized electron asymmetry experiments, *i.e.*, SAMPLE, the PVA4 experiment at Mainz, and the HAPPEX and G0 experiments at Jefferson Lab, have focussed on the strange quark content of the nucleon. These are reviewed in Ref. 129, where it is shown that they can also provide significant constraints on C_{1u} and C_{1d} which complement those from atomic parity violation (see Fig. 10.2).

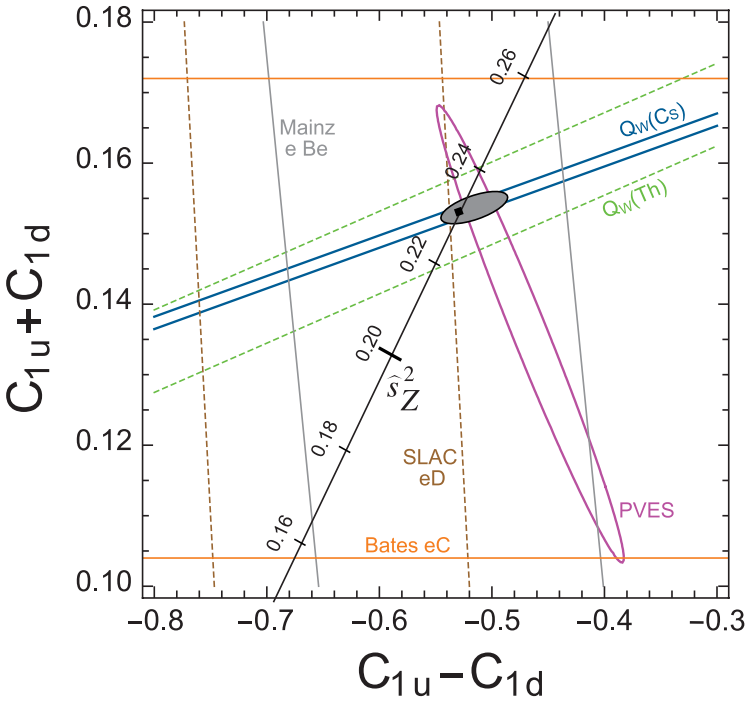

Figure 10.2: Constraints on the effective couplings, C_{1u} and C_{1d}, from recent (PVES) and older polarized parity violating electron scattering, and from atomic parity violation (APV) at 1 σ, as well as the 90% C.L. global best fit (shaded) and the SM prediction as a function of the weak mixing angle $\widehat{s}^2_Z$. (The SM best fit value $\widehat{s}^2_Z = 0.23116$ is also indicated.)

The parity violating asymmetry, A_{PV}, in fixed target polarized Møller scattering, $e^-e^- \to e^-e^-$, is defined as in Eq. (10.28) and reads [130],

$$\frac{A_{PV}}{Q^2} = -2\,C_{2e}\frac{G_F}{\sqrt{2}\pi\alpha}\frac{1-y}{1+y^4+(1-y)^4}\ , \tag{10.31}$$

where y is again the energy transfer. It has been measured at low $Q^2 = 0.026$ GeV^2 in the SLAC E158 experiment [131], with the result $A_{PV} = (-1.31 \pm 0.14_{\rm stat.} \pm 0.10_{\rm syst.}) \times 10^{-7}$. Expressed in terms of the weak mixing angle in the $\overline{\rm MS}$ scheme, this yields $\widehat{s}^2(Q^2) =$

0.2403 ± 0.0013, and established the scale dependence of the weak mixing angle (see Fig. 10.3) at the level of 6.4 standard deviations. One can also define the so-called weak charge of the electron (*cf.* Eq. (10.32) below) as $Q_W(e) \equiv -2\,C_{2e} = -0.0403 \pm 0.0053$ (the implications are discussed in Ref. 133).

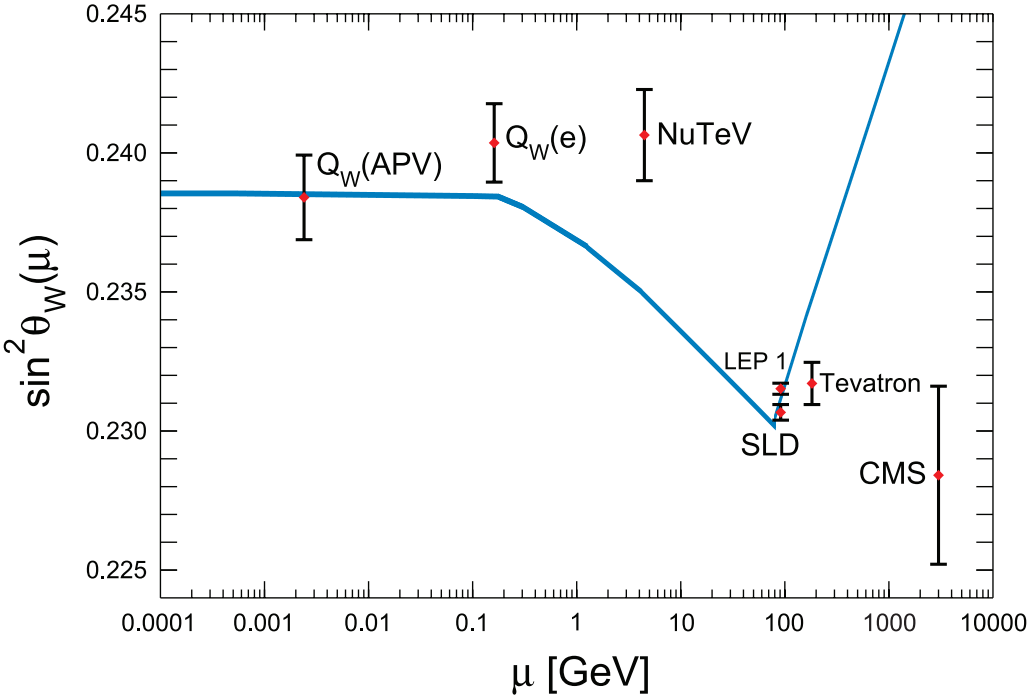

Figure 10.3: Scale dependence of the weak mixing angle defined in the $\overline{\rm MS}$ scheme [132] (for the scale dependence of the weak mixing angle defined in a mass-dependent renormalization scheme, see Ref. 133). The minimum of the curve corresponds to $Q = M_W$, below which we switch to an effective theory with the $W^\pm$ bosons integrated out, and where the β-function for the weak mixing angle changes sign. At the location of the W boson mass and each fermion mass there are also discontinuities arising from scheme dependent matching terms which are necessary to ensure that the various effective field theories within a given loop order describe the same physics. However, in the $\overline{\rm MS}$ scheme these are very small numerically and barely visible in the figure provided one decouples quarks at $Q = \widehat{m}_q(\widehat{m}_q)$. The width of the curve reflects the theory uncertainty from strong interaction effects which at low energies is at the level of $\pm 7 \times 10^{-5}$ [132]. Following the estimate [135] of the typical momentum transfer for parity violation experiments in Cs, the location of the APV data point is given by $\mu = 2.4$ MeV. For NuTeV we display the updated value from Ref. 134 and chose $\mu = \sqrt{20}$ GeV which is about half-way between the averages of $\sqrt{Q^2}$ for ν and $\overline{\nu}$ interactions at NuTeV. The Tevatron measurements are strongly dominated by invariant masses of the final state dilepton pair of $\mathcal{O}(M_Z)$ and can thus be considered as additional Z pole data points. However, for clarity we displayed the point horizontally to the right. Similar remarks apply to the first measurement at the LHC by the CMS collaboration.

In a similar experiment and at about the same Q^2, Qweak at Jefferson Lab [136] will be able to measure the weak charge of the proton, $Q_W(p) = -2\,[2\,C_{1u} + C_{1d}]$, and $\sin^2\theta_W$ in polarized ep scattering with relative precisions of 4% and 0.3%, respectively.

There are precise experiments measuring atomic parity violation (APV) [137] in cesium [138,139] (at the 0.4% level [138]), thallium [140], lead [141], and bismuth [142]. The EW physics is contained in the weak charges which are defined by,

$$Q_W(Z,N) \equiv -2\,[C_{1u}\,(2Z+N) + C_{1d}(Z+2N)] \approx Z(1-4\sin^2\theta_W) - N. \qquad (10.32)$$

E.g., $Q_W(^{133}\mathrm{Cs})$ is extracted by measuring experimentally the ratio of the parity violating amplitude, E_{PNC}, to the Stark vector transition polarizability, β, and by calculating theoretically E_{PNC} in terms of Q_W. One can then write,

$$Q_W = N \left(\frac{\mathrm{Im}\,E_{\mathrm{PNC}}}{\beta}\right)_{\mathrm{exp.}} \left(\frac{|e|\,a_B}{\mathrm{Im}\,E_{\mathrm{PNC}}}\frac{Q_W}{N}\right)_{\mathrm{th.}} \left(\frac{\beta}{a_B^3}\right)_{\mathrm{exp.+th.}} \left(\frac{a_B^2}{|e|}\right).$$

The uncertainties associated with atomic wave functions are quite small for cesium [143]. The semi-empirical value of β used in early analyses added another source of theoretical uncertainty [144]. However, the ratio of the off-diagonal hyperfine amplitude to the polarizability was subsequently measured directly by the Boulder group [145]. Combined with the precisely known hyperfine amplitude [146] one finds, $\beta = 26.991 \pm 0.046$, in excellent agreement with the earlier results, reducing the overall theory uncertainty (while slightly increasing the experimental error). The recent state-of-the-art many body calculation [147] yields, $\mathrm{Im}\,E_{\mathrm{PNC}} = (0.8906 \pm 0.0026) \times 10^{-11}|e|\,a_B\,Q_W/N$, while the two measurements [138,139] combine to give $\mathrm{Im}\,E_{\mathrm{PNC}}/\beta = -1.5924 \pm 0.0055$ mV/cm, and we obtain $Q_W(^{133}_{78}\mathrm{Cs}) = -73.20 \pm 0.35$. Thus, the various theoretical efforts in Refs. 147 and 148 together with an update of the SM calculation [149] including a very recent dispersion analysis of the γZ-box contribution [150] removed an earlier 2.3 σ deviation from the SM (see the year 2000 edition of this *Review*). The theoretical uncertainties are 3% for thallium [151] but larger for the other atoms. The Boulder experiment in cesium also observed the parity-violating weak corrections to the nuclear electromagnetic vertex (the anapole moment [152]) .

In the future it could be possible to further reduce the theoretical wave function uncertainties by taking the ratios of parity violation in different isotopes [137,153]. There would still be some residual uncertainties from differences in the neutron charge radii, however [154]. Experiments in hydrogen and deuterium are another possibility for reducing the atomic theory uncertainties [155], while measurements of single trapped radium ions are promising [156] because of the much larger parity violating effect.

10.4. *W* and *Z* boson physics

10.4.1. e^+e^- *scattering below the Z pole* :

The forward-backward asymmetry for $e^+e^- \to \ell^+\ell^-$, $\ell = \mu$ or τ, is defined as

$$A_{FB} \equiv \frac{\sigma_F - \sigma_B}{\sigma_F + \sigma_B} \ , \tag{10.33}$$

where $\sigma_F\,(\sigma_B)$ is the cross-section for ℓ^- to travel forward (backward) with respect to the e^- direction. A_{FB} and R, the total cross-section relative to pure QED, are given by

$$R = F_1 \ , \qquad\qquad A_{FB} = \frac{3}{4}\frac{F_2}{F_1} \ , \tag{10.34}$$

where

$$F_1 = 1 - 2\chi_0\, g_V^e\, g_V^\ell\, \cos\delta_R + \chi_0^2 \left(g_V^{e2} + g_A^{e2}\right)\left(g_V^{\ell 2} + g_A^{\ell 2}\right), \tag{10.35a}$$

$$F_2 = -2\chi_0\, g_A^e\, g_A^\ell\, \cos\delta_R + 4\chi_0^2\, g_A^e\, g_A^\ell\, g_V^e\, g_V^\ell \ , \tag{10.35b}$$

$$\tan\delta_R = \frac{M_Z\Gamma_Z}{M_Z^2 - s} \ , \quad \chi_0 = \frac{G_F}{2\sqrt{2}\pi\alpha}\frac{sM_Z^2}{\left[(M_Z^2 - s)^2 + M_Z^2\Gamma_Z^2\right]^{1/2}} \ , \tag{10.36}$$

and where $\sqrt{s}$ is the CM energy. Eqs. (10.35) are valid at tree level. If the data are radiatively corrected for QED effects (as described in Sec. 10.2), then the remaining EW corrections can be incorporated [157,158] (in an approximation adequate for existing PEP, PETRA, and TRISTAN data, which are well below the Z pole) by replacing χ_0 by $\chi(s) \equiv (1 + \rho_t)\,\chi_0(s)\,\alpha/\alpha(s)$, where $\alpha(s)$ is the running QED coupling, and evaluating g_V in the $\overline{\rm MS}$ scheme. Reviews and formulae for $e^+e^- \to$ hadrons may be found in Ref. 159.

10.4.2. *Z pole physics* :

At LEP 1 and the SLC, there were high-precision measurements of various Z pole observables [11,160–166], as summarized in Table 10.5. These include the Z mass and total width, Γ_Z, and partial widths $\Gamma(f\overline{f})$ for $Z \to f\overline{f}$ where fermion $f = e$, μ, τ, hadrons, b, or c. It is convenient to use the variables M_Z, Γ_Z, $R_\ell \equiv \Gamma({\rm had})/\Gamma(\ell^+\ell^-)$ $(\ell = e, \mu, \tau)$, $\sigma_{\rm had} \equiv 12\pi\,\Gamma(e^+e^-)\,\Gamma({\rm had})/M_Z^2\,\Gamma_Z^2$, $R_b \equiv \Gamma(b\overline{b})/\Gamma({\rm had})$, and $R_c \equiv \Gamma(c\overline{c})/\Gamma({\rm had})$, most of which are weakly correlated experimentally. ($\Gamma({\rm had})$ is the partial width into hadrons.) The three values for R_ℓ are not inconsistent with lepton universality (although R_τ is somewhat low compared to R_e and R_μ), but we use the general analysis in which the three observables are treated as independent. Similar remarks apply to $A_{FB}^{0,\ell}$ defined in Eq. (10.39) ($A_{FB}^{0,\tau}$ is somewhat high). $\mathcal{O}(\alpha^3)$ QED corrections introduce a large anti-correlation (-30%) between Γ_Z and $\sigma_{\rm had}$. The anti-correlation between R_b and R_c is -18% [11]. The R_ℓ are insensitive to m_t except for the $Z \to b\overline{b}$ vertex and final state corrections and the implicit dependence through $\sin^2\theta_W$. Thus, they are especially useful for constraining α_s. The width for invisible decays [11],

$\Gamma(\text{inv}) = \Gamma_Z - 3\,\Gamma(\ell^+\ell^-) - \Gamma(\text{had}) = 499.0 \pm 1.5$ MeV, can be used to determine the number of neutrino flavors much lighter than $M_Z/2$, $N_\nu = \Gamma(\text{inv})/\Gamma^{\text{theory}}(\nu\overline{\nu}) = 2.984 \pm 0.009$ for $(m_t, M_H) = (173.4, 117)$ GeV.

There were also measurements of various Z pole asymmetries. These include the polarization or left-right asymmetry

$$A_{LR} \equiv \frac{\sigma_L - \sigma_R}{\sigma_L + \sigma_R} \ , \tag{10.37}$$

where $\sigma_L(\sigma_R)$ is the cross-section for a left-(right-)handed incident electron. A_{LR} was measured precisely by the SLD collaboration at the SLC [162], and has the advantages of being extremely sensitive to $\sin^2\theta_W$ and that systematic uncertainties largely cancel. In addition, SLD extracted the final-state couplings (defined below), A_b, A_c [11], A_s [163], A_τ, and A_μ [164], from left-right forward-backward asymmetries, using

$$A_{LR}^{FB}(f) = \frac{\sigma_{LF}^f - \sigma_{LB}^f - \sigma_{RF}^f + \sigma_{RB}^f}{\sigma_{LF}^f + \sigma_{LB}^f + \sigma_{RF}^f + \sigma_{RB}^f} = \frac{3}{4} A_f \ , \tag{10.38}$$

where, for example, σ_{LF}^f is the cross-section for a left-handed incident electron to produce a fermion f traveling in the forward hemisphere. Similarly, A_τ was measured at LEP 1 [11] through the negative total τ polarization, $\mathcal{P}_\tau$, and A_e was extracted from the angular distribution of $\mathcal{P}_\tau$. An equation such as (10.38) assumes that initial state QED corrections, photon exchange, γ–Z interference, the tiny EW boxes, and corrections for $\sqrt{s} \neq M_Z$ are removed from the data, leaving the pure EW asymmetries. This allows the use of effective tree-level expressions,

$$A_{LR} = A_e P_e \ , \qquad\qquad A_{FB} = \frac{3}{4} A_f \, \frac{A_e + P_e}{1 + P_e A_e} \ , \tag{10.39}$$

where

$$A_f \equiv \frac{2\overline{g}_V^f \, \overline{g}_A^f}{\overline{g}_V^{f\,2} + \overline{g}_A^{f\,2}} \ . \tag{10.40}$$

P_e is the initial e^- polarization, so that the second equality in Eq. (10.38) is reproduced for $P_e = 1$, and the Z pole forward-backward asymmetries at LEP 1 ($P_e = 0$) are given by $A_{FB}^{(0,f)} = \frac{3}{4} A_e A_f$ where $f = e,\ \mu,\ \tau,\ b,\ c,\ s$ [165], and q, and where $A_{FB}^{(0,q)}$ refers to the hadronic charge asymmetry. Corrections for t-channel exchange and s/t-channel interference cause $A_{FB}^{(0,e)}$ to be strongly anti-correlated with R_e (-37%). The correlation between $A_{FB}^{(0,b)}$ and $A_{FB}^{(0,c)}$ amounts to 15%. The initial state coupling, A_e, was also determined through the left-right charge asymmetry [166] and in polarized Bhabba scattering [164] at the SLC.

As an example of the precision of the Z-pole observables, the values of $\bar{g}_A^f$ and $\bar{g}_V^f$, $f = e, \mu, \tau, \ell$, extracted from the LEP and SLC lineshape and asymmetry data is shown in

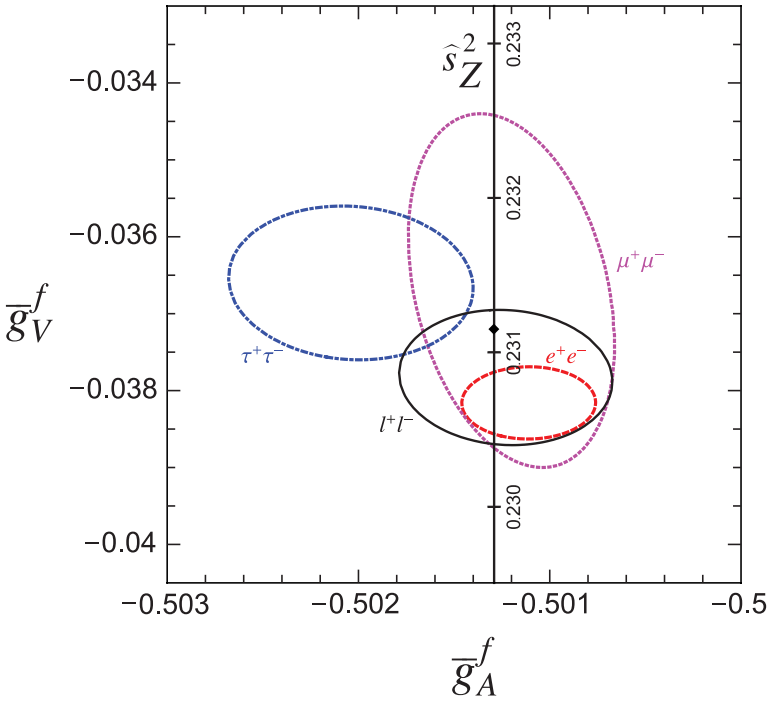

Figure 10.4: 1 σ (39.35% C.L.) contours for the Z-pole observables $\bar{g}^f_A$ and $\bar{g}^f_V$, $f = e, \mu, \tau$ obtained at LEP and SLC [11], compared to the SM expectation as a function of $\widehat{s}^2_Z$. (The SM best fit value $\widehat{s}^2_Z = 0.23116$ is also indicated.) Also shown is the 90% CL allowed region in $\bar{g}^\ell_{A,V}$ obtained assuming lepton universality.

Fig. 10.4, which should be compared with Fig. 10.1. (The two sets of parameters coincide in the SM at tree-level.)

As for hadron colliders, the forward-backward asymmetry, A_{FB}, for e^+e^- final states (with invariant masses restricted to or dominated by values around M_Z) in $p\bar{p}$ collisions has been measured by the DØ [167] and CDF [168] collaborations and values for $\overline{s}^2_\ell$ were extracted, which combine to $\overline{s}^2_\ell = 0.23200 \pm 0.00076$ (assuming common PDF uncertainties). By varying the invariant mass and the scattering angle (and assuming the electron couplings), information on the effective Z couplings to light quarks, $\overline{g}^{u,d}_{V,A}$, could also be obtained [167,169], but with large uncertainties and mutual correlations and not independently of $\overline{s}^2_\ell$ above. Similar analyses have also been reported by the H1 and ZEUS collaborations at HERA [170] and by the LEP collaborations [11]. This kind of measurement is harder in the pp environment due to the difficulty to assign the initial quark and antiquark in the underlying Drell-Yan process to the protons. Nevertheless, the CMS collaboration [171] already reported a first measurement, $\bar{s}^2_Z = 0.2287 \pm 0.0032$.

10.4.3. *LEP 2* :

LEP 2 [172] ran at several energies above the Z pole up to ~ 209 GeV. Measurements were made of a number of observables, including the cross-sections for $e^+e^- \to f\bar{f}$ for $f = q, \mu^-, \tau^-$; the differential cross-sections for $f = e^-, \mu^-, \tau^-$; R_q for $q = b, c$; $A_{FB}(f)$ for $f = \mu, \tau, b, c$; W branching ratios; and WW, $WW\gamma$, ZZ, single W, and single Z cross-sections. They are in good agreement with the SM predictions, with the exceptions of the total hadronic cross-section (1.7 σ high), R_b (2.1 σ low), and $A_{FB}(b)$ (1.6 σ low). Also, the negative result of the direct search for the SM Higgs boson excluded M_H values below 114.4 GeV at the 95% CL [173]. This result is complementary to and can be combined with [174] the limits inferred from the EW precision data.

The Z boson properties are extracted assuming the SM expressions for the γ–Z interference terms. These have also been tested experimentally by performing more general fits [172,175] to the LEP 1 and LEP 2 data. Assuming family universality this approach introduces three additional parameters relative to the standard fit [11], describing the γ–Z interference contribution to the total hadronic and leptonic cross-sections, $j^{\rm tot}_{\rm had}$ and $j^{\rm tot}_{\ell}$, and to the leptonic forward-backward asymmetry, $j^{\rm fb}_{\ell}$. *E.g.*,

$$j^{\rm tot}_{\rm had} \sim g^{\ell}_V g^{\rm had}_V = 0.277 \pm 0.065, \tag{10.41}$$

which is in agreement with the SM expectation [11] of 0.21 ± 0.01. These are valuable tests of the SM; but it should be cautioned that new physics is not expected to be described by this set of parameters, since (i) they do not account for extra interactions beyond the standard weak neutral-current, and (ii) the photonic amplitude remains fixed to its SM value.

Strong constraints on anomalous triple and quartic gauge couplings have been obtained at LEP 2 and the Tevatron as described in the Gauge & Higgs Bosons Particle Listings.

10.4.4. *W and Z decays* :

The partial decay width for gauge bosons to decay into massless fermions $f_1\overline{f}_2$ (the numerical values include the small EW radiative corrections and final state mass effects) is given by

$$\Gamma(W^+ \to e^+\nu_e) = \frac{G_F M_W^3}{6\sqrt{2}\pi} \approx 226.36 \pm 0.05 \text{ MeV} , \tag{10.42a}$$

$$\Gamma(W^+ \to u_i\overline{d}_j) = \frac{C G_F M_W^3}{6\sqrt{2}\pi} |V_{ij}|^2 \approx 706.34 \pm 0.16 \text{ MeV } |V_{ij}|^2, \tag{10.42b}$$

$$\Gamma(Z \to \psi_i\overline{\psi}_i) = \frac{C G_F M_Z^3}{6\sqrt{2}\pi} \left[g_V^{i2} + g_A^{i2}\right] \approx \begin{cases} 167.22 \pm 0.01 \text{ MeV } (\nu\overline{\nu}), \\ 84.00 \pm 0.01 \text{ MeV } (e^+e^-), \\ 300.26 \pm 0.05 \text{ MeV } (u\overline{u}), \\ 383.04 \pm 0.05 \text{ MeV } (d\overline{d}), \\ 375.98 \mp 0.03 \text{ MeV } (b\overline{b}). \end{cases} \tag{10.42c}$$

For leptons $C = 1$, while for quarks

$$C = 3\left[1 + \frac{\alpha_s(M_V)}{\pi} + 1.409\,\frac{\alpha_s^2}{\pi^2} - 12.77\,\frac{\alpha_s^3}{\pi^3} - 80.0\,\frac{\alpha_s^4}{\pi^4}\right], \tag{10.43}$$

where the 3 is due to color and the factor in brackets represents the universal part of the QCD corrections [176] for massless quarks [177]. The $\mathcal{O}(\alpha_s^4)$ contribution in Eq. (10.43) is recent [178]. The $Z \to f\bar{f}$ widths contain a number of additional corrections: which are different for vector and axial-vector partial widths and are included through order α_s^3 and $\widehat{m}_q^4(M_Z^2)$ unless they are tiny; and singlet contributions starting from two-loop order which are large, strongly top quark mass dependent, family universal, and flavor non-universal [181]. The QED factor $1 + 3\alpha q_f^2/4\pi$, as well as two-loop order $\alpha\alpha_s$ and α^2 self-energy corrections [182] are also included. Working in the on-shell scheme, *i.e.*, expressing the widths in terms of $G_F M_{W,Z}^3$, incorporates the largest radiative corrections from the running QED coupling [63,183]. EW corrections to the Z widths are then incorporated by replacing $g_{V,A}^{i2}$ by $\overline{g}_{V,A}^{i2}$. Hence, in the on-shell scheme the Z widths are proportional to $\rho_i \sim 1 + \rho_t$. The $\overline{\rm MS}$ normalization accounts also for the leading EW corrections [68]. There is additional (negative) quadratic m_t dependence in the $Z \to b\bar{b}$ vertex corrections [184] which causes $\Gamma(b\bar{b})$ to decrease with m_t. The dominant effect is to multiply $\Gamma(b\bar{b})$ by the vertex correction $1 + \delta\rho_{b\bar{b}}$, where $\delta\rho_{b\bar{b}} \sim 10^{-2}(-\frac{1}{2}\frac{m_t^2}{M_Z^2} + \frac{1}{5})$. In practice, the corrections are included in ρ_b and κ_b, as discussed in Sec. 10.2.

For three fermion families the total widths are predicted to be

$$\Gamma_Z \approx 2.4960 \pm 0.0002 \text{ GeV}\,, \qquad \Gamma_W \approx 2.0915 \pm 0.0005 \text{ GeV}\,. \tag{10.44}$$

We have assumed $\alpha_s(M_Z) = 0.1200$. An uncertainty in α_s of ± 0.002 introduces an additional uncertainty of 0.06% in the hadronic widths, corresponding to ± 1 MeV in Γ_Z. These predictions are to be compared with the experimental results, $\Gamma_Z = 2.4952 \pm 0.0023$ GeV [11] and $\Gamma_W = 2.085 \pm 0.042$ GeV [185] (see the Gauge & Higgs Boson Particle Listings for more details).

10.5. Precision flavor physics

In addition to cross-sections, asymmetries, parity violation, W and Z decays, there is a large number of experiments and observables testing the flavor structure of the SM. These are addressed elsewhere in this *Review*, and are generally not included in this Section. However, we identify three precision observables with sensitivity to similar types of new physics as the other processes discussed here. The branching fraction of the flavor changing transition $b \to s\gamma$ is of comparatively low precision, but since it is a loop-level process (in the SM) its sensitivity to new physics (and SM parameters, such as heavy quark masses) is enhanced. A discussion can be found in earlier editions of this *Review*. The τ-lepton lifetime and leptonic branching ratios are primarily sensitive to α_s and not affected significantly by many types of new physics. However, having an independent and reliable low energy measurement of α_s in a global analysis allows the

comparison with the Z lineshape determination of α_s which shifts easily in the presence of new physics contributions. By far the most precise observable discussed here is the anomalous magnetic moment of the muon (the electron magnetic moment is measured to even greater precision and can be used to determine α, but its new physics sensitivity is suppressed by an additional factor of m_e^2/m_μ^2). Its combined experimental and theoretical uncertainty is comparable to typical new physics contributions.

The extraction of α_s from the τ lifetime [186] is standing out from other determinations because of a variety of independent reasons: (i) the τ-scale is low, so that upon extrapolation to the Z scale (where it can be compared to the theoretically clean Z lineshape determinations) the α_s error shrinks by about an order of magnitude; (ii) yet, this scale is high enough that perturbation theory and the operator product expansion (OPE) can be applied; (iii) these observables are fully inclusive and thus free of fragmentation and hadronization effects that would have to be modeled or measured; (iv) duality violation (DV) effects are most problematic near the branch cut but there they are suppressed by a double zero at $s = m_\tau^2$; (v) there are data [43] to constrain non-perturbative effects both within ($\delta_{D=6,8}$) and breaking (δ_{DV}) the OPE; (vi) a complete four-loop order QCD calculation is available [178]; (vii) large effects associated with the QCD β-function can be re-summed [187] in what has become known as contour improved perturbation theory (CIPT). However, while there is no doubt that CIPT shows faster convergence in the lower (calculable) orders, doubts have been cast on the method by the observation that at least in a specific model [188], which includes the exactly known coefficients and theoretical constraints on the large-order behavior, ordinary fixed order perturbation theory (FOPT) may nevertheless give a better approximation to the full result. We therefore use the expressions [54,177,178,189],

$$\tau_\tau = \hbar \frac{1-\mathcal{B}_\tau^s}{\Gamma_\tau^e + \Gamma_\tau^\mu + \Gamma_\tau^{ud}} = 291.13 \pm 0.43 \text{ fs}, \tag{10.45}$$

$$\Gamma_\tau^{ud} = \frac{G_F^2 m_\tau^5 |V_{ud}|^2}{64\pi^3} S(m_\tau, M_Z) \left(1 + \frac{3}{5}\,\frac{m_\tau^2 - m_\mu^2}{M_W^2}\right) \times$$

$$[1 + \frac{\alpha_s(m_\tau)}{\pi} + 5.202\,\frac{\alpha_s^2}{\pi^2} + 26.37\,\frac{\alpha_s^3}{\pi^3} + 127.1\,\frac{\alpha_s^4}{\pi^4} + \frac{\widehat{\alpha}}{\pi}(\frac{85}{24} - \frac{\pi^2}{2}) + \delta_q], \tag{10.46}$$

and Γ_τ^e and Γ_τ^μ can be taken from Eq. (10.6) with obvious replacements. The relative fraction of decays with $\Delta S = -1$, $\mathcal{B}_\tau^s = 0.0286 \pm 0.0007$, is based on experimental data since the value for the strange quark mass, $\widehat{m}_s(m_\tau)$, is not well known and the QCD expansion proportional to $\widehat{m}_s^2$ converges poorly and cannot be trusted. $S(m_\tau, M_Z) = 1.01907 \pm 0.0003$ is a logarithmically enhanced EW correction factor with higher orders re-summed [190]. δ_q contains the dimension six and eight terms in the OPE, as well as DV effects, $\delta_{D=6,8} + \delta_{DV} = -0.004 \pm 0.012$ [191]. Depending on how $\delta_{D=6}$, $\delta_{D=8}$, and δ_{DV} are extracted, there are strong correlations not only between them, but also with the gluon condensate ($D = 4$) and possibly $D > 8$ terms. These latter are suppressed in Eq. (10.46) by additional factors of α_s, but not so for more general

weight functions. A simultaneous fit to all non-perturbative terms [191] (as is necessary if one wants to avoid *ad hoc* assumptions) indicates that the α_s errors may have been underestimated in the past. Higher statistics τ decay data [45] and spectral functions from e^+e^- annihilation (providing a larger fit window and thus more discriminatory power and smaller correlations) are likely to reduce the δ_q error in the future. Also included in δ_q are quark mass effects and the $D = 4$ condensate contributions. An uncertainty of similar size arises from the truncation of the FOPT series and is conservatively taken as the α_s^4 term (this is re-calculated in each call of the fits, leading to an α_s-dependent and thus asymmetric error) until a better understanding of the numerical differences between FOPT and CIPT has been gained. Our perturbative error covers almost the entire range from using CIPT to assuming that the nearly geometric series in Eq. (10.46) continues to higher orders. The experimental uncertainty in Eq. (10.45), is from the combination of the two leptonic branching ratios with the direct τ_τ. Included are also various smaller uncertainties (± 0.5 fs) from other sources which are dominated by the evolution from the Z scale. In total we obtain a $\sim 2\%$ determination of $\alpha_s(M_Z) = 0.1193^{+0.0022}_{-0.0020}$, which corresponds to $\alpha_s(m_\tau) = 0.327^{+0.019}_{-0.016}$, and updates the result of Refs. 54 and 192. For more details, see Refs. 191 and 193 where the τ spectral functions are used as additional input.

The world average of the muon anomalous magnetic moment[‡],

$$a_\mu^{\rm exp} = \frac{g_\mu - 2}{2} = (1165920.80 \pm 0.63) \times 10^{-9}, \qquad (10.47)$$

is dominated by the final result of the E821 collaboration at BNL [194]. The QED contribution has been calculated to four loops [195] (fully analytically to three loops [196,197]) , and the leading logarithms are included to five loops [198,199]. The estimated SM EW contribution [200–202], $a_\mu^{\rm EW} = (1.52 \pm 0.03) \times 10^{-9}$, which includes leading two-loop [201] and three-loop [202] corrections, is at the level of twice the current uncertainty.

The limiting factor in the interpretation of the result are the uncertainties from the two- and three-loop hadronic contribution. *E.g.,* Ref. 20 obtained the value $a_\mu^{\rm had} = (69.23 \pm 0.42) \times 10^{-9}$ which combines CMD-2 [47] and SND [48] $e^+e^- \to$ hadrons cross-section data with radiative return results from BaBar [50] and KLOE [51]. This value suggests a 3.6 σ discrepancy between Eq. (10.47) and the SM prediction. An alternative analysis [20] using τ decay data and isospin symmetry (CVC) yields

[‡] In what follows, we summarize the most important aspects of $g_\mu - 2$, and give some details about the evaluation in our fits. For more details see the dedicated contribution by A. Höcker and W. Marciano in this *Review*. There are some small numerical differences (at the level of 0.1 standard deviation), which are well understood and mostly arise because internal consistency of the fits requires the calculation of all observables from analytical expressions and common inputs and fit parameters, so that an independent evaluation is necessary for this Section. Note, that in the spirit of a global analysis based on all available information we have chosen here to average in the τ decay data, as well.

$a_\mu^{\rm had} = (70.15 \pm 0.47) \times 10^{-9}$. This result implies a smaller conflict (2.4 σ) with Eq. (10.47). Thus, there is also a discrepancy between the spectral functions obtained from the two methods. For example, if one uses the e^+e^- data and CVC to predict the branching ratio for $\tau^- \to \nu_\tau \pi^- \pi^0$ decays [20] we obtain an average of $\mathcal{B}_{\rm CVC} = 24.93 \pm 0.13 \pm 0.22_{\rm CVC}$, while the average of the directly measured branching ratio yields 25.51 ± 0.09, which is 2.3 σ higher. It is important to understand the origin of this difference, but two observations point to the conclusion that at least some of it is experimental: (i) There is also a direct discrepancy of 1.9 σ between $\mathcal{B}_{\rm CVC}$ derived from BaBar (which is not inconsistent with τ decays) and KLOE. (ii) Isospin violating corrections have been studied in detail in Ref. 203 and found to be largely under control. The largest effect is due to higher-order EW corrections [204] but introduces a negligible uncertainty [190]. Nevertheless, $a_\mu^{\rm had}$ is often evaluated excluding the τ decay data arguing [205] that CVC breaking effects (*e.g.*, through a relatively large mass difference between the $\rho^\pm$ and ρ^0 vector mesons) may be larger than expected. (This may also be relevant [205] in the context of the NuTeV result discussed above.) Experimentally [45], this mass difference is indeed larger than expected, but then one would also expect a significant width difference which is contrary to observation [45]. Fortunately, due to the suppression at large s (from where the conflicts originate) these problems are less pronounced as far as $a_\mu^{\rm had}$ is concerned. In the following we view all differences in spectral functions as (systematic) fluctuations and average the results.

An additional uncertainty is induced by the hadronic three-loop light-by-light scattering contribution. Two recent and inherently different model calculations yield $a_\mu^{\rm LBLS} = (+1.36 \pm 0.25) \times 10^{-9}$ [206] and $a_\mu^{\rm LBLS} = +1.37^{+0.15}_{-0.27} \times 10^{-9}$ [207] which are higher than previous evaluations [208,209]. The sign of this effect is opposite [208] to the one quoted in the 2002 edition of this *Review*, and has subsequently been confirmed by two other groups [209]. There is also the upper bound $a_\mu^{\rm LBLS} < 1.59 \times 10^{-9}$ [207] but this requires an *ad hoc* assumption, too. The recent Ref. 210 quotes the value $a_\mu^{\rm LBLS} = (+1.05 \pm 0.26) \times 10^{-9}$, which we shift by 2×10^{-11} to account for the more accurate charm quark treatment of Ref. 207. We also increase the error to cover all evaluations, and we will use $a_\mu^{\rm LBLS} = (+1.07 \pm 0.32) \times 10^{-9}$ in the fits.

Other hadronic effects at three-loop order contribute [211] $a_\mu^{\rm had}(\alpha^3) = (-1.00 \pm 0.06) \times 10^{-9}$. Correlations with the two-loop hadronic contribution and with $\Delta\alpha(M_Z)$ (see Sec. 10.2) were considered in Ref. 197 which also contains analytic results for the perturbative QCD contribution.

Altogether, the SM prediction is

$$a_\mu^{\rm theory} = (1165918.41 \pm 0.48) \times 10^{-9} \ , \tag{10.48}$$

where the error is from the hadronic uncertainties excluding parametric ones such as from α_s and the heavy quark masses. Using a correlation of about 84% from the data input to the vacuum polarization integrals [20], we estimate the correlation of the total (experimental plus theoretical) uncertainty in a_μ with $\Delta\alpha(M_Z)$ as 24%. The overall 3.0 σ discrepancy between the experimental and theoretical a_μ values could be due to fluctuations (the E821 result is statistics dominated) or underestimates of the theoretical

uncertainties. On the other hand, $g_\mu - 2$ is also affected by many types of new physics, such as supersymmetric models with large $\tan\beta$ and moderately light superparticle masses [212]. Thus, the deviation could also arise from physics beyond the SM.

10.6. Global fit results

In this section we present the results of global fits to the experimental data discussed in Sec. 10.3–Sec. 10.5. For earlier analyses see Refs. 128 and 213.

Table 10.4: Principal non-Z pole observables, compared with the SM best fit predictions. The first M_W value is from the Tevatron [214] and the second one from LEP 2 [172]. e-DIS [129] and the ν-DIS constraints from CDHS [102], CHARM [103], and CCFR [104] are included, as well, but not shown in the Table. The world averages for $g^{\nu e}_{V,A}$ are dominated by the CHARM II [98] results, $g^{\nu e}_V = -0.035 \pm 0.017$ and $g^{\nu e}_A = -0.503 \pm 0.017$. The errors are the total (experimental plus theoretical) uncertainties. The τ_τ value is the τ lifetime world average computed by combining the direct measurements with values derived from the leptonic branching ratios [54]; in this case, the theory uncertainty is included in the SM prediction. In all other SM predictions, the uncertainty is from M_Z, M_H, m_t, m_b, m_c, $\widehat{\alpha}(M_Z)$, and α_s, and their correlations have been accounted for. The column denoted Pull gives the standard deviations for the principal fit with M_H free, while the column denoted Dev. (Deviation) is for $M_H = 124.5$ GeV [215] fixed.

Quantity	Value	Standard Model	Pull	Dev.
m_t [GeV]	173.4 ± 1.0	173.5 ± 1.0	-0.1	-0.3
M_W [GeV]	80.420 ± 0.031	80.381 ± 0.014	1.2	1.6
	80.376 ± 0.033		-0.2	0.2
$g^{\nu e}_V$	-0.040 ± 0.015	-0.0398 ± 0.0003	0.0	0.0
$g^{\nu e}_A$	-0.507 ± 0.014	-0.5064 ± 0.0001	0.0	0.0
$Q_W(e)$	-0.0403 ± 0.0053	-0.0474 ± 0.0005	1.3	1.3
Q_W(Cs)	-73.20 ± 0.35	-73.23 ± 0.02	0.1	0.1
Q_W(Tl)	-116.4 ± 3.6	-116.88 ± 0.03	0.1	0.1
τ_τ [fs]	291.13 ± 0.43	290.75 ± 2.51	0.1	0.1
$\frac{1}{2}(g_\mu - 2 - \frac{\alpha}{\pi})$	$(4511.07 \pm 0.77) \times 10^{-9}$	$(4508.70 \pm 0.09) \times 10^{-9}$	3.0	3.0

The values for m_t [56–58], M_W [172,214], neutrino scattering [96–104], the weak charges of the electron [131], cesium [138,139] and thallium [140], the muon anomalous magnetic moment [194], and the τ lifetime are listed in Table 10.4. Likewise, the principal Z pole observables can be found in Table 10.5 where the LEP 1 averages of the ALEPH, DELPHI, L3, and OPAL results include common systematic errors and correlations [11]. The heavy flavor results of LEP 1 and SLD are based on common inputs and correlated,

Table 10.5: Principal Z pole observables and their SM predictions (*cf.* Table 10.4). The first $\overline{s}^2_\ell(A^{(0,q)}_{FB})$ is the effective angle extracted from the hadronic charge asymmetry, the second is the combined value from DØ [167] and CDF [168], and the third is from CMS [171]. The three values of A_e are (i) from A_{LR} for hadronic final states [162]; (ii) from A_{LR} for leptonic final states and from polarized Bhabba scattering [164]; and (iii) from the angular distribution of the τ polarization at LEP 1. The two A_τ values are from SLD and the total τ polarization, respectively.

Quantity	Value	Standard Model	Pull	Dev.
M_Z [GeV]	91.1876 ± 0.0021	91.1874 ± 0.0021	0.1	0.0
Γ_Z [GeV]	2.4952 ± 0.0023	2.4961 ± 0.0010	-0.4	-0.2
Γ(had) [GeV]	1.7444 ± 0.0020	1.7426 ± 0.0010	—	—
Γ(inv) [MeV]	499.0 ± 1.5	501.69 ± 0.06	—	—
$\Gamma(\ell^+\ell^-)$ [MeV]	83.984 ± 0.086	84.005 ± 0.015	—	—
$\sigma_{\rm had}$[nb]	41.541 ± 0.037	41.477 ± 0.009	1.7	1.7
R_e	20.804 ± 0.050	20.744 ± 0.011	1.2	1.3
R_μ	20.785 ± 0.033	20.744 ± 0.011	1.2	1.3
R_τ	20.764 ± 0.045	20.789 ± 0.011	-0.6	-0.5
R_b	0.21629 ± 0.00066	0.21576 ± 0.00004	0.8	0.8
R_c	0.1721 ± 0.0030	0.17227 ± 0.00004	-0.1	-0.1
$A^{(0,e)}_{FB}$	0.0145 ± 0.0025	0.01633 ± 0.00021	-0.7	-0.7
$A^{(0,\mu)}_{FB}$	0.0169 ± 0.0013		0.4	0.6
$A^{(0,\tau)}_{FB}$	0.0188 ± 0.0017		1.5	1.6
$A^{(0,b)}_{FB}$	0.0992 ± 0.0016	0.1034 ± 0.0007	-2.6	-2.3
$A^{(0,c)}_{FB}$	0.0707 ± 0.0035	0.0739 ± 0.0005	-0.9	-0.8
$A^{(0,s)}_{FB}$	0.0976 ± 0.0114	0.1035 ± 0.0007	-0.5	-0.5
$\overline{s}^2_\ell(A^{(0,q)}_{FB})$	0.2324 ± 0.0012	0.23146 ± 0.00012	0.8	0.7
	0.23200 ± 0.00076		0.7	0.6
	0.2287 ± 0.0032		-0.9	-0.9
A_e	0.15138 ± 0.00216	0.1475 ± 0.0010	1.8	2.1
	0.1544 ± 0.0060		1.1	1.3
	0.1498 ± 0.0049		0.5	0.6
A_μ	0.142 ± 0.015		-0.4	-0.3
A_τ	0.136 ± 0.015		-0.8	-0.7
	0.1439 ± 0.0043		-0.8	-0.7
A_b	0.923 ± 0.020	0.9348 ± 0.0001	-0.6	-0.6
A_c	0.670 ± 0.027	0.6680 ± 0.0004	0.1	0.1
A_s	0.895 ± 0.091	0.9357 ± 0.0001	-0.4	-0.4

Table 10.6: Principal SM fit result including mutual correlations (all masses in GeV). Note that $\widehat{m}_c(\widehat{m}_c)$ induces a significant uncertainty in the running of α beyond $\Delta\alpha^{(3)}_{\rm had}(1.8\ {\rm GeV})$ resulting in a relatively large correlation with M_H. Since this effect is proportional to the quark's electric charge squared it is much smaller for $\widehat{m}_b(\widehat{m}_b)$.

M_Z	91.1874 ± 0.0021	1.00	−0.01	0.00	0.00	−0.01	0.00	0.14
$\widehat{m}_t(\widehat{m}_t)$	163.71 ± 0.95	−0.01	1.00	0.01	−0.01	−0.15	0.00	0.31
$\widehat{m}_b(\widehat{m}_b)$	4.197 ± 0.025	0.00	0.01	1.00	0.24	−0.04	0.01	0.04
$\widehat{m}_c(\widehat{m}_c)$	$1.266^{+0.032}_{-0.040}$	0.00	−0.01	0.24	1.00	0.09	0.03	0.14
$\alpha_s(M_Z)$	0.1196 ± 0.0017	−0.01	−0.15	−0.04	0.09	1.00	−0.01	−0.05
$\Delta\alpha^{(3)}_{\rm had}(1.8\ {\rm GeV})$	0.00561 ± 0.00008	0.00	0.00	0.01	0.03	−0.01	1.00	−0.16
M_H	99^{+28}_{-23}	0.14	0.31	0.04	0.14	−0.05	−0.16	1.00

as well [11]. Note that the values of $\Gamma(\ell^+\ell^-)$, Γ(had), and Γ(inv) are not independent of Γ_Z, the R_ℓ, and $\sigma_{\rm had}$ and that the SM errors in those latter are largely dominated by the uncertainty in α_s. Also shown in both Tables are the SM predictions for the values of M_Z, M_H, $\alpha_s(M_Z)$, $\Delta\alpha^{(3)}_{\rm had}$ and the heavy quark masses shown in Table 10.6. The predictions result from a global least-square (χ^2) fit to all data using the minimization package MINUIT [216] and the EW library GAPP [21]. In most cases, we treat all input errors (the uncertainties of the values) as Gaussian. The reason is not that we assume that theoretical and systematic errors are intrinsically bell-shaped (which they are not) but because in most cases the input errors are combinations of many different (including statistical) error sources, which should yield approximately Gaussian *combined* errors by the large number theorem. Thus, if either the statistical components dominate or there are many components of similar size. An exception is the theory dominated error on the τ lifetime, which we recalculate in each χ^2-function call since it depends itself on α_s. Sizes and shapes of the output errors (the uncertainties of the predictions and the SM fit parameters) are fully determined by the fit, and 1 σ errors are defined to correspond to $\Delta\chi^2 = \chi^2 - \chi^2_{\rm min} = 1$, and do not necessarily correspond to the 68.3% probability range or the 39.3% probability contour (for 2 parameters).

The agreement is generally very good. Despite the few discrepancies discussed in the following, the fit describes well the data with a χ^2/d.o.f. = 45.0/42. The probability of a larger χ^2 is 35%. Only the final result for $g_\mu - 2$ from BNL and $A_{FB}^{(0,b)}$ from LEP 1 are currently showing large (3.0 σ and 2.6 σ) deviations. In addition, A^0_{LR} (SLD) from hadronic final states differs by 1.8 σ. g_L^2 from NuTeV is nominally in conflict with the SM, as well, but the precise status is under investigation (see Sec. 10.3).

A_b can be extracted from $A_{FB}^{(0,b)}$ when $A_e = 0.1501 \pm 0.0016$ is taken from a fit to

leptonic asymmetries (using lepton universality). The result, $A_b = 0.881 \pm 0.017$, is 3.2 σ below the SM prediction[§] and also 1.6 σ below $A_b = 0.923 \pm 0.020$ obtained from $A_{LR}^{FB}(b)$ at SLD. Thus, it appears that at least some of the problem in $A_{FB}^{(0,b)}$ is experimental. Note, however, that the uncertainty in $A_{FB}^{(0,b)}$ is strongly statistics dominated. The combined value, $A_b = 0.899 \pm 0.013$ deviates by 2.8 σ. It would be difficult to account for this 4.0% deviation by new physics that enters only at the level of radiative corrections since about a 20% correction to $\widehat{\kappa}_b$ would be necessary to account for the central value of A_b [217]. If this deviation is due to new physics, it is most likely of tree-level type affecting preferentially the third generation. Examples include the decay of a scalar neutrino resonance [218], mixing of the b quark with heavy exotics [219], and a heavy Z' with family-nonuniversal couplings [220,221]. It is difficult, however, to simultaneously account for R_b, which has been measured on the Z peak and off-peak [222] at LEP 1. An average of R_b measurements at LEP 2 at energies between 133 and 207 GeV is 2.1 σ below the SM prediction, while $A_{FB}^{(b)}$ (LEP 2) is 1.6 σ low [172].

The left-right asymmetry, $A_{LR}^0 = 0.15138 \pm 0.00216$ [162], based on all hadronic data from 1992–1998 differs 1.8 σ from the SM expectation of 0.1475 ± 0.0010. The combined value of $A_\ell = 0.1513 \pm 0.0021$ from SLD (using lepton-family universality and including correlations) is also 1.8 σ above the SM prediction; but there is experimental agreement between this SLD value and the LEP 1 value, $A_\ell = 0.1481 \pm 0.0027$, obtained from a fit to $A_{FB}^{(0,\ell)}$, $A_e(\mathcal{P}_\tau)$, and $A_\tau(\mathcal{P}_\tau)$, again assuming universality.

The observables in Table 10.4 and Table 10.5, as well as some other less precise observables, are used in the global fits described below. In all fits, the errors include full statistical, systematic, and theoretical uncertainties. The correlations on the LEP 1 lineshape and τ polarization, the LEP/SLD heavy flavor observables, the SLD lepton asymmetries, and the deep inelastic and ν-e scattering observables, are included. The theoretical correlations between $\Delta\alpha_{\rm had}^{(5)}$ and $g_\mu - 2$, and between the charm and bottom quark masses, are also accounted for.

The data allow a simultaneous determination of M_Z, M_H, m_t, and the strong coupling $\alpha_s(M_Z)$. ($\widehat{m}_c$, $\widehat{m}_b$, and $\Delta\alpha_{\rm had}^{(3)}$ are also allowed to float in the fits, subject to the theoretical constraints [19,54] described in Sec. 10.2. These are correlated with α_s.) α_s is determined mainly from R_ℓ, Γ_Z, $\sigma_{\rm had}$, and τ_τ and is only weakly correlated with the other variables. The global fit to all data, including the hadron collider average $m_t = 173.4 \pm 1.0$ GeV, yields the result in Table 10.6 (the $\overline{\rm MS}$ top quark mass given there corresponds to $m_t = 173.5 \pm 1.0$ GeV). The weak mixing angle is determined to

$$\widehat{s}^2_Z = 0.23116 \pm 0.00012, \qquad\qquad s^2_W = 0.22296 \pm 0.00028,$$

while the corresponding effective angle is related by Eq. (10.18), *i.e.*, $\overline{s}^2_\ell = 0.23146 \pm 0.00012$.

[§] Alternatively, one can use $A_\ell = 0.1481 \pm 0.0027$, which is from LEP 1 alone and in excellent agreement with the SM, and obtain $A_b = 0.893 \pm 0.022$ which is 1.9 σ low. This illustrates that some of the discrepancy is related to the one in A_{LR}.

As described in Sec. 10.2 and the paragraph following Eq. (10.47) in Sec. 10.5, there is considerable stress in the experimental e^+e^- spectral functions and also conflict when these are compared with τ decay spectral functions. These are below or above the 2σ level (depending on what is actually compared) but not larger than the deviations of some other quantities entering our analyses. The number and size or these deviations are not inconsistent with what one would expect to happen as a result of random fluctuations. It is nevertheless instructive to study the effect of doubling the uncertainty in $\Delta\alpha^{(3)}_{\rm had}(1.8\ {\rm GeV}) = (55.50 \pm 0.78) \times 10^{-4}$, (see Sec. 10.2) on the extracted Higgs mass. The result, $M_H = 95^{+28}_{-23}$ GeV, demonstrates that the uncertainty in $\Delta\alpha_{\rm had}$ is currently of only secondary importance. Note also, that a shift of ± 0.0001 in $\Delta\alpha^{(3)}_{\rm had}(1.8\ {\rm GeV})$ corresponds to a shift of ∓ 5 GeV in M_H or about one fifth of its total uncertainty. The hadronic contribution to $\alpha(M_Z)$ is correlated with $g_\mu - 2$ (see Sec. 10.5). The measurement of the latter is higher than the SM prediction, and its inclusion in the fit favors a larger $\alpha(M_Z)$ and a lower M_H (currently by about 4 GeV).

The weak mixing angle can be determined from Z pole observables, M_W, and from a variety of neutral-current processes spanning a very wide Q^2 range. The results (for the older low energy neutral-current data see Refs. 128 and 213) shown in Table 10.7 are in reasonable agreement with each other, indicating the quantitative success of the SM. The largest discrepancy is the value $\widehat{s}^2_Z = 0.23193 \pm 0.00028$ from the forward-backward asymmetries into bottom and charm quarks, which is 2.8 σ above the value 0.23116 ± 0.00012 from the global fit to all data. Similarly, $\widehat{s}^2_Z = 0.23067 \pm 0.00029$ from the SLD asymmetries (in both cases when combined with M_Z) is 1.8 σ low. The SLD result has the additional difficulty (within the SM) of implying very low and excluded [173] Higgs masses. This is also true for $\widehat{s}^2_Z = 0.23098 \pm 0.00022$ from M_W and M_Z and — as a consequence — for the global fit. We have therefore included in Table 10.4 and Table 10.5 an additional column (denoted Deviation) indicating the deviations if $M_H = 124.5$ GeV [215] is fixed.

The extracted Z pole value of $\alpha_s(M_Z)$ is based on a formula with negligible theoretical uncertainty if one assumes the exact validity of the SM. One should keep in mind, however, that this value, $\alpha_s(M_Z) = 0.1197 \pm 0.0028$, is very sensitive to such types of new physics as non-universal vertex corrections. In contrast, the value derived from τ decays, $\alpha_s(M_Z) = 0.1193^{+0.0022}_{-0.0020}$, is theory dominated but less sensitive to new physics. The two values are in remarkable agreement with each other. They are also in perfect agreement with the averages from jet-event shapes in e^+e^- annihilation (0.1172 ± 0.0037) and lattice simulations (0.1185 ± 0.0007), whereas the DIS average (0.1150 ± 0.0021) is somewhat lower. For more details, other determinations, and references, see our Section 9 on "Quantum Chromodynamics" in this *Review*.

Using $\alpha(M_Z)$ and $\widehat{s}^2_Z$ as inputs, one can predict $\alpha_s(M_Z)$ assuming grand unification. One predicts [223] $\alpha_s(M_Z) = 0.130 \pm 0.001 \pm 0.01$ for the simplest theories based on the minimal supersymmetric extension of the SM, where the first (second) uncertainty is from the inputs (thresholds). This is slightly larger, but consistent with the experimental $\alpha_s(M_Z) = 0.1196 \pm 0.0017$ from the Z lineshape and the τ lifetime, as well as with most other determinations. Non-supersymmetric unified theories predict the low value

Table 10.7: Values of $\widehat{s}^2_Z$, s^2_W, α_s, and M_H [in GeV] for various (combinations of) observables. Unless indicated otherwise, the top quark mass, $m_t = 173.4 \pm 1.0$ GeV, is used as an additional constraint in the fits. The (†) symbol indicates a fixed parameter.

Data	$\widehat{s}^2_Z$	s^2_W	$\alpha_s(M_Z)$	M_H
All data	0.23116(12)	0.22295(28)	0.1196(17)	99^{+28}_{-23}
All indirect (no m_t)	0.23118(14)	0.22285(35)	0.1197(17)	$134^{+144}_{-\ 65}$
Z pole (no m_t)	0.23121(17)	0.22318(60)	0.1197(28)	$102^{+133}_{-\ 51}$
LEP 1 (no m_t)	0.23152(20)	0.22383(67)	0.1213(30)	191^{+266}_{-105}
SLD + M_Z	0.23067(28)	0.22204(54)	0.1185 (†)	39^{+31}_{-19}
$A_{FB}^{(b,c)}$ + M_Z	0.23193(28)	0.22494(76)	0.1185 (†)	444^{+300}_{-178}
M_W + M_Z	0.23098(22)	0.22262(47)	0.1185 (†)	75^{+39}_{-30}
M_Z	0.23124(5)	0.22318(13)	0.1185 (†)	124.5 (†)
$Q_W(e)$	0.2332(15)	0.2252(15)	0.1185 (†)	124.5 (†)
Q_W (APV)	0.2311(16)	0.2230(17)	0.1185 (†)	124.5 (†)
ν_μ-N DIS (isoscalar)	0.2332(39)	0.2251(39)	0.1185 (†)	124.5 (†)
Elastic $\nu_\mu(\overline{\nu}_\mu)$-$e$	0.2311(77)	0.2230(77)	0.1185 (†)	124.5 (†)
e-D DIS (SLAC)	0.222(18)	0.214(18)	0.1185 (†)	124.5 (†)
Elastic $\nu_\mu(\overline{\nu}_\mu)$-$p$	0.211(33)	0.203(33)	0.1185 (†)	124.5 (†)

$\alpha_s(M_Z) = 0.073 \pm 0.001 \pm 0.001$. See also the note on "Supersymmetry" in the Searches Particle Listings.

The data indicate a preference for a small Higgs mass. There is a strong correlation between the quadratic m_t and logarithmic M_H terms in $\widehat{\rho}$ in all of the indirect data except for the $Z \to b\overline{b}$ vertex. Therefore, observables (other than R_b) which favor m_t values higher than the Tevatron range favor lower values of M_H. M_W has additional M_H dependence through $\Delta\widehat{r}_W$ which is not coupled to m_t^2 effects. The strongest individual pulls toward smaller M_H are from M_W and A^0_{LR}, while $A_{FB}^{(0,b)}$ favors higher values. The difference in χ^2 for the global fit is $\Delta\chi^2 = \chi^2(M_H = 314\ \text{GeV}) - \chi^2_{\text{min}} = 25$. Hence, the data favor a small value of M_H, as in supersymmetric extensions of the SM. The central value of the global fit result, $M_H = 99^{+28}_{-23}$ GeV, is below the direct lower bound from LEP 2, $M_H \geq 114.4$ GeV (95% CL) [173], which was very recently extended slightly by ATLAS to $M_H \geq 115.5$ GeV [224].

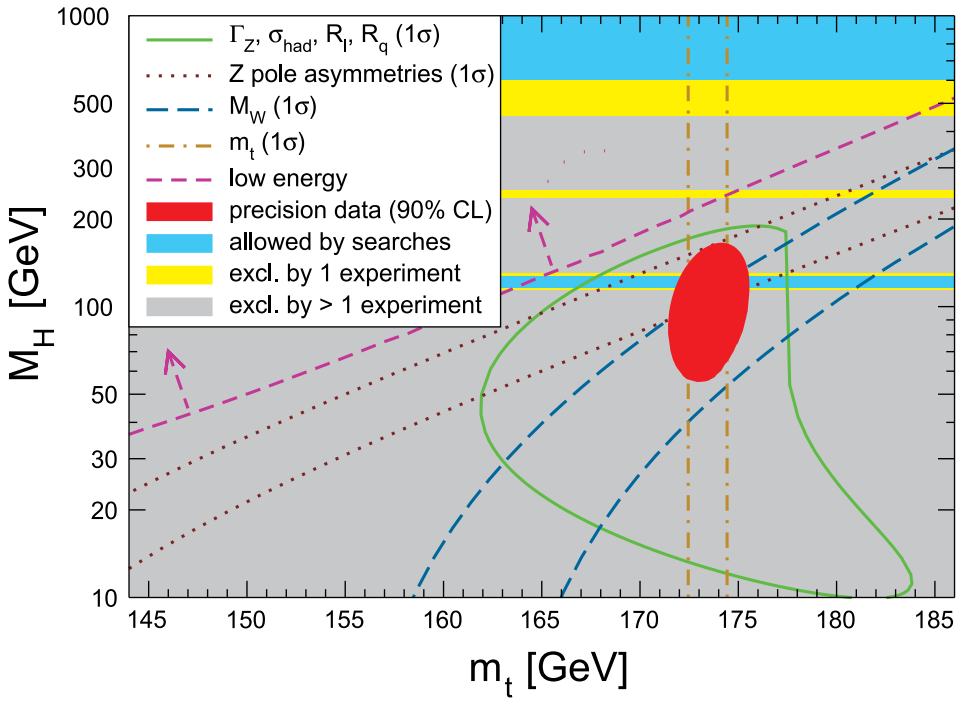

Figure 10.5: One-standard-deviation (39.35%) uncertainties in M_H as a function of m_t for various inputs, and the 90% CL region ($\Delta\chi^2 = 4.605$) allowed by all data. $\alpha_s(M_Z) = 0.1185$ is assumed except for the fits including the Z lineshape or low energy data. The bright (yellow) bands are excluded by one experiment and the remaining (gray) regions are ruled out by more than one experiment (95% CL).

The 90% central confidence range from all precision data is

$$68 \text{ GeV} \leq M_H \leq 155 \text{ GeV}. \tag{10.49}$$

Including the results of the direct searches at LEP 2 [173] and the Tevatron [225] as extra contributions to the likelihood function reduces the 95% upper limit to $M_H \leq 150$ GeV. As two further refinements, we account for (i) theoretical uncertainties from uncalculated higher order contributions by allowing the T parameter (see next subsection) subject to the constraint $T = 0 \pm 0.02$, (ii) the M_H dependence of the correlation matrix which gives slightly more weight to lower Higgs masses [226]. The resulting limits at 95 (90, 99)% CL are, respectively,

$$M_H \leq 175 \text{ (148, 210) GeV}. \tag{10.50}$$

In their Higgs searches in pp collisions with CM energy of 7 TeV, both ATLAS [224] and CMS [227] find results consistent with Eq. (10.50) and currently report $\gtrsim 2\ \sigma$ excess fluctuation near $M_H = 119.5$ GeV (CMS only), $M_H = 124$ GeV (CMS), and $M_H = 126$ GeV (ATLAS only). Of course, these excesses do not constitute a discovery. However, it is useful to take them at face value for comparison with the precision data in Table 10.4, Table 10.5, and Table 10.7. A combination of all available data yields (at the 68% CL) [215]

$$M_H = 124.5 \pm 0.8 \text{ GeV}. \tag{10.51}$$

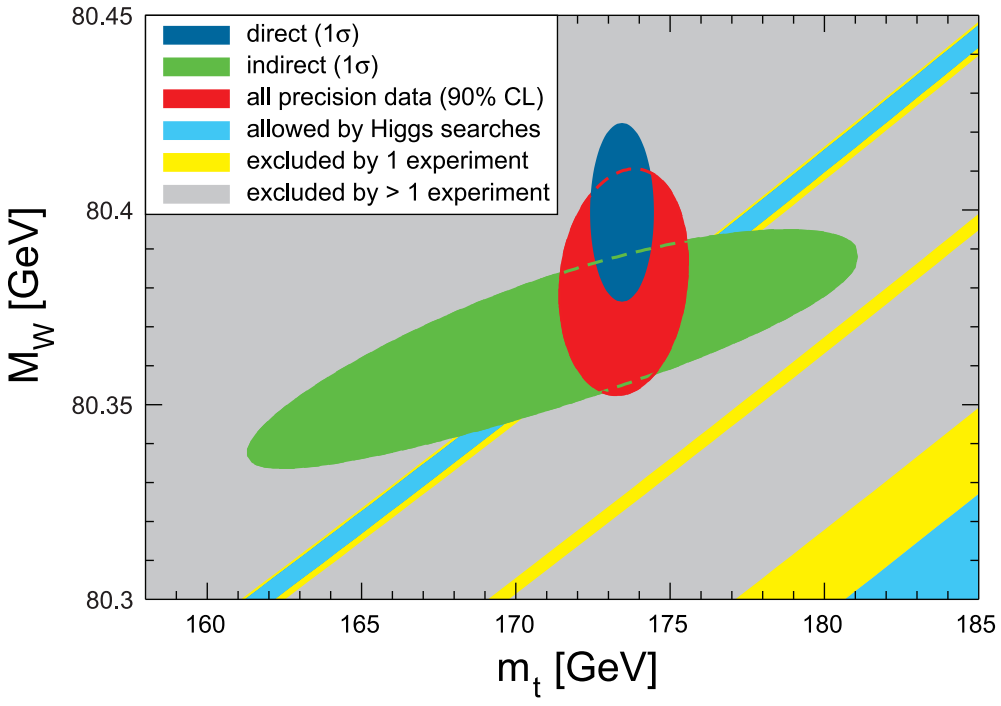

Figure 10.6: One-standard-deviation (39.35%) region in M_W as a function of m_t for the direct and indirect precision data, and the 90% CL region ($\Delta\chi^2 = 4.605$) allowed by all precision data. The SM predictions are also indicated, where the blue bands for Higgs masses between 115.5 and 127 GeV and beyond 600 GeV are currently allowed at the 95% CL. The bright (yellow) bands are excluded by one experiment and the remaining (gray) regions are ruled out by more than one experiment (95% CL).

The resulting probability distribution has a twin peak structure (besides a smaller maximum at $M_H = 118.5$ GeV) with almost equal probability at $M_H = 124$ GeV and $M_H = 125$ GeV [215].

One can also carry out a fit to the indirect data alone, *i.e.*, without including the constraint, $m_t = 173.4 \pm 1.0$ GeV, from the hadron colliders. (The indirect prediction is for the $\overline{\rm MS}$ mass, $\widehat{m}_t(\widehat{m}_t) = 167.5^{+8.9}_{-7.3}$ GeV, which is in the end converted to the pole mass). One obtains $m_t = 177.5^{+9.4}_{-7.8}$ GeV, in perfect agreement with the direct Tevatron/LHC average. Using this indirect top mass value, the tendency for a light Higgs persists and Eq. (10.49) becomes 46 GeV $\leq M_H \leq$ 306 GeV. The relations between M_H and m_t for various observables are shown in Fig. 10.5.

One can also determine the radiative correction parameters Δr: from the global fit one obtains $\Delta r = 0.0352 \pm 0.0009$ and $\Delta\widehat{r}_W = 0.06945 \pm 0.00019$. M_W measurements [172,214] (when combined with M_Z) are equivalent to measurements of $\Delta r = 0.0342 \pm 0.0015$, which is 0.9 σ below the result from all other data, $\Delta r = 0.0358 \pm 0.0011$. Fig. 10.6 shows the 1 σ contours in the M_W-m_t plane from the direct and indirect determinations, as well as the combined 90% CL region. The indirect determination uses M_Z from LEP 1 as input, which is defined assuming an s-dependent decay width. M_W then

Table 10.8: Values of the model-independent neutral-current parameters, compared with the SM predictions. There is a second $g^{\nu e}_{V,A}$ solution, given approximately by $g^{\nu e}_V \leftrightarrow g^{\nu e}_A$, which is eliminated by e^+e^- data under the assumption that the neutral current is dominated by the exchange of a single Z boson. The ϵ_L, as well as the ϵ_R, are strongly correlated and non-Gaussian, so that for implementations we recommend the parametrization using g_i^2 and $\theta_i = \tan^{-1}[\epsilon_i(u)/\epsilon_i(d)]$, $i = L$ or R. The analysis of more recent low energy experiments in polarized electron scattering performed in Ref. 129 is included by means of the two orthogonal constraints, $\cos\gamma\, C_{1d} - \sin\gamma\, C_{1u} = 0.342 \pm 0.063$ and $\sin\gamma\, C_{1d} + \cos\gamma\, C_{1u} = -0.0285 \pm 0.0043$, where $\tan\gamma \approx 0.445$. In the SM predictions, the uncertainty is from M_Z, M_H, m_t, m_b, m_c, $\widehat{\alpha}(M_Z)$, and α_s.

Quantity	Experimental Value	SM	Correlation		
$\epsilon_L(u)$	0.328 ± 0.016	0.3461(1)			
$\epsilon_L(d)$	-0.440 ± 0.011	$-0.4292(1)$	non-		
$\epsilon_R(u)$	-0.179 ± 0.013	$-0.1549(1)$	Gaussian		
$\epsilon_R(d)$	$-0.027\ ^{+0.077}_{-0.048}$	0.0775			
g_L^2	0.3009 ± 0.0028	0.3040(2)			
g_R^2	0.0328 ± 0.0030	0.0300	small		
θ_L	2.50 ± 0.035	2.4630(1)			
θ_R	$4.56\ ^{+0.42}_{-0.27}$	5.1765			
$g^{\nu e}_V$	-0.040 ± 0.015	$-0.0399(2)$			-0.05
$g^{\nu e}_A$	-0.507 ± 0.014	$-0.5064(1)$			
$C_{1u} + C_{1d}$	0.1537 ± 0.0011	0.1530(1)	0.64	-0.18	-0.01
$C_{1u} - C_{1d}$	-0.516 ± 0.014	$-0.5300(3)$		-0.27	-0.02
$C_{2u} + C_{2d}$	-0.21 ± 0.57	-0.0089			-0.30
$C_{2u} - C_{2d}$	-0.077 ± 0.044	$-0.0627(5)$			
$Q_W(e) = -2C_{2e}$	-0.0403 ± 0.0053	$-0.0474(5)$			

corresponds to the s-dependent width definition, as well, and can be directly compared with the results from the Tevatron and LEP 2 which have been obtained using the same definition. The difference to a constant width definition is formally only of $\mathcal{O}(\alpha^2)$, but is strongly enhanced since the decay channels add up coherently. It is about 34 MeV for M_Z and 27 MeV for M_W. The residual difference between working consistently with one or the other definition is about 3 MeV, *i.e.*, of typical size for non-enhanced $\mathcal{O}(\alpha^2)$

corrections [74–77].

Most of the parameters relevant to ν-hadron, ν-e, e-hadron, and $e^-e^\pm$ processes are determined uniquely and precisely from the data in "model-independent" fits (*i.e.*, fits which allow for an arbitrary EW gauge theory). The values for the parameters defined in Eqs. (10.19)–(10.22) are given in Table 10.8 along with the predictions of the SM. The agreement is very good. (The ν-hadron results including the original NuTeV data can be found in the 2006 edition of this *Review*, and fits with modified NuTeV constraints in the 2008 and 2010 editions.) The off Z pole e^+e^- results are difficult to present in a model-independent way because Z propagator effects are non-negligible at TRISTAN, PETRA, PEP, and LEP 2 energies. However, assuming e-μ-τ universality, the low energy lepton asymmetries imply [159] $4\,(g_A^e)^2 = 0.99 \pm 0.05$, in good agreement with the SM prediction $\simeq 1$.

10.7. Constraints on new physics

The Z pole, W mass, and low energy data can be used to search for and set limits on deviations from the SM. We will mainly discuss the effects of exotic particles (with heavy masses $M_{\rm new} \gg M_Z$ in an expansion in $M_Z/M_{\rm new}$) on the gauge boson self-energies. (Brief remarks are made on new physics which is not of this type.) Most of the effects on precision measurements can be described by three gauge self-energy parameters S, T, and U. We will define these, as well as related parameters, such as ρ_0, ϵ_i, and $\widehat{\epsilon}_i$, to arise from new physics only. *I.e.*, they are equal to zero ($\rho_0 = 1$) exactly in the SM, and do not include any (loop induced) contributions that depend on m_t or M_H, which are treated separately. Our treatment differs from most of the original papers.

Many extensions of the SM can be described by the ρ_0 parameter,

$$\rho_0 \equiv \frac{M_W^2}{M_Z^2\,\widehat{c}_Z^{\,2}\,\widehat{\rho}}\,, \tag{10.52}$$

which describes new sources of SU(2) breaking that cannot be accounted for by the SM Higgs doublet or m_t effects. $\widehat{\rho}$ is calculated as in Eq. (10.13) assuming the validity of the SM. In the presence of $\rho_0 \neq 1$, Eq. (10.52) generalizes the second Eq. (10.13) while the first remains unchanged. Provided that the new physics which yields $\rho_0 \neq 1$ is a small perturbation which does not significantly affect the radiative corrections, ρ_0 can be regarded as a phenomenological parameter which multiplies G_F in Eqs. (10.19)–(10.22), (10.36), and Γ_Z in Eq. (10.42*c*). There are enough data to determine ρ_0, M_H, m_t, and α_s, simultaneously. From the global fit,

$$\rho_0 = 1.0004^{+0.0003}_{-0.0004}\,, \tag{10.53}$$

$$115.5\ {\rm GeV} \leq M_H \leq 127\ {\rm GeV}, \tag{10.54}$$

$$m_t = 173.4 \pm 1.0\ {\rm GeV}, \tag{10.55}$$

$$\alpha_s(M_Z) = 0.1195 \pm 0.0017, \tag{10.56}$$

where the limits on M_H are nominal direct search bounds at the 95% CL [173,224,227]. In addition, the LHC is not yet sensitive to very large values of $M_H > 600$ GeV which are thus not ruled out either. In this very high mass scenario, we obtain,

$$\rho_0 = 1.0024^{+0.0010}_{-0.0003} \ , \tag{10.57}$$

$$0.6 \text{ TeV} \leq M_H \leq 1.2 \text{ TeV}, \tag{10.58}$$

$$\alpha_s(M_Z) = 0.1191 \pm 0.0016, \tag{10.59}$$

with the same m_t. Finally, if the direct search results are ignored entirely one finds $M_H = 189^{+568}_{-114}$ GeV and $\rho_0 = 1.0008^{+0.0020}_{-0.0011}$. The result in Eq. (10.53) is slightly above but consistent with the SM expectation, $\rho_0 = 1$. It can be used to constrain higher-dimensional Higgs representations to have vacuum expectation values of less than a few percent of those of the doublets. Indeed, the relation between M_W and M_Z is modified if there are Higgs multiplets with weak isospin $> 1/2$ with significant vacuum expectation values. For a general (charge-conserving) Higgs structure,

$$\rho_0 = \frac{\sum_i [t(i)(t(i)+1) - t_3(i)^2]|v_i|^2}{2\sum_i t_3(i)^2 |v_i|^2}, \tag{10.60}$$

where v_i is the expectation value of the neutral component of a Higgs multiplet with weak isospin $t(i)$ and third component $t_3(i)$. In order to calculate to higher orders in such theories one must define a set of four fundamental renormalized parameters which one may conveniently choose to be α, G_F, M_Z, and M_W, since M_W and M_Z are directly measurable. Then $\widehat{s}^2_Z$ and ρ_0 can be considered dependent parameters.

Eq. (10.53) can also be used to constrain other types of new physics. For example, non-degenerate multiplets of heavy fermions or scalars break the vector part of weak SU(2) and lead to a decrease in the value of M_Z/M_W. A non-degenerate SU(2) doublet $\binom{f_1}{f_2}$ yields a positive contribution to ρ_0 [228] of

$$\frac{C\,G_F}{8\sqrt{2}\pi^2}\Delta m^2, \tag{10.61}$$

where

$$\Delta m^2 \equiv m_1^2 + m_2^2 - \frac{4m_1^2 m_2^2}{m_1^2 - m_2^2}\ln\frac{m_1}{m_2} \geq (m_1 - m_2)^2, \tag{10.62}$$

and $C = 1$ (3) for color singlets (triplets). Thus, in the presence of such multiplets,

$$\rho_0 = 1 + \frac{3\,G_F}{8\sqrt{2}\pi^2}\sum_i \frac{C_i}{3}\,\Delta m_i^2 \ , \tag{10.63}$$

where the sum includes fourth-family quark or lepton doublets, $\binom{t'}{b'}$ or $\binom{E^0}{E^-}$, right-handed (mirror) doublets, non-degenerate vector-like fermion doublets (with an extra factor of 2), and scalar doublets such as $\binom{\tilde{t}}{\tilde{b}}$ in Supersymmetry (in the absence of L–R mixing).

Eq. (10.53) taken together with Eq. (10.63) implies at the 95% CL,

$$\sum_i \frac{C_i}{3}\,\Delta m_i^2 \leq (52\ \text{GeV})^2. \tag{10.64}$$

Non-degenerate multiplets usually imply $\rho_0 > 1$. Similarly, heavy Z' bosons decrease the prediction for M_Z due to mixing and generally lead to $\rho_0 > 1$ [229]. On the other hand, additional Higgs doublets which participate in spontaneous symmetry breaking [230] or heavy lepton doublets involving Majorana neutrinos [231], both of which have more complicated expressions, as well as the vacuum expectation values of Higgs triplets or higher-dimensional representations can contribute to ρ_0 with either sign. Allowing for the presence of heavy degenerate chiral multiplets (the S parameter, to be discussed below) affects the determination of ρ_0 from the data, at present leading to a larger value (for fixed M_H).

A number of authors [232–237] have considered the general effects on neutral-current and Z and W boson observables of various types of heavy (*i.e.*, $M_{\rm new} \gg M_Z$) physics which contribute to the W and Z self-energies but which do not have any direct coupling to the ordinary fermions. In addition to non-degenerate multiplets, which break the vector part of weak SU(2), these include heavy degenerate multiplets of chiral fermions which break the axial generators. The effects of one degenerate chiral doublet are small, but in Technicolor theories there may be many chiral doublets and therefore significant effects [232].

Such effects can be described by just three parameters, S, T, and U, at the (EW) one-loop level. (Three additional parameters are needed if the new physics scale is comparable to M_Z [238]. Further generalizations, including effects relevant to LEP 2, are described in Ref. 239.) T is proportional to the difference between the W and Z self-energies at $Q^2 = 0$ (*i.e.*, vector SU(2)-breaking), while S ($S + U$) is associated with the difference between the Z (W) self-energy at $Q^2 = M_{Z,W}^2$ and $Q^2 = 0$ (axial SU(2)-breaking). Denoting the contributions of new physics to the various self-energies by $\Pi_{ij}^{\rm new}$, we have

$$\widehat{\alpha}(M_Z)T \equiv \frac{\Pi_{WW}^{\rm new}(0)}{M_W^2} - \frac{\Pi_{ZZ}^{\rm new}(0)}{M_Z^2}\ , \tag{10.65a}$$

$$\begin{aligned}\frac{\widehat{\alpha}(M_Z)}{4\,\widehat{s}_Z^2\widehat{c}_Z^2}S \equiv{}& \frac{\Pi_{ZZ}^{\rm new}(M_Z^2) - \Pi_{ZZ}^{\rm new}(0)}{M_Z^2} - \\ & \frac{\widehat{c}_Z^2 - \widehat{s}_Z^2}{\widehat{c}_Z\widehat{s}_Z}\,\frac{\Pi_{Z\gamma}^{\rm new}(M_Z^2)}{M_Z^2} - \frac{\Pi_{\gamma\gamma}^{\rm new}(M_Z^2)}{M_Z^2}\ ,\end{aligned} \tag{10.65b}$$

$$\begin{aligned}\frac{\widehat{\alpha}(M_Z)}{4\,\widehat{s}_Z^2}(S+U) \equiv{}& \frac{\Pi_{WW}^{\rm new}(M_W^2) - \Pi_{WW}^{\rm new}(0)}{M_W^2} - \\ & \frac{\widehat{c}_Z}{\widehat{s}_Z}\,\frac{\Pi_{Z\gamma}^{\rm new}(M_Z^2)}{M_Z^2} - \frac{\Pi_{\gamma\gamma}^{\rm new}(M_Z^2)}{M_Z^2}\ .\end{aligned} \tag{10.65c}$$

S, T, and U are defined with a factor proportional to $\widehat{\alpha}$ removed, so that they are expected to be of order unity in the presence of new physics. In the $\overline{\rm MS}$ scheme as defined in Ref. 66, the last two terms in Eqs. (10.65*b*) and (10.65*c*) can be omitted (as was done in some earlier editions of this *Review*). These three parameters are related to other parameters (S_i, h_i, $\widehat{\epsilon}_i$) defined in Refs. [66,233,234] by

$$\begin{aligned} T &= h_V = \widehat{\epsilon}_1/\widehat{\alpha}(M_Z), \\ S &= h_{AZ} = S_Z = 4\,\widehat{s}^2_Z\,\widehat{\epsilon}_3/\widehat{\alpha}(M_Z), \\ U &= h_{AW} - h_{AZ} = S_W - S_Z = -4\,\widehat{s}^2_Z\,\widehat{\epsilon}_2/\widehat{\alpha}(M_Z). \end{aligned} \tag{10.66}$$

A heavy non-degenerate multiplet of fermions or scalars contributes positively to T as

$$\rho_0 - 1 = \frac{1}{1 - \widehat{\alpha}(M_Z)T} - 1 \simeq \widehat{\alpha}(M_Z)T, \tag{10.67}$$

where ρ_0 is given in Eq. (10.63). The effects of non-standard Higgs representations cannot be separated from heavy non-degenerate multiplets unless the new physics has other consequences, such as vertex corrections. Most of the original papers defined T to include the effects of loops only. However, we will redefine T to include all new sources of SU(2) breaking, including non-standard Higgs, so that T and ρ_0 are equivalent by Eq. (10.67).

A multiplet of heavy degenerate chiral fermions yields

$$S = \frac{C}{3\pi}\sum_i \Big(t_{3L}(i) - t_{3R}(i)\Big)^2, \tag{10.68}$$

where $t_{3L,R}(i)$ is the third component of weak isospin of the left-(right-)handed component of fermion i and C is the number of colors. For example, a heavy degenerate ordinary or mirror family would contribute $2/3\pi$ to S. In Technicolor models with QCD-like dynamics, one expects [232] $S \sim 0.45$ for an iso-doublet of techni-fermions, assuming $N_{TC} = 4$ techni-colors, while $S \sim 1.62$ for a full techni-generation with $N_{TC} = 4$; T is harder to estimate because it is model-dependent. In these examples one has $S \geq 0$. However, the QCD-like models are excluded on other grounds (flavor changing neutral-currents, and too-light quarks and pseudo-Goldstone bosons [240]) . In particular, these estimates do not apply to models of walking Technicolor [240], for which S can be smaller or even negative [241]. Other situations in which $S < 0$, such as loops involving scalars or Majorana particles, are also possible [242]. The simplest origin of $S < 0$ would probably be an additional heavy Z' boson [229], which could mimic $S < 0$. Supersymmetric extensions of the SM generally give very small effects. See Refs. 243 and 244 and the note on "Supersymmetry" in the Searches Particle Listings for a complete set of references.

Most simple types of new physics yield $U = 0$, although there are counter-examples, such as the effects of anomalous triple gauge vertices [234].

The SM expressions for observables are replaced by

$$M_Z^2 = M_{Z0}^2 \, \frac{1 - \widehat{\alpha}(M_Z)T}{1 - G_F M_{Z0}^2 S/2\sqrt{2}\pi} \ ,$$
$$M_W^2 = M_{W0}^2 \, \frac{1}{1 - G_F M_{W0}^2 (S+U)/2\sqrt{2}\pi} \ , \tag{10.69}$$

where M_{Z0} and M_{W0} are the SM expressions (as functions of m_t and M_H) in the $\overline{\rm MS}$ scheme. Furthermore,

$$\Gamma_Z = \frac{M_Z^3 \beta_Z}{1 - \widehat{\alpha}(M_Z)T}, \qquad \Gamma_W = M_W^3 \beta_W, \qquad A_i = \frac{A_{i0}}{1 - \widehat{\alpha}(M_Z)T} \ , \tag{10.70}$$

where β_Z and β_W are the SM expressions for the reduced widths Γ_{Z0}/M_{Z0}^3 and Γ_{W0}/M_{W0}^3, M_Z and M_W are the physical masses, and A_i (A_{i0}) is a neutral-current amplitude (in the SM).

The data allow a simultaneous determination of $\widehat{s}^2_Z$ (from the Z pole asymmetries), S (from M_Z), U (from M_W), T (mainly from Γ_Z), α_s (from R_ℓ, $\sigma_{\rm had}$, and τ_τ), and m_t (from the hadron colliders), with little correlation among the SM parameters:

$$S = 0.00^{+0.11}_{-0.10},$$
$$T = 0.02^{+0.11}_{-0.12},$$
$$U = 0.08 \pm 0.11, \tag{10.71}$$

and $\widehat{s}^2_Z = 0.23125 \pm 0.00016$, $\alpha_s(M_Z) = 0.1197 \pm 0.0018$, $m_t = 173.4 \pm 1.0$ GeV, where the uncertainties are from the inputs. We have used 115.5 GeV $< M_H <$ 127 GeV which is the allowed low mass window from LEP and the LHC. The SM parameters (U) can be determined with no (little) M_H dependence. On the other hand, S, T, and M_H cannot be obtained simultaneously from the precision data alone, because the Higgs boson loops themselves are resembled approximately by oblique effects. Negative (positive) contributions to the S (T) parameter can weaken or entirely remove the strong constraints on M_H from the SM fits. Specific models in which a large M_H is compensated by new physics are reviewed in Ref. 245. The parameters in Eqs. (10.71), which by definition are due to new physics only, are in reasonable agreement with the SM values of zero. Fixing $U = 0$ (as is also done in Fig. 10.7) moves S and T slightly upwards,

$$S = 0.04 \pm 0.09,$$
$$T = 0.07 \pm 0.08. \tag{10.72}$$

The correlation between S and T in this fit amounts to 88%.

Using Eq. (10.67), the value of ρ_0 corresponding to T in Eq. (10.71) is 1.0001 ± 0.0009, while the one corresponding to Eq. (10.72) is $1.0005^{+0.0007}_{-0.0006}$. The values of the $\widehat{\epsilon}$ parameters defined in Eq. (10.66) are

$$\begin{aligned} \widehat{\epsilon}_3 &= \ \ 0.0000 \pm 0.0008, \\ \widehat{\epsilon}_1 &= \ \ 0.0001 \pm 0.0009 \\ \widehat{\epsilon}_2 &= -0.0006 \pm 0.0009. \end{aligned} \tag{10.73}$$

Unlike the original definition, we defined the quantities in Eqs. (10.73) to vanish identically in the absence of new physics and to correspond directly to the parameters S, T, and U in Eqs. (10.71). There is a strong correlation (89%) between the S and T parameters. The U parameter is -49% (-70%) anti-correlated with S (T). The allowed regions in S–T are shown in Fig. 10.7. From Eqs. (10.71) one obtains $S \leq 0.17$ and $T \leq 0.20$ at 95% CL.

If one assumes that the excess Higgs candidates seen at the LHC are statistical fluctuations then (in the presence of new physics significantly affecting gauge boson self-energies) there is still the possibility for a heavy Higgs scenario. If one fixes $M_H = 600$ GeV (as is still allowed by direct searches) and requires the constraint $S \geq 0$ (as is appropriate in QCD-like Technicolor models) then $S \leq 0.13$ (Bayesian) or $S \leq 0.11$ (frequentist). This rules out simple Technicolor models with many techni-doublets and QCD-like dynamics.

The S parameter can also be used to constrain the number of fermion families, *under the assumption* that there are no new contributions to T or U and therefore that any new families are degenerate; then an extra generation of SM fermions is excluded at the 5.7 σ level corresponding to $N_F = 2.91^{+0.19}_{-0.25}$ (with M_H in the allowed low mass window). This is in agreement with a fit to the number of light neutrinos, $N_\nu = 2.989 \pm 0.007$. However, the S parameter fits are valid even for a very heavy fourth family neutrino. This restriction can be relaxed by allowing T to vary as well, since $T > 0$ is expected from a non-degenerate extra family. Fixing $S = 2/3\pi$, the global fit favors a fourth family contribution to T of 0.21 ± 0.04. However, the quality of the fit deteriorates ($\Delta\chi^2 = 3.8$ relative to the SM fit with M_H forced not to drop below its ATLAS bound of 115.5 GeV) so that this tuned T scenario is also disfavored but less so than in the past. In fact, tuned mass splittings of the extra leptons and quarks [246] can yield fits with only moderately higher χ^2 values (by about 1 unit) than for the SM. A more detailed analysis is also required if the extra neutrino (or the extra down-type quark) is close to its direct mass limit [247]. Thus, a fourth family is disfavored but not excluded by the current EW precision data. Similar remarks apply to a heavy mirror family [248] involving right-handed SU(2) doublets and left-handed singlets. A more recent and detailed discussion can be found in Ref. 249. One important consequence of a heavy fourth family is to increase the Higgs production cross section by gluon fusion by a factor ~ 9, which considerably strengthens the exclusion limits from direct searches at the Tevatron [250] and LHC [251]. Additional heavy ordinary or mirror generations may also require large Yukawa and Higgs couplings that may lead to Landau poles at low scales [252]. In contrast, heavy degenerate non-chiral (also known as vector-like or

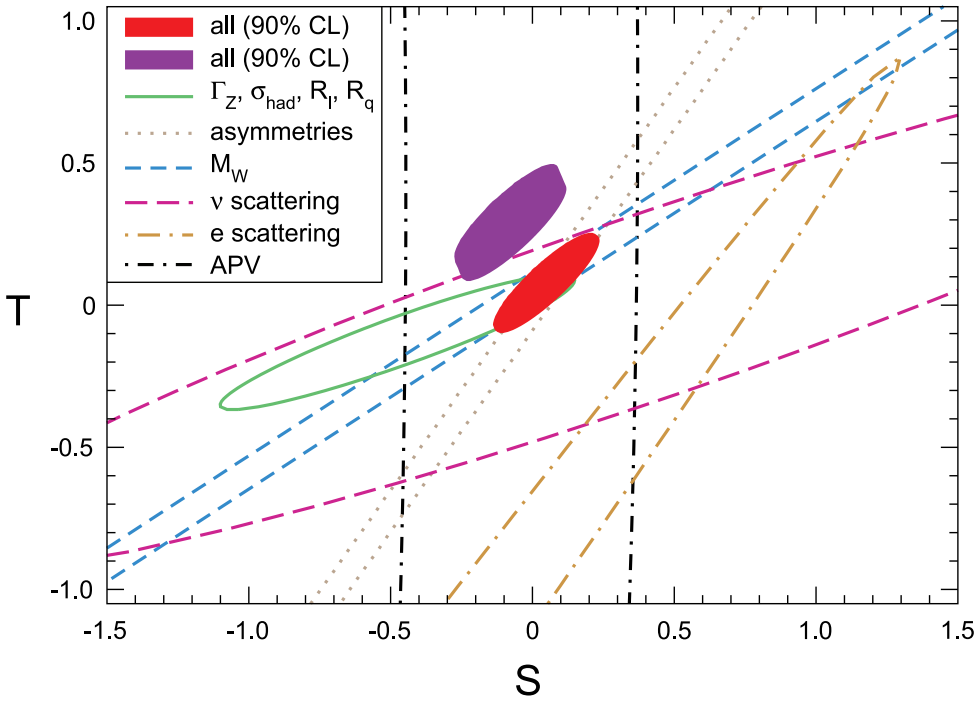

Figure 10.7: 1 σ constraints (39.35%) on S and T from various inputs combined with M_Z. S and T represent the contributions of new physics only. (Uncertainties from m_t are included in the errors.) The contours assume 115.5 GeV $< M_H <$ 127 GeV except for the larger (violet) one for all data which is for 600 GeV $< M_H <$ 1 TeV. Data sets not involving M_W are insensitive to U. Due to higher order effects, however, $U = 0$ has to be assumed in all fits. α_s is constrained using the τ lifetime as additional input in all fits. The long-dashed (magenta) contour from ν scattering is now consistent with the global average (see Sec. 10.3). The long-dash-dotted (orange) contour from polarized e scattering [129,131] is the upper tip of an elongated ellipse centered at around $S = -14$ and $T = -20$. At first sight it looks as if it is deviating strongly but it is off by only 1.8 σ. This illusion arises because $\Delta\chi^2 > 0.77$ everywhere on the visible part of the contour.

exotic) multiplets, which are predicted in many grand unified theories [253] and other extensions of the SM, do not contribute to S, T, and U (or to ρ_0), and do not require large coupling constants. Such exotic multiplets may occur in partial families, as in E_6 models, or as complete vector-like families [254].

There is no simple parametrization to describe the effects of every type of new physics on every possible observable. The S, T, and U formalism describes many types of heavy physics which affect only the gauge self-energies, and it can be applied to all precision observables. However, new physics which couples directly to ordinary fermions, such as heavy Z' bosons [229], mixing with exotic fermions [255], or leptoquark exchange [172,256] cannot be fully parametrized in the S, T, and U framework. It is convenient to treat these types of new physics by parameterizations that are specialized

to that particular class of theories (*e.g.*, extra Z' bosons), or to consider specific models (which might contain, *e.g.,* Z' bosons and exotic fermions with correlated parameters). Fits to Supersymmetric models are described in Ref. 244. Models involving strong dynamics (such as (extended) Technicolor) for EW breaking are considered in Ref. 257. The effects of compactified extra spatial dimensions at the TeV scale are reviewed in Ref. 258, and constraints on Little Higgs models in Ref. 259. The implications of non-standard Higgs sectors, e.g., involving Higgs singlets or triplets, are discussed in Ref. 260, while additional Higgs doublets are considered in Ref. 230. Limits on new four-Fermi operators and on leptoquarks using LEP 2 and lower energy data are given in Refs. 172 and 261. Constraints on various types of new physics are reviewed in Refs. [7,128,149,161,262,263], and implications for the LHC in Ref. 264.

An alternate formalism [265] defines parameters, ϵ_1, ϵ_2, ϵ_3, and ϵ_b in terms of the specific observables M_W/M_Z, $\Gamma_{\ell\ell}$, $A_{FB}^{(0,\ell)}$, and R_b. The definitions coincide with those for $\widehat{\epsilon}_i$ in Eqs. (10.65) and (10.66) for physics which affects gauge self-energies only, but the ϵ's now parametrize arbitrary types of new physics. However, the ϵ's are not related to other observables unless additional model-dependent assumptions are made. Another approach [266] parametrizes new physics in terms of gauge-invariant sets of operators. It is especially powerful in studying the effects of new physics on non-Abelian gauge vertices. The most general approach introduces deviation vectors [262]. Each type of new physics defines a deviation vector, the components of which are the deviations of each observable from its SM prediction, normalized to the experimental uncertainty. The length (direction) of the vector represents the strength (type) of new physics.

One of the best motivated kinds of physics beyond the SM besides Supersymmetry are extra Z' bosons [267]. They do not spoil the observed approximate gauge coupling unification, and appear copiously in many Grand Unified Theories (GUTs), most Superstring models [268], as well as in dynamical symmetry breaking [257] and Little Higgs models [259]. For example, the SO(10) GUT contains an extra U(1) as can be seen from its maximal subgroup, $\mathrm{SU}(5) \times \mathrm{U}(1)_\chi$. Similarly, the E_6 GUT contains the subgroup $\mathrm{SO}(10) \times \mathrm{U}(1)_\psi$. The Z_ψ possesses only axial-vector couplings to the ordinary fermions, and its mass is generally less constrained. The Z_η boson is the linear combination $\sqrt{3/8}\, Z_\chi - \sqrt{5/8}\, Z_\psi$. The Z_{LR} boson occurs in left-right models with gauge group $\mathrm{SU}(3)_C \times \mathrm{SU}(2)_L \times \mathrm{SU}(2)_R \times \mathrm{U}(1)_{B-L} \subset \mathrm{SO}(10)$, and the secluded Z_S emerges in a supersymmetric bottom-up scenario [269]. The sequential Z_{SM} boson is defined to have the same couplings to fermions as the SM Z boson. Such a boson is not expected in the context of gauge theories unless it has different couplings to exotic fermions than the ordinary Z boson. However, it serves as a useful reference case when comparing constraints from various sources. It could also play the role of an excited state of the ordinary Z boson in models with extra dimensions at the weak scale [258]. Finally, we consider a Superstring motivated Z_{string} boson appearing in a specific model [270]. The potential Z' boson is in general a superposition of the SM Z and the new boson

Table 10.9: 95% CL lower mass limits (in GeV) from low energy and Z pole data on various extra Z' gauge bosons, appearing in models of unification and string theory. More general parametrizations are described in Refs. 267 and 272. The EW results [273] are for Higgs sectors consisting of doublets and singlets only ($\rho_0 = 1$) with unspecified $U(1)'$ charges. The next two columns show the limits from ATLAS [274] and CMS [275] from the combination of both lepton channels. The CDF [276] and DØ [277] bounds from searches for $\bar{p}p \to \mu^+\mu^-$ and e^+e^-, respectively, are listed in the next two columns, followed by the LEP 2 $e^+e^- \to f\bar{f}$ bounds [172] (assuming $\theta = 0$). The Tevatron bounds would be moderately weakened if there are open supersymmetric or exotic decay channels [278]. The last column shows the 1 σ ranges for M_H when it is left unconstrained in the EW fits.

Z'	EW	ATLAS	CMS	CDF	DØ	LEP 2	M_H
Z_χ	1,141	1,640	–	930	903	673	$171^{+493}_{-\ 89}$
Z_ψ	147	1,490	1,620	917	891	481	$97^{+\ 31}_{-\ 25}$
Z_η	427	1,540	–	938	923	434	423^{+577}_{-350}
Z_{LR}	998	–	–	–	–	804	$804^{+174}_{-\ 35}$
Z_S	1,257	1,600	–	858	822	–	$149^{+353}_{-\ 68}$
Z_{SM}	1,403	1,830	1,940	1,071	1,023	1,787	331^{+669}_{-246}
$Z_{\rm string}$	1,362	–	–	–	–	–	$134^{+209}_{-\ 58}$

associated with the extra U(1). The mixing angle θ satisfies,

$$\tan^2\theta = \frac{M^2_{Z^0_1} - M^2_Z}{M^2_{Z'} - M^2_{Z^0_1}} \ ,$$

where $M_{Z^0_1}$ is the SM value for M_Z in the absence of mixing. Note, that $M_Z < M_{Z^0_1}$, and that the SM Z couplings are changed by the mixing. The couplings of the heavier Z' may also be modified by kinetic mixing [267,271]. If the Higgs $U(1)'$ quantum numbers are known, there will be an extra constraint,

$$\theta = C\,\frac{g_2}{g_1}\,\frac{M^2_Z}{M^2_{Z'}} \ ,$$

where $g_{1,2}$ are the U(1) and $U(1)'$ gauge couplings with $g_2 = \sqrt{\frac{5}{3}}\sin\theta_W\sqrt{\lambda}\,g_1$ and $g_1 = \sqrt{g^2 + g'^2}$. $\lambda \sim 1$ (which we assume) if the GUT group breaks directly to $SU(3)\times SU(2)\times U(1)\times U(1)'$. C is a function of vacuum expectation values. For minimal Higgs sectors it can be found in Ref. 229. Table 10.9 shows the 95% CL lower mass

limits [273] for $\rho_0 = 1$ and 114.4 GeV $\leq M_H \leq 1$ TeV. The last column shows the 1 σ ranges for M_H when it is left unconstrained. In cases of specific minimal Higgs sectors where C is known, the Z' mass limits from the EW precision data are generally pushed into the TeV region in which case they are still competitive with those from the LHC, and they are also competitive in the case of large g_2 [279]. The limits on $|\theta|$ are typically smaller than a few $\times 10^{-3}$. For more details see [267,273,280,281] and the note on "The Z' Searches" in the Gauge & Higgs Boson Particle Listings. Also listed in Table 10.9 are the direct lower limits on Z' production from the LHC [274,275] and the Tevatron [276,277], as well as the LEP 2 bounds [172].

Acknowledgments:

We are indebted to M. Davier, B. Malaescu, and K. Maltman for providing us with additional information about their work in a form suitable to be included in our fits. We also thank R. H. Bernstein, K. S. McFarland, H. Schellman, and G. P. Zeller for discussions on the NuTeV analysis. This work was supported in part by CONACyT (México) contract 82291–F and by PASPA (DGAPA–UNAM).

References:

1. S. L. Glashow, Nucl. Phys. **22**, 579 (1961);
   S. Weinberg, Phys. Rev. Lett. **19**, 1264 (1967);
   A. Salam, p. 367 of *Elementary Particle Theory*, ed. N. Svartholm (Almquist and Wiksells, Stockholm, 1969);
   S.L. Glashow, J. Iliopoulos, and L. Maiani, Phys. Rev. **D2**, 1285 (1970).
2. CKMfitter Group: J. Charles *et al.*, Eur. Phys. J. **C41**, 1 (2005);
   CKMfitter Group: S. T'Jampens *et al.*, PoS **ICHEP2010**, 269 (2010).
3. For reviews, see the Section on "Higgs Bosons: Theory and Searches" in this *Review*;
   J. Gunion *et al.*, *The Higgs Hunter's Guide*, (Addison-Wesley, Redwood City, 1990);
   M. Carena and H.E. Haber, Prog. in Part. Nucl. Phys. **50**, 63 (2003);
   A. Djouadi, Phys. Reports **457**, 1 (2008).
4. For reviews, see E.D. Commins and P.H. Bucksbaum, *Weak Interactions of Leptons and Quarks*, (Cambridge Univ. Press, 1983);
   G. Barbiellini and C. Santoni, Riv. Nuovo Cimento **9(2)**, 1 (1986);
   N. Severijns, M. Beck, and O. Naviliat-Cuncic, Rev. Mod. Phys. **78**, 991 (2006);
   W. Fetscher and H.J. Gerber, p. 657 of Ref. 5;
   J. Deutsch and P. Quin, p. 706 of Ref. 5;
   P. Herczeg, p. 786 of Ref. 5;
   P. Herczeg, Prog. in Part. Nucl. Phys. **46**, 413 (2001).
5. *Precision Tests of the Standard Electroweak Model*, ed. P. Langacker (World Scientific, Singapore, 1995).
6. J. Erler and M.J. Ramsey-Musolf, Prog. in Part. Nucl. Phys. **54**, 351 (2005).
7. P. Langacker, *The Standard Model and Beyond*, (CRC Press, New York, 2009).
8. T. Kinoshita, *Quantum Electrodynamics*, (World Scientific, Singapore, 1990).
9. S. G. Karshenboim, Phys. Reports **422**, 1 (2005).

10. P.J. Mohr, B.N. Taylor, and D.B. Newell, Rev. Mod. Phys. **80**, 633 (2008); for updates see `http://physics.nist.gov/cuu/Constants/`.
11. ALEPH, DELPHI, L3, OPAL, SLD, LEP Electroweak Working Group, SLD Electroweak and Heavy Flavour Groups: S. Schael *et al.*, Phys. Reports **427**, 257 (2006); for updates see `http://lepewwg.web.cern.ch/LEPEWWG/`.
12. MuLan: D. M. Webber *et al.*, Phys. Rev. Lett. **106**, 041803 (2011).
13. T. Kinoshita and A. Sirlin, Phys. Rev. **113**, 1652 (1959).
14. T. van Ritbergen and R.G. Stuart, Nucl. Phys. **B564**, 343 (2000); M. Steinhauser and T. Seidensticker, Phys. Lett. **B467**, 271 (1999).
15. Y. Nir, Phys. Lett. **B221**, 184 (1989).
16. A. Pak and A. Czarnecki, Phys. Rev. Lett. **100**, 241807 (2008).
17. For a review, see S. Mele, `arXiv:hep-ex/0610037`.
18. S. Fanchiotti, B. Kniehl, and A. Sirlin, Phys. Rev. **D48**, 307 (1993) and references therein.
19. J. Erler, Phys. Rev. **D59**, 054008 (1999).
20. M. Davier *et al.*, Eur. Phys. J. **C71**, 1515 (2011); the quoted value uses additional information thankfully provided to us by the authors in a private communication.
21. J. Erler, `hep-ph/0005084`.
22. M. Steinhauser, Phys. Lett. **B429**, 158 (1998).
23. A.D. Martin and D. Zeppenfeld, Phys. Lett. **B345**, 558 (1995).
24. S. Eidelman and F. Jegerlehner, Z. Phys. **C67**, 585 (1995).
25. B.V. Geshkenbein and V.L. Morgunov, Phys. Lett. **B352**, 456 (1995).
26. H. Burkhardt and B. Pietrzyk, Phys. Lett. **B356**, 398 (1995).
27. M.L. Swartz, Phys. Rev. **D53**, 5268 (1996).
28. R. Alemany, M. Davier, and A. Höcker, Eur. Phys. J. **C2**, 123 (1998).
29. N.V. Krasnikov and R. Rodenberg, Nuovo Cimento **111A**, 217 (1998).
30. M. Davier and A. Höcker, Phys. Lett. **B419**, 419 (1998).
31. J.H. Kühn and M. Steinhauser, Phys. Lett. **B437**, 425 (1998).
32. M. Davier and A. Höcker, Phys. Lett. **B435**, 427 (1998).
33. S. Groote *et al.*, Phys. Lett. **B440**, 375 (1998).
34. A.D. Martin, J. Outhwaite, and M.G. Ryskin, Phys. Lett. **B492**, 69 (2000).
35. H. Burkhardt and B. Pietrzyk, Phys. Lett. **B513**, 46 (2001).
36. J.F. de Troconiz and F.J. Yndurain, Phys. Rev. **D65**, 093002 (2002).
37. F. Jegerlehner, Nucl. Phys. Proc. Suppl. **126**, 325 (2004).
38. K. Hagiwara *et al.*, Phys. Rev. **D69**, 093003 (2004).
39. H. Burkhardt and B. Pietrzyk, Phys. Rev. **D72**, 057501 (2005).
40. K. Hagiwara *et al.*, Phys. Lett. **B649**, 173 (2007).
41. F. Jegerlehner, Nucl. Phys. Proc. Suppl. **181**, 135 (2008).
42. K. Hagiwara *et al.*, J. Phys. **G38**, 085003 (2011).
43. OPAL: K. Ackerstaff *et al.*, Eur. Phys. J. **C7**, 571 (1999).
44. CLEO: S. Anderson *et al.*, Phys. Rev. **D61**, 112002 (2000).
45. ALEPH: S. Schael *et al.*, Phys. Reports **421**, 191 (2005).
46. Belle: M. Fujikawa *et al.*: Phys. Rev. **D78**, 072006 (2008).

47. CMD-2: R.R. Akhmetshin *et al.*, Phys. Lett. **B578**, 285 (2004);
CMD-2: V.M. Aulchenko *et al.*, JETP Lett. **82**, 743 (2005);
CMD-2: R.R. Akhmetshin *et al.*, JETP Lett. **84**, 413 (2006);
CMD-2: R.R. Akhmetshin *et al.*, Phys. Lett. **B648**, 28 (2007).
48. SND: M.N. Achasov *et al.*, Sov. Phys. JETP **103**, 380 (2006).
49. A.B. Arbuzov *et al.*, JHEP **9812**, 009 (1998);
S. Binner, J.H. Kühn, and K. Melnikov, Phys. Lett. **B459**, 279 (1999).
50. BaBar: B. Aubert *et al.*, Phys. Rev. **D70**, 072004 (2004);
BaBar: B. Aubert *et al.*, Phys. Rev. **D71**, 052001 (2005);
BaBar: B. Aubert *et al.*, Phys. Rev. **D73**, 052003 (2006);
BaBar: B. Aubert *et al.*, Phys. Rev. **D76**, 092005 (2007);
BaBar: B. Aubert *et al.*, Phys. Rev. Lett. **103**, 231801 (2009).
51. KLOE: F. Ambrosino *et al.*, Phys. Lett. **B670**, 285 (2009);
KLOE: F. Ambrosino *et al.*, Phys. Lett. **B700**, 102 (2011).
52. See *e.g.*, CMD and OLYA: L.M. Barkov *et al.*, Nucl. Phys. **B256**, 365 (1985).
53. V.A. Novikov *et al.*, Phys. Reports **41**, 1 (1978).
54. J. Erler and M. Luo, Phys. Lett. **B558**, 125 (2003).
55. K. G. Chetyrkin *et al.*, Phys. Rev. **D80**, 074010 (2009).
56. Tevatron Electroweak Working Group, CDF and DØ: `arXiv:1107.5255 [hep-ex]`.
57. CMS: `cdsweb.cern.ch/record/1356578/files/TOP-10-009-pas.pdf`.
58. ATLAS: `cdsweb.cern.ch/record/1376412/files/ATLAS-CONF-2011-120.pdf`.
59. M. Beneke, Phys. Reports **317**, 1 (1999).
60. K. G. Chetyrkin and M. Steinhauser, Nucl. Phys. **B573**, 617 (2000);
K. Melnikov and T. van Ritbergen, Phys. Lett. **B482**, 99 (2000).
61. S.J. Brodsky, G.P. Lepage, and P.B. Mackenzie, Phys. Rev. **D28**, 228 (1983).
62. N. Gray *et al.*, Z. Phys. **C48**, 673 (1990).
63. A. Sirlin, Phys. Rev. **D22**, 971 (1980);
D.C. Kennedy *et al.*, Nucl. Phys. **B321**, 83 (1989);
D.Yu. Bardin *et al.*, Z. Phys. **C44**, 493 (1989);
W. Hollik, Fortsch. Phys. **38**, 165 (1990);
for reviews, see W. Hollik, pp. 37 and 117, and W. Marciano, p. 170 of Ref. 5.
64. V.A. Novikov, L.B. Okun, and M.I. Vysotsky, Nucl. Phys. **B397**, 35 (1993).
65. W. Hollik in Ref. 63 and references therein.
66. W.J. Marciano and J.L. Rosner, Phys. Rev. Lett. **65**, 2963 (1990).
67. G. Degrassi, S. Fanchiotti, and A. Sirlin, Nucl. Phys. **B351**, 49 (1991).
68. G. Degrassi and A. Sirlin, Nucl. Phys. **B352**, 342 (1991).
69. P. Gambino and A. Sirlin, Phys. Rev. **D49**, 1160 (1994).
70. ZFITTER: A.B. Arbuzov *et al.*, Comput. Phys. Commun. **174**, 728 (2006) and references therein.
71. R. Barbieri *et al.*, Nucl. Phys. **B409**, 105 (1993).
72. J. Fleischer, O.V. Tarasov, and F. Jegerlehner, Phys. Lett. **B319**, 249 (1993).
73. G. Degrassi, P. Gambino, and A. Vicini, Phys. Lett. **B383**, 219 (1996);
G. Degrassi, P. Gambino, and A. Sirlin, Phys. Lett. **B394**, 188 (1997).

74. A. Freitas *et al.*, Phys. Lett. **B495**, 338 (2000) and *ibid.*, **570**, 260(E) (2003); M. Awramik and M. Czakon, Phys. Lett. **B568**, 48 (2003).
75. A. Freitas *et al.*, Nucl. Phys. **B632**, 189 (2002) and *ibid.*, **666**, 305(E) (2003); M. Awramik and M. Czakon, Phys. Rev. Lett. **89**, 241801 (2002); A. Onishchenko and O. Veretin, Phys. Lett. **B551**, 111 (2003).
76. M. Awramik *et al.*, Phys. Rev. Lett. **93**, 201805 (2004); W. Hollik, U. Meier, and S. Uccirati, Nucl. Phys. **B731**, 213 (2005).
77. M. Awramik, M. Czakon, and A. Freitas, JHEP **0611**, 048 (2006); W. Hollik, U. Meier, and S. Uccirati, Nucl. Phys. **B765**, 154 (2007).
78. A. Djouadi and C. Verzegnassi, Phys. Lett. **B195**, 265 (1987); A. Djouadi, Nuovo Cimento **100A**, 357 (1988).
79. K.G. Chetyrkin, J.H. Kühn, and M. Steinhauser, Phys. Lett. **B351**, 331 (1995); L. Avdeev *et al.*, Phys. Lett. **B336**, 560 (1994) and *ibid.*, **B349**, 597(E) (1995).
80. B.A. Kniehl, J.H. Kühn, and R.G. Stuart, Phys. Lett. **B214**, 621 (1988); B.A. Kniehl, Nucl. Phys. **B347**, 86 (1990); F. Halzen and B.A. Kniehl, Nucl. Phys. **B353**, 567 (1991); A. Djouadi and P. Gambino, Phys. Rev. **D49**, 3499 (1994) and *ibid.*, **53**, 4111(E) (1996).
81. K.G. Chetyrkin, J.H. Kühn, and M. Steinhauser, Phys. Rev. Lett. **75**, 3394 (1995).
82. J.J. van der Bij *et al.*, Phys. Lett. **B498**, 156 (2001).
83. M. Faisst *et al.*, Nucl. Phys. **B665**, 649 (2003).
84. R. Boughezal, J.B. Tausk, and J.J. van der Bij, Nucl. Phys. **B725**, 3 (2005).
85. A. Anselm, N. Dombey, and E. Leader, Phys. Lett. **B312**, 232 (1993).
86. Y. Schröder and M. Steinhauser, Phys. Lett. **B622**, 124 (2005).
87. K.G. Chetyrkin *et al.*, Phys. Rev. Lett. **97**, 102003 (2006); R. Boughezal and M. Czakon, Nucl. Phys. **B755**, 221 (2006).
88. J. Fleischer *et al.*, Phys. Lett. **B293**, 437 (1992); K.G. Chetyrkin, A. Kwiatkowski, and M. Steinhauser, Mod. Phys. Lett. **A8**, 2785 (1993).
89. R. Harlander, T. Seidensticker, and M. Steinhauser, Phys. Lett. **B426**, 125 (1998); J. Fleischer *et al.*, Phys. Lett. **B459**, 625 (1999).
90. M. Awramik *et al.*, Nucl. Phys. **B813**, 174 (2009).
91. A. Czarnecki and J.H. Kühn, Phys. Rev. Lett. **77**, 3955 (1996).
92. Gfitter: H. Flacher *et al.*, Eur. Phys. J. **C60**, 543 (2009).
93. J.M. Conrad, M.H. Shaevitz, and T. Bolton, Rev. Mod. Phys. **70**, 1341 (1998).
94. Z. Berezhiani and A. Rossi, Phys. Lett. **B535**, 207 (2002); S. Davidson *et al.*, JHEP **0303**, 011 (2003); A. Friedland, C. Lunardini and C. Pena-Garay, Phys. Lett. **B594**, 347 (2004).
95. J. Panman, p. 504 of Ref. 5.
96. CHARM: J. Dorenbosch *et al.*, Z. Phys. **C41**, 567 (1989).
97. CALO: L.A. Ahrens *et al.*, Phys. Rev. **D41**, 3297 (1990).
98. CHARM II: P. Vilain *et al.*, Phys. Lett. **B335**, 246 (1994).
99. ILM: R.C. Allen *et al.*, Phys. Rev. **D47**, 11 (1993); LSND: L.B. Auerbach *et al.*, Phys. Rev. **D63**, 112001 (2001).

100. TEXONO: M. Deniz *et al.*, Phys. Rev. **D81**, 072001 (2010).
101. For reviews, see G.L. Fogli and D. Haidt, Z. Phys. **C40**, 379 (1988); F. Perrier, p. 385 of Ref. 5.
102. CDHS: A. Blondel *et al.*, Z. Phys. **C45**, 361 (1990).
103. CHARM: J.V. Allaby *et al.*, Z. Phys. **C36**, 611 (1987).
104. CCFR: K.S. McFarland *et al.*, Eur. Phys. J. **C1**, 509 (1998).
105. R.M. Barnett, Phys. Rev. **D14**, 70 (1976); H. Georgi and H.D. Politzer, Phys. Rev. **D14**, 1829 (1976).
106. LAB-E: S.A. Rabinowitz *et al.*, Phys. Rev. Lett. **70**, 134 (1993).
107. E.A. Paschos and L. Wolfenstein, Phys. Rev. **D7**, 91 (1973).
108. NuTeV: G.P. Zeller *et al.*, Phys. Rev. Lett. **88**, 091802 (2002).
109. D. Mason *et al.*, Phys. Rev. Lett. **99**, 192001 (2007).
110. S. Kretzer, D. Mason, and F. Olness, Phys. Rev. **D65**, 074010 (2002).
111. J. Pumplin *et al.*, JHEP **0207**, 012 (2002); S. Kretzer *et al.*, Phys. Rev. Lett. **93**, 041802 (2004).
112. S. Alekhin, S.A. Kulagin, and R. Petti, Phys. Lett. **B675**, 433 (2009).
113. W. Bentz *et al.*, Phys. Lett. **B693**, 462 (2010).
114. E. Sather, Phys. Lett. **B274**, 433 (1992); E.N. Rodionov, A.W. Thomas, and J.T. Londergan, Mod. Phys. Lett. **A9**, 1799 (1994).
115. A.D. Martin *et al.*, Eur. Phys. J. **C35**, 325 (2004).
116. J.T. Londergan and A.W. Thomas, Phys. Rev. **D67**, 111901 (2003).
117. M. Glück, P. Jimenez-Delgado, and E. Reya, Phys. Rev. Lett. **95**, 022002 (2005).
118. S. Kumano, Phys. Rev. **D66**, 111301 (2002); S.A. Kulagin, Phys. Rev. **D67**, 091301 (2003); S.J. Brodsky, I. Schmidt, and J.J. Yang, Phys. Rev. **D70**, 116003 (2004); M. Hirai, S. Kumano, and T. H. Nagai, Phys. Rev. **D71**, 113007 (2005); G.A. Miller and A.W. Thomas, Int. J. Mod. Phys. A **20**, 95 (2005).
119. I.C. Cloet, W. Bentz, and A.W. Thomas, Phys. Rev. Lett. **102**, 252301 (2009).
120. K.P.O. Diener, S. Dittmaier, and W. Hollik, Phys. Rev. **D69**, 073005 (2004); A.B. Arbuzov, D.Y. Bardin, and L.V. Kalinovskaya, JHEP **0506**, 078 (2005); K. Park, U. Baur, and D. Wackeroth, `arXiv:0910.5013 [hep-ph]`.
121. K.P.O. Diener, S. Dittmaier, and W. Hollik, Phys. Rev. **D72**, 093002 (2005).
122. B.A. Dobrescu and R.K. Ellis, Phys. Rev. **D69**, 114014 (2004).
123. For a review, see S. Davidson *et al.*, JHEP **0202**, 037 (2002).
124. SSF: C.Y. Prescott *et al.*, Phys. Lett. **B84**, 524 (1979).
125. E.J. Beise, M.L. Pitt, and D.T. Spayde, Prog. in Part. Nucl. Phys. **54**, 289 (2005).
126. S.L. Zhu *et al.*, Phys. Rev. **D62**, 033008 (2000).
127. P. Souder, p. 599 of Ref. 5.
128. P. Langacker, p. 883 of Ref. 5.
129. R.D. Young *et al.*, Phys. Rev. Lett. **99**, 122003 (2007).
130. E. Derman and W.J. Marciano, Annals Phys. **121**, 147 (1979).
131. E158: P.L. Anthony *et al.*, Phys. Rev. Lett. **95**, 081601 (2005).
132. J. Erler and M.J. Ramsey-Musolf, Phys. Rev. **D72**, 073003 (2005).

133. A. Czarnecki and W.J. Marciano, Int. J. Mod. Phys. A **15**, 2365 (2000).
134. K.S. McFarland, in the *Proceedings of DIS* 2008.
135. C. Bouchiat and C.A. Piketty, Phys. Lett. **B128**, 73 (1983).
136. Qweak: M.T. Gericke *et al.*, AIP Conf. Proc. **1149**, 237 (2009);
the implications are discussed in Ref. 149.
137. For reviews and references to earlier work, see M.A. Bouchiat and L. Pottier, Science **234**, 1203 (1986);
B.P. Masterson and C.E. Wieman, p. 545 of Ref. 5.
138. Cesium (Boulder): C.S. Wood *et al.*, Science **275**, 1759 (1997).
139. Cesium (Paris): J. Guéna, M. Lintz, and M.A. Bouchiat, Phys. Rev. **A71**, 042108 (2005).
140. Thallium (Oxford): N.H. Edwards *et al.*, Phys. Rev. Lett. **74**, 2654 (1995);
Thallium (Seattle): P.A. Vetter *et al.*, Phys. Rev. Lett. **74**, 2658 (1995).
141. Lead (Seattle): D.M. Meekhof *et al.*, Phys. Rev. Lett. **71**, 3442 (1993).
142. Bismuth (Oxford): M.J.D. MacPherson *et al.*, Phys. Rev. Lett. **67**, 2784 (1991).
143. V.A. Dzuba, V.V. Flambaum, and O.P. Sushkov, Phys. Lett. **141A**, 147 (1989);
S.A. Blundell, J. Sapirstein, and W.R. Johnson, Phys. Rev. **D45**, 1602 (1992);
For reviews, see S.A. Blundell, W.R. Johnson, and J. Sapirstein, p. 577 of Ref. 5;
J.S.M. Ginges and V.V. Flambaum, Phys. Reports **397**, 63 (2004);
J. Guéna, M. Lintz, and M. A. Bouchiat, Mod. Phys. Lett. **A20**, 375 (2005);
A. Derevianko and S.G. Porsev, Eur. Phys. J. A **32**, 517 (2007).
144. V.A. Dzuba, V.V. Flambaum, and O.P. Sushkov, Phys. Rev. **A56**, R4357 (1997).
145. S.C. Bennett and C.E. Wieman, Phys. Rev. Lett. **82**, 2484 (1999).
146. M.A. Bouchiat and J. Guéna, J. Phys. (France) **49**, 2037 (1988).
147. S. G. Porsev, K. Beloy, and A. Derevianko, Phys. Rev. Lett. **102**, 181601 (2009).
148. A. Derevianko, Phys. Rev. Lett. **85**, 1618 (2000);
V.A. Dzuba, C. Harabati, and W.R. Johnson, Phys. Rev. **A63**, 044103 (2001);
M.G. Kozlov, S.G. Porsev, and I.I. Tupitsyn, Phys. Rev. Lett. **86**, 3260 (2001);
W.R. Johnson, I. Bednyakov, and G. Soff, Phys. Rev. Lett. **87**, 233001 (2001);
A.I. Milstein and O.P. Sushkov, Phys. Rev. **A66**, 022108 (2002);
V.A. Dzuba, V.V. Flambaum, and J.S. Ginges, Phys. Rev. **D66**, 076013 (2002);
M.Y. Kuchiev and V.V. Flambaum, Phys. Rev. Lett. **89**, 283002 (2002);
A.I. Milstein, O.P. Sushkov, and I.S. Terekhov, Phys. Rev. Lett. **89**, 283003 (2002);
V.V. Flambaum and J.S.M. Ginges, Phys. Rev. **A72**, 052115 (2005).
149. J. Erler, A. Kurylov, and M.J. Ramsey-Musolf, Phys. Rev. **D68**, 016006 (2003).
150. P.G. Blunden, W. Melnitchouk, and A.W. Thomas, Phys. Rev. Lett. **107**, 081801 (2011).
151. V.A. Dzuba *et al.*, J. Phys. **B20**, 3297 (1987).
152. Ya.B. Zel'dovich, Sov. Phys. JETP **6**, 1184 (1958);
for recent discussions, see V.V. Flambaum and D.W. Murray, Phys. Rev. **C56**, 1641 (1997);
W.C. Haxton and C.E. Wieman, Ann. Rev. Nucl. Part. Sci. **51**, 261 (2001).
153. J.L. Rosner, Phys. Rev. **D53**, 2724 (1996).

154. S.J. Pollock, E.N. Fortson, and L. Wilets, Phys. Rev. **C46**, 2587 (1992); B.Q. Chen and P. Vogel, Phys. Rev. **C48**, 1392 (1993).
155. R.W. Dunford and R.J. Holt, J. Phys. **G34**, 2099 (2007).
156. O.O. Versolato *et al.*, Hyperfine Interact. **199**, 9 (2011).
157. B.W. Lynn and R.G. Stuart, Nucl. Phys. **B253**, 216 (1985).
158. *Physics at LEP*, ed. J. Ellis and R. Peccei, CERN 86–02, Vol. 1.
159. PETRA: S.L. Wu, Phys. Reports **107**, 59 (1984); C. Kiesling, *Tests of the Standard Theory of Electroweak Interactions*, (Springer-Verlag, New York, 1988); R. Marshall, Z. Phys. **C43**, 607 (1989); Y. Mori *et al.*, Phys. Lett. **B218**, 499 (1989); D. Haidt, p. 203 of Ref. 5.
160. For reviews, see D. Schaile, p. 215, and A. Blondel, p. 277 of Ref. 5; P. Langacker [7]; and S. Riemann [161].
161. S. Riemann, Rept. on Prog. in Phys. **73**, 126201 (2010).
162. SLD: K. Abe *et al.*, Phys. Rev. Lett. **84**, 5945 (2000).
163. SLD: K. Abe *et al.*, Phys. Rev. Lett. **85**, 5059 (2000).
164. SLD: K. Abe *et al.*, Phys. Rev. Lett. **86**, 1162 (2001).
165. DELPHI: P. Abreu *et al.*, Z. Phys. **C67**, 1 (1995); OPAL: K. Ackerstaff *et al.*, Z. Phys. **C76**, 387 (1997).
166. SLD: K. Abe *et al.*, Phys. Rev. Lett. **78**, 17 (1997).
167. DØ: V.M. Abazov *et al.*, Phys. Rev. **D84**, 012007 (2011).
168. CDF: J. Han *et al.*, `arXiv:1110.0153 [hep-ex]`.
169. CDF: D. Acosta *et al.*, Phys. Rev. **D71**, 052002 (2005).
170. H1: A. Aktas *et al.*, Phys. Lett. **B632**, 35 (2006); H1 and ZEUS: Z. Zhang, Nucl. Phys. Proc. Suppl. **191**, 271 (2009).
171. CMS: S. Chatrchyan *et al.*, Phys. Rev. **D84**, 112002 (2011).
172. ALEPH, DELPHI, L3, OPAL, and LEP Electroweak Working Group: J. Alcarez *et al.*, `hep-ex/0612034`.
173. ALEPH, DELPHI, L3, OPAL, and the LEP Working Group for Higgs Boson Searches: D. Abbaneo *et al.*, Phys. Lett. **B565**, 61 (2003).
174. J. Erler, Phys. Rev. **D81**, 051301 (R) (2010); see also Ref. 92.
175. A. Leike, T. Riemann, and J. Rose, Phys. Lett. **B273**, 513 (1991); T. Riemann, Phys. Lett. **B293**, 451 (1992).
176. A comprehensive report and further references can be found in K.G. Chetyrkin, J.H. Kühn, and A. Kwiatkowski, Phys. Reports **277**, 189 (1996).
177. J. Schwinger, *Particles, Sources, and Fields*, Vol. II, (Addison-Wesley, New York, 1973); K.G. Chetyrkin, A.L. Kataev, and F.V. Tkachev, Phys. Lett. **B85**, 277 (1979); M. Dine and J. Sapirstein, Phys. Rev. Lett. **43**, 668 (1979); W. Celmaster and R.J. Gonsalves, Phys. Rev. Lett. **44**, 560 (1980); S.G. Gorishnii, A.L. Kataev, and S.A. Larin, Phys. Lett. **B259**, 144 (1991); L.R. Surguladze, M.A. Samuel, Phys. Rev. Lett. **66**, 560 (1991) and *ibid.*, 2416(E).

178. P.A. Baikov, K.G. Chetyrkin, and J.H. Kühn, Phys. Rev. Lett. **101**, 012002 (2008).
179. W. Bernreuther and W. Wetzel, Phys. Rev. **D24**, 2724 (1982);
B.A. Kniehl, Phys. Lett. **B237**, 127 (1990);
K.G. Chetyrkin, Phys. Lett. **B307**, 169 (1993);
A.H. Hoang *et al.*, Phys. Lett. **B338**, 330 (1994);
S.A. Larin, T. van Ritbergen, and J.A.M. Vermaseren, Nucl. Phys. **B438**, 278 (1995).
180. T.H. Chang, K.J.F. Gaemers, and W.L. van Neerven, Nucl. Phys. **B202**, 407 (1980);
J. Jersak, E. Laermann, and P.M. Zerwas, Phys. Rev. **D25**, 1218 (1982);
S.G. Gorishnii, A.L. Kataev, and S.A. Larin, Nuovo Cimento **92**, 117 (1986);
K.G. Chetyrkin and J.H. Kühn, Phys. Lett. **B248**, 359 (1990);
K.G. Chetyrkin, J.H. Kühn, and A. Kwiatkowski, Phys. Lett. **B282**, 221 (1992);
K.G. Chetyrkin and J.H. Kühn, Phys. Lett. **B406**, 102 (1997).
181. B.A. Kniehl and J.H. Kühn, Nucl. Phys. **B329**, 547 (1990);
K.G. Chetyrkin and A. Kwiatkowski, Phys. Lett. **B319**, 307 (1993);
S.A. Larin, T. van Ritbergen, and J.A.M. Vermaseren, Phys. Lett. **B320**, 159 (1994);
K.G. Chetyrkin and O.V. Tarasov, Phys. Lett. **B327**, 114 (1994).
182. A.L. Kataev, Phys. Lett. **B287**, 209 (1992).
183. D. Albert *et al.*, Nucl. Phys. **B166**, 460 (1980);
F. Jegerlehner, Z. Phys. **C32**, 425 (1986);
A. Djouadi, J.H. Kühn, and P.M. Zerwas, Z. Phys. **C46**, 411 (1990);
A. Borrelli *et al.*, Nucl. Phys. **B333**, 357 (1990).
184. A.A. Akhundov, D.Yu. Bardin, and T. Riemann, Nucl. Phys. **B276**, 1 (1986);
W. Beenakker and W. Hollik, Z. Phys. **C40**, 141 (1988);
B.W. Lynn and R.G. Stuart, Phys. Lett. **B352**, 676 (1990);
J. Bernabeu, A. Pich, and A. Santamaria, Phys. Lett. **B200**, 569 (1988) and Nucl. Phys. **B363**, 326 (1991).
185. Tevatron Electroweak Working Group, CDF and DØ: `1003.2826 [hep-ex]`.
186. E. Braaten, S. Narison, and A. Pich, Nucl. Phys. **B373**, 581 (1992).
187. F. Le Diberder and A. Pich, Phys. Lett. **B286**, 147 (1992).
188. M. Beneke and M. Jamin, JHEP **0809**, 044 (2008).
189. E. Braaten and C.S. Li, Phys. Rev. **D42**, 3888 (1990).
190. J. Erler, Rev. Mex. Fis. **50**, 200 (2004).
191. D. Boito *et al.*, Phys. Rev. **D84**, 113006 (2011);
D. Boito *et al.*, `arXiv:1203.3146 [hep-ph]`.
192. J. Erler, `arXiv:1102.5520 [hep-ph]`.
193. M. Davier *et al.*, Eur. Phys. J. **C56**, 305 (2008);
K. Maltman and T. Yavin, Phys. Rev. **D78**, 094020 (2008).
194. E821: G.W. Bennett *et al.*, Phys. Rev. Lett. **92**, 161802 (2004).
195. T. Kinoshita and M. Nio, Phys. Rev. **D70**, 113001 (2004);
M. Passera, J. Phys. **G31**, R75 (2005);
T. Kinoshita, Nucl. Phys. Proc. Suppl. **144**, 206 (2005).

196. G. Li, R. Mendel, and M.A. Samuel, Phys. Rev. **D47**, 1723 (1993);
S. Laporta and E. Remiddi, Phys. Lett. **B301**, 440 (1993);
S. Laporta and E. Remiddi, Phys. Lett. **B379**, 283 (1996);
A. Czarnecki and M. Skrzypek, Phys. Lett. **B449**, 354 (1999).

197. J. Erler and M. Luo, Phys. Rev. Lett. **87**, 071804 (2001).

198. A.L. Kataev, Nucl. Phys. Proc. Suppl. **155**, 369 (2006);
T. Kinoshita and M. Nio, Phys. Rev. **D73**, 053007 (2006).

199. For reviews, see V.W. Hughes and T. Kinoshita, Rev. Mod. Phys. **71**, S133 (1999);
A. Czarnecki and W.J. Marciano, Phys. Rev. **D64**, 013014 (2001);
T. Kinoshita, J. Phys. **G29**, 9 (2003);
M. Davier and W.J. Marciano, Ann. Rev. Nucl. Part. Sci. **54**, 115 (2004);
J.P. Miller, E. de Rafael, and B.L. Roberts, Rept. Prog. Phys. **70**, 795 (2007);
F. Jegerlehner, Acta Phys. Polon. **B38**, 3021 (2007).

200. S.J. Brodsky and J.D. Sullivan, Phys. Rev. **D156**, 1644 (1967);
T. Burnett and M.J. Levine, Phys. Lett. **B24**, 467 (1967);
R. Jackiw and S. Weinberg, Phys. Rev. **D5**, 2473 (1972);
I. Bars and M. Yoshimura, Phys. Rev. **D6**, 374 (1972);
K. Fujikawa, B.W. Lee, and A.I. Sanda, Phys. Rev. **D6**, 2923 (1972);
G. Altarelli, N. Cabibbo, and L. Maiani, Phys. Lett. **B40**, 415 (1972);
W.A. Bardeen, R. Gastmans, and B.E. Laurup, Nucl. Phys. **B46**, 315 (1972).

201. T.V. Kukhto *et al.*, Nucl. Phys. **B371**, 567 (1992);
S. Peris, M. Perrottet, and E. de Rafael, Phys. Lett. **B355**, 523 (1995);
A. Czarnecki, B. Krause, and W.J. Marciano, Phys. Rev. **D52**, 2619 (1995);
A. Czarnecki, B. Krause, and W.J. Marciano, Phys. Rev. Lett. **76**, 3267 (1996).

202. G. Degrassi and G. Giudice, Phys. Rev. **D58**, 053007 (1998).

203. V. Cirigliano, G. Ecker, and H. Neufeld, JHEP **0208**, 002 (2002);
K. Maltman and C.E. Wolfe, Phys. Rev. **D73**, 013004 (2006);
M. Davier *et al.*, Eur. Phys. J. **C66**, 127 (2010).

204. W.J. Marciano and A. Sirlin, Phys. Rev. Lett. **61**, 1815 (1988).

205. S. Ghozzi and F. Jegerlehner, Phys. Lett. **B583**, 222 (2004).

206. K. Melnikov and A. Vainshtein, Phys. Rev. **D70**, 113006 (2004).

207. J. Erler and G. Toledo Sánchez, Phys. Rev. Lett. **97**, 161801 (2006).

208. M. Knecht and A. Nyffeler, Phys. Rev. **D65**, 073034 (2002).

209. M. Hayakawa and T. Kinoshita, `hep-ph/0112102`;
J. Bijnens, E. Pallante, and J. Prades, Nucl. Phys. **B626**, 410 (2002);
A recent discussion is in J. Bijnens and J. Prades, Mod. Phys. Lett. **A22**, 767 (2007).

210. J. Prades, E. de Rafael, and A. Vainshtein, `0901.0306 [hep-ph]`.

211. B. Krause, Phys. Lett. **B390**, 392 (1997).

212. J.L. Lopez, D.V. Nanopoulos, and X. Wang, Phys. Rev. **D49**, 366 (1994);
for recent reviews, see Ref. 199.

213. U. Amaldi *et al.*, Phys. Rev. **D36**, 1385 (1987);
G. Costa *et al.*, Nucl. Phys. **B297**, 244 (1988);

P. Langacker and M. Luo, Phys. Rev. **D44**, 817 (1991);
J. Erler and P. Langacker, Phys. Rev. **D52**, 441 (1995).
214. Tevatron Electroweak Working Group, CDF and DØ: 0908.1374 [hep-ex].
215. J. Erler, arXiv:1201.0695 [hep-ph].
216. F. James and M. Roos, Comput. Phys. Commun. **10**, 343 (1975).
217. For a more recent study, see J. Cao and J.M. Yang, JHEP **0812**, 006 (2008).
218. J. Erler, J.L. Feng, and N. Polonsky, Phys. Rev. Lett. **78**, 3063 (1997).
219. D. Choudhury, T.M.P. Tait, and C.E.M. Wagner, Phys. Rev. **D65**, 053002 (2002).
220. J. Erler and P. Langacker, Phys. Rev. Lett. **84**, 212 (2000).
221. P. Langacker and M. Plümacher, Phys. Rev. **D62**, 013006 (2000).
222. DELPHI: P. Abreu *et al.*, Eur. Phys. J. **C10**, 415 (1999).
223. P. Langacker and N. Polonsky, Phys. Rev. **D52**, 3081 (1995);
J. Bagger, K.T. Matchev, and D. Pierce, Phys. Lett. **B348**, 443 (1995).
224. F. Gianotti, CERN public seminar, ATLAS-CONF-2011-163.
225. CDF and DØ: arXiv:1107.5518 [hep-ex].
226. J. Erler, Phys. Rev. **D63**, 071301 (R) (2001).
227. G. Tonelli, CERN public seminar, CMS-HIG-11-032.
228. M. Veltman, Nucl. Phys. **B123**, 89 (1977);
M. Chanowitz, M.A. Furman, and I. Hinchliffe, Phys. Lett. **B78**, 285 (1978);
The two-loop correction has been obtained by J.J. van der Bij and F. Hoogeveen, Nucl. Phys. **B283**, 477 (1987).
229. P. Langacker and M. Luo, Phys. Rev. **D45**, 278 (1992) and refs. therein.
230. A. Denner, R.J. Guth, and J.H. Kühn, Phys. Lett. **B240**, 438 (1990);
W. Grimus *et al.*, J. Phys. G **35**, 075001 (2008);
H. E. Haber and D. O'Neil, Phys. Rev. **D83**, 055017 (2011).
231. S. Bertolini and A. Sirlin, Phys. Lett. **B257**, 179 (1991).
232. M. Peskin and T. Takeuchi, Phys. Rev. Lett. **65**, 964 (1990);
M. Peskin and T. Takeuchi, Phys. Rev. **D46**, 381 (1992);
M. Golden and L. Randall, Nucl. Phys. **B361**, 3 (1991).
233. D. Kennedy and P. Langacker, Phys. Rev. **D44**, 1591 (1991).
234. G. Altarelli and R. Barbieri, Phys. Lett. **B253**, 161 (1990).
235. B. Holdom and J. Terning, Phys. Lett. **B247**, 88 (1990).
236. B.W. Lynn, M.E. Peskin, and R.G. Stuart, p. 90 of Ref. 158.
237. An alternative formulation is given by K. Hagiwara *et al.*, Z. Phys. **C64**, 559 (1994), and *ibid.*, **68**, 352(E) (1995);
K. Hagiwara, D. Haidt, and S. Matsumoto, Eur. Phys. J. **C2**, 95 (1998).
238. I. Maksymyk, C.P. Burgess, and D. London, Phys. Rev. **D50**, 529 (1994);
C.P. Burgess *et al.*, Phys. Lett. **B326**, 276 (1994).
239. R. Barbieri *et al.*, Nucl. Phys. **B703**, 127 (2004).
240. K. Lane, hep-ph/0202255.
241. E. Gates and J. Terning, Phys. Rev. Lett. **67**, 1840 (1991);
R. Sundrum and S.D.H. Hsu, Nucl. Phys. **B391**, 127 (1993);
R. Sundrum, Nucl. Phys. **B395**, 60 (1993);
M. Luty and R. Sundrum, Phys. Rev. Lett. **70**, 529 (1993);

T. Appelquist and J. Terning, Phys. Lett. **B315**, 139 (1993);
D.D. Dietrich, F. Sannino, and K. Tuominen, Phys. Rev. **D72**, 055001 (2005);
N.D. Christensen and R. Shrock, Phys. Lett. **B632**, 92 (2006);
M. Harada, M. Kurachi, and K. Yamawaki, Prog. Theor. Phys. **115**, 765 (2006).

242. H. Georgi, Nucl. Phys. **B363**, 301 (1991);
M.J. Dugan and L. Randall, Phys. Lett. **B264**, 154 (1991).

243. R. Barbieri *et al.*, Nucl. Phys. **B341**, 309 (1990).

244. J. Erler and D.M. Pierce, Nucl. Phys. **B526**, 53 (1998);
G.C. Cho and K. Hagiwara, Nucl. Phys. **B574**, 623 (2000);
G. Altarelli *et al.*, JHEP **0106**, 018 (2001);
S. Heinemeyer, W. Hollik, and G. Weiglein, Phys. Reports **425**, 265 (2006);
S.P. Martin, K. Tobe, and J.D. Wells, Phys. Rev. **D71**, 073014 (2005);
G. Marandella, C. Schappacher, and A. Strumia, Nucl. Phys. **B715**, 173 (2005);
S. Heinemeyer *et al.*, JHEP **0608**, 052 (2006);
M.J. Ramsey-Musolf and S. Su, Phys. Reports **456**, 1 (2008);
J.R. Ellis *et al.*, JHEP **0708**, 083 (2007);
A. Djouadi, Phys. Reports **459**, 1 (2008);
S. Heinemeyer *et al.*, JHEP **0804**, 039 (2008).

245. M.E. Peskin and J.D. Wells, Phys. Rev. **D64**, 093003 (2001).

246. G.D. Kribs *et al.*, Phys. Rev. **D76**, 075016 (2007).

247. H.J. He, N. Polonsky, and S. Su, Phys. Rev. **D64**, 053004 (2001);
V.A. Novikov *et al.*, Sov. Phys. JETP **76**, 127 (2002);
S.S. Bulanov *et al.*, Yad. Fiz. **66**, 2219 (2003) and refs. therein.

248. J. Maalampi and M. Roos, Phys. Reports **186**, 53 (1990).

249. J. Erler and P. Langacker, Phys. Rev. Lett. **105**, 031801 (2010).

250. CDF and DØ: D. Benjamin, `arXiv:1108.3331 [hep-ex]`.

251. ATLAS: `http://atlas.ch/news/2011/Higgs-note.pdf`.

252. Z. Murdock, S. Nandi and Z. Tavartkiladze, Phys. Lett. **B668**, 303 (2008).

253. For reviews, see the Section on "Grand Unified Theories" in this *Review*;
P. Langacker, Phys. Reports **72**, 185 (1981);
J.L. Hewett and T.G. Rizzo, Phys. Reports **183**, 193 (1989);
for collider implications, see T.C. Andre and J.L. Rosner, Phys. Rev. **D69**, 035009 (2004);
J. Kang, P. Langacker and B.D. Nelson, Phys. Rev. **D77**, 035003 (2008).

254. S.P. Martin, Phys. Rev. **D81**, 035004 (2010);
P.W. Graham *et al.*, Phys. Rev. **D81**, 055016 (2010).

255. P. Langacker and D. London, Phys. Rev. **D38**, 886 (1988);
D. London, p. 951 of Ref. 5;
a recent analysis is F. del Aguila, J. de Blas and M. Perez-Victoria, Phys. Rev. **D78**, 013010 (2008).

256. M. Chemtob, Prog. in Part. Nucl. Phys. **54**, 71 (2005);
R. Barbier *et al.*, Phys. Reports **420**, 1 (2005).

257. R.S. Chivukula and E.H. Simmons, Phys. Rev. **D66**, 015006 (2002);
C.T. Hill and E.H. Simmons, Phys. Reports **381**, 235 (2003);
R.S. Chivukula *et al.*, Phys. Rev. **D70**, 075008 (2004).

258. K. Agashe *et al.*, JHEP **0308**, 050 (2003);
M. Carena *et al.*, Phys. Rev. **D68**, 035010 (2003);
I. Gogoladze and C. Macesanu, Phys. Rev. **D74**, 093012 (2006);
I. Antoniadis, `hep-th/0102202` see also the note on "Extra Dimensions" in the Searches Particle Listings.

259. T. Han, H.E. Logan, and L.T. Wang, JHEP **0601**, 099 (2006);
M. Perelstein, Prog. in Part. Nucl. Phys. **58**, 247 (2007).

260. E. Accomando *et al.*, `arXiv:hep-ph/0608079`;
V. Barger *et al.*, Phys. Rev. **D77**, 035005 (2008);
W. Grimus *et al.*, Nucl. Phys. **B801**, 81 (2008);
M. Maniatis, Int. J. Mod. Phys. **A25**, 3505 (2010);
U. Ellwanger, C. Hugonie, and A.M. Teixeira, Phys. Reports **496**, 1 (2010);
M.C. Chen, S. Dawson, and C.B. Jackson, Phys. Rev. **D78**, 093001 (2008).

261. G.C. Cho, K. Hagiwara, and S. Matsumoto, Eur. Phys. J. **C5**, 155 (1998);
K. Cheung, Phys. Lett. **B517**, 167 (2001);
Z. Han and W. Skiba, Phys. Rev. **D71**, 075009 (2005).

262. P. Langacker, M. Luo, and A.K. Mann, Rev. Mod. Phys. **64**, 87 (1992);
M. Luo, p. 977 of Ref. 5.

263. F.S. Merritt *et al.*, p. 19 of *Particle Physics: Perspectives and Opportunities: Report of the DPF Committee on Long Term Planning*, ed. R. Peccei *et al.* (World Scientific, Singapore, 1995);
M. Baak *et al.*, `arXiv:1107.0975 [hep-ph]`.

264. D.E. Morrissey, T. Plehn, and T.M.P. Tait, `arXiv:0912.3259 [hep-ph]`.

265. G. Altarelli, R. Barbieri, and S. Jadach, Nucl. Phys. **B369**, 3 (1992) and *ibid.*, **B376**, 444(E) (1992).

266. A. De Rújula *et al.*, Nucl. Phys. **B384**, 3 (1992);
K. Hagiwara *et al.*, Phys. Rev. **D48**, 2182 (1993);
C.P. Burgess *et al.*, Phys. Rev. **D49**, 6115 (1994);
Z. Han and W. Skiba, Phys. Rev. **D71**, 075009 (2005);
G. Cacciapaglia *et al.*, Phys. Rev. **D74**, 033011 (2006);
V. Bernard *et al.*, JHEP **0801**, 015 (2008);
Z. Han, Int. J. Mod. Phys. A **23**, 2653 (2008).

267. For reviews, see A. Leike, Phys. Reports **317**, 143 (1999);
P. Langacker, Rev. Mod. Phys. **81**, 1199 (2009).

268. M. Cvetic and P. Langacker, Phys. Rev. **D54**, 3570 (1996).

269. J. Erler, P. Langacker, and T. Li, Phys. Rev. **D66**, 015002 (2002).

270. S. Chaudhuri *et al.*, Nucl. Phys. **B456**, 89 (1995);
G. Cleaver *et al.*, Phys. Rev. **D59**, 055005 (1999).

271. B. Holdom, Phys. Lett. **B166**, 196 (1986).

272. M. Carena *et al.*, Phys. Rev. **D70**, 093009 (2004).

273. J. Erler, P. Langacker, S. Munir and E. Rojas, JHEP **0908**, 017 (2009).

274. ATLAS: G. Aad *et al.*, Phys. Rev. Lett. **107**, 272002 (2011).
275. CMS: cdsweb.cern.ch/record/1369192/files/EXO-11-019-pas.pdf.
276. CDF: T. Aaltonen *et al.*, Phys. Rev. Lett. **106**, 121801 (2011).
277. DØ: V.M. Abazov *et al.*, Phys. Lett. **B695**, 88 (2011).
278. J. Kang and P. Langacker, Phys. Rev. **D71**, 035014 (2005);
C. -F. Chang, K. Cheung, and T. -C. Yuan, JHEP **1109**, 058 (2011).
279. J. Erler *et al.*, JHEP **1111**, 076 (2011).
280. F. del Aguila, J. de Blas, and M. Perez-Victoria, JHEP **1009**, 033 (2010).
281. T. Appelquist, B.A. Dobrescu, and A.R. Hopper, Phys. Rev. **D68**, 035012 (2003);
R.S. Chivukula *et al.*, Phys. Rev. **D69**, 015009 (2004).